DISSERTATION

Sample preparation for matrix-assisted laser desorption/ionization mass spectrometry (MALDI MS) and gas phase electrophoretic macromolecular mobility analyzer (GEMMA) related to proteins, polymers and intact *Fusarium* spores

Ausgeführt zum Zwecke der Erlangung des akademischen Grades eines

Doktors der Naturwissenschaften

unter der Leitung von

Univ. Prof. Dr. Günter Allmaier

E 164

Instistut für Chemische Technologien und Analytik

Eingereicht an der Technischen Universität Wien

Fakultät für Technische Chemie

von

Mag. Jasmin HIRSCHMANN

9805232

Stifterstraße 10a

4663 Laakirchen

Wien, 19. Mai 2008

Name der Kandidatin: Mag. Jasmin Hirschmann

Name der Prüfer: Univ. Prof. Dr. Günter Allmaier, AO Univ. Prof. Dr. Andreas Rizzi

Titel der Dissertation: Sample preparation for matrix-assisted laser desorption/ionization mass spectrometry (MALDI MS) and gas phase electrophoretic macromolecular mobility analysis (GEMMA) related to proteins, polymers and intact *Fusarium* spores

Zusammenfassung:

Im Rahmen dieser Dissertation wurden zwei Substanzklassen, nämlich (Glyko)Proteine sowie wasserlösliche Polyethylenglykole (PEG) mittels MALDI MS (Matrix-unterstützter Laser Desorptions-/Ionisationsmassenspektrometrie) und GEMMA (Gas Phase Electrophoretic Macromolecular Mobility Analyzer) untersucht, wobei die exakte Molekulargewichts-bestimmung bzw. die Bestimmung der Polymerverteilung im Zentrum des Interesses standen. Ein zweiter Fokus lag auf der MALDI MS Untersuchung intakter Pilzsporen. Des Weiteren wurden enzymatisch generierte Peptide von (Glyko)Proteinen untersucht, um optimale „peptide mass fingerprinting (PMF)" Bedingungen für die Proteinidentifizierung zu finden. Die dafür notwendige Probenvorbereitung ist sowohl von den instrumentellen Anforderungen als auch stark von den Analyteigenschaften abhängig und bedarf daher einer Entwicklung und Optimierung in vielerlei Richtungen.

Eine Vielzahl an Probenvorbereitungsschritten ist für die Charakterisierung von Proteinen und noch viel mehr von Glykoproteinen (z.B. Erythropoietine) notwendig, von denen einige sehr zeit- und arbeitsintensiv sind. Vor allem die Sichtbarmachung der Protein- bzw. Glykoproteinbanden nach der Auftrennung mittels ein- oder zweidimensionaler planarer Gelelektrophorese ist zeitaufwendig, da besonders die kovalent gebundenen Zuckerstrukturen die Wechselwirkung zwischen dem Proteinrückgrad und den Farbpigmenten be- oder sogar verhindern. Unterstützt man den Färbeprozess mit optimierter Mikrowellenstrahlung, kann die Färbedauer bei gleichbleibender Sensitivität signifikant verkürzt werden. Außerdem findet durch die Mikrowellenbehandlung eine zusätzliche Denaturierung der Proteine statt und die Gelmatrix wird aufgeweitet, wodurch der enzymatische Verdau und die anschließende Extraktion der Peptide aus der Gelmatrix positiv beeinflusst werden. Nach PMF mittels MALDI-MS konnten höhere Aminosäuresequenzabdeckungen erzielt werden, ein wichtiger Faktor für die Identifizierung von (Glyko)Proteinen.

Die Charakterisierung des von Willebrand Faktors (vWF), eines adhäsiven Glykoproteins, war auf Grund seines hohen Molekulargewichtes und seiner Multimerstruktur eine große

Herausforderung für MALDI MS und GEMMA. Es wurde ein Probenvorbereitungsprotokoll, bestehend aus Aufreinigung, Reduktion der Disulfidbrücken und Entfernung von Salzen und Detergenzien, entwickelt, das erstmals eine exakte Molekulargewichtsbestimmung mittels MALDI MS und GEMMA ermöglichte.

PEGs (mit reaktiven Gruppen) werden auf Grund ihrer Eigenschaften, nicht toxisch, nicht immunogen und wasserlöslich, oft für die Konjugation an Proteine oder Peptide herangezogen. Bevor jedoch PEGs für pharmazeutische Anwendungen eingesetzt werden können, müssen sie genau charakterisiert werden, wobei das Hauptaugenmerk auf einer exakten Molekulargewichtsbestimmung und der Bestimmung der Polydispersität jedes einzelnen Batches liegt. Eine Gegenüberstellung der GEMMA und MALDI MS Polymerdaten einiger PEGs ergab eine gute Übereinstimmung der beiden Methoden und auch eine gute Übereinstimmung mit den Daten (basierend auf orthogonalen Techniken), die von der Herstellerfirma angegeben wurden.

Die Identifizierung und Klassifizierung von Mikroorganismen, wie Bakterien und Pilze, ist von großer Bedeutung in der Landwirtschaft, Lebensmitteltechnologie und in der medizinischen Forschung und Diagnostik. Viele mikrobiologische Standardmethoden sind jedoch mit hohem Zeit-, Kosten- und Arbeitsaufwand verbunden. ICMS (Intact Cell Mass Spectrometry) basierend auf MALDI Flugzeit MS stellt eine schnelle und zuverlässige Alternative dar. Es konnten erstmals Oberflächenproteinprofile von intakten Sporen unterschiedlicher *Fusarium* Spezies mit einer speziell optimierten Präparationstechnik generiert werden und auf Grund von Profilunterschieden in den Massenspektren konnten die *Fusarien* differenziert und identifiziert werden (im Falle des Vorhandenseins von Referenzspektren). Der Focus lag dabei auf in Österreich vorkommenden, mykotoxin-produzierenden *Fusarium* Spezies. Dafür musste eine Waschprozedur für die Sporen (nach der Züchtung), ein optimiertes MALDI Matrixsystem und eine passende Probenpräparation sowie ein neues MALDI MS Setup entwickelt werden.

Name der Kandidatin: Mag. Jasmin Hirschmann

Namen der Prüfer: Univ. Prof. Dr. Günter Allmaier, AO Univ. Prof. Dr. Andreas Rizzi

Titel der Dissertation: Sample preparation for matrix-assisted laser desorption/ionization mass spectrometry (MALDI MS) and gas phase electrophoretic macromolecular mobility analysis (GEMMA) related to proteins, polymers and intact *Fusarium* spores.

Abstract:

Within the scope of this Ph. D. thesis two types of analytes, namely (glyco)proteins and water-soluble synthetic polymers, were investigated by means of matrix-assisted laser desorption/ionization time-of-flight (TOF) mass spectrometry (MALDI MS) and gas phase electrophoretic macromolecular mobility analyzer (GEMMA). The main focus was the accurate molecular mass determination and the determination of the polymer distribution. Furthermore intact spores from *Fusarium* species were characterized by means of MALDI MS. Whereas the third topic concentrated on the optimization of peptide mass fingerprinting (PMF) conditions by means of analysis of proteolytic (glyco)peptides. A continuous optimization of the required sample preparation was necessary and strongly dependent on the instrumental requirements as well as on the properties exhibited by the analyte itself.

A high number of sample preparation steps are necessary for the characterization of proteins by PMF especially of glycoproteins (e.g. erythropoietins) and some of them are quite time as well as labor intensive. Especially the visualization of (glyco)protein bands separated by 1- or 2-dimensional planar gel electrophoresis can be quiet challenging, because the covalently linked carbohydrate moieties can inhibit the protein-dye interaction or protein-silver reaction and therefore slow down or even completely prevent the staining process. By supporting the staining process with optimized microwave irradiation a significant reduction of the staining duration without loss of sensitivity could be achieved. Furthermore the microwave treatment leads to increased denaturation of the analytes and to an expansion of the surrounding gel matrix, thus improving the enzymatic digestion and the subsequent extraction process of the generated peptides. The mass spectrometric analysis (PMF) of the proteolytic peptides yielded a higher amino acid sequence coverage, which is important for identification of intact (glyco)proteins.

The characterization of von Willebrand factor (vWF), an adhesive glycoprotein circulating in the human blood plasma, is quiet challenging due to its high molecular weight and its multimeric character. A sample preparation procedure consisting of desalting/purification

(removal of salts and detergents) and reduction of disulfide bridges was developed, which enabled an accurate molecular weight determination by means of MALDI linear TOF MS and nano electrospray (nES) GEMMA.

Due to its outstanding properties, non-toxic, non-immunogenic, and high solubility in water, poly(ethylene glycols) (PEGs) carrying a reactive group are commonly used for conjugation to proteins or peptides. Nevertheless, prior to pharmaceutical application the PEGs have to be characterized according to their accurate molecular weight and their degree of polydispersity. The techniques nES GEMMA and MALDI MS of such PEGs yielded high-quality data which were quite comparable as well as in excellent agreement with the data stated by the manufacturer (based on orthogonal techniques as e.g. size exclusion chromatography with light scattering).

Identification and classification of micro-organisms, e.g. bacteria and fungi, is of great importance in the field of agriculture, food production, homeland security as well as in medical research and diagnosis. Most of the commonly used microbiological techniques are highly time, cost and labor intensive. Therefore intact cell mass spectrometry (ICMS) based on MALDI TOF MS offers a fast and reliable alternative. Mass spectrometric profiles of the analytes present on the surface of the intact micro-organism are generated. According to occurring differences in the profiles the micro-organisms can be differentiated and identified. For the first time spores of mycotoxin-producing *Fusarium* species common in Austria were analyzed by means of such an approach. A washing procedure for the spores (after cultivation), MALDI matrix system, sample preparation and MALDI MS setup, has been developed successfully and allowed the differentiation of various *Fusarium* species.

„Die Neugier steht immer an erster Stelle eines Problems, das gelöst werden will"

(Galileo Galilei)

Table of Contents

1 Introduction to MALDI-TOF MS and GEMMA for the characterization of biopolymers and synthetic polymers

Characterization of biomolecules and polymers can be performed with a variety of analytical methods[1], such as gel electrophoresis, immunology, chromatography, spectroscopy, and mass spectrometry. Each of these analytical methods shows individual advantages as well as disadvantages, but they all require some sort of sample preparation procedures (purification, concentration, desalting and solubilisation etc.) as salts, detergents or contaminations present in the for example biological sample influence their analytical characteristics and the analytical process in general. This Ph.D. thesis deals with several sample preparation approaches required for the characterization of peptides, (glyco)proteins, synthetic polymers and intact micro-organisms performed subsequently by means of vacuum matrix-assisted laser desorption/ionization mass spectrometry time-of-flight mass spectrometry (MALDI-TOF MS) and nano electrospray gas phase electrophoretic macromolecular mobility analysis (GEMMA).

Nowadays mass spectrometric approaches such as MALDI or electrospray ionization (ESI) MS are commonly used for the characterization of biomolecules, biopolymers and technical polymers with respect to molecular weight determination, heterogeneity, elucidation of posttranslational modifications of proteins or investigation of the degree of polydispersity. MALDI-TOF MS exhibits a number of advantages which makes it suited for the characterization of a wide range of analytes, such as peptides [2, 3], (glyco)proteins [4], intact micro-organisms [5] and synthetic polymers [6]. It offers a high tolerance (relative to ESI related techniques) against salts and detergents as well as fast and accurate determination of the analytes molecular weight. Furthermore the generation of mainly singly charged molecular ions facilitates the ease of data interpretation. In combination with a linear TOF mass analyzer, which theoretically allows an unlimited accessible m/z range, MALDI MS provides in a large number of cases molecular weight as well as heterogeneity information of the investigated analyte. Nevertheless, depending on the analyte various MALDI matrix compounds can be applied and for each individual matrix/analyte system the sample preparation technique as well as the UV laser irradiation conditions have to be optimized in terms of obtainable mass spectral information (peak

number and intensity) and mass spectra reproducibility. An essential prerequisite to obtain optimal MALDI mass spectra are the evenly embedding of the analyte into the matrix crystal and the formation of a homogeneous matrix/analyte crystal layer on the MALDI target. Beside the choice of the matrix compound and the sample preparation technique itself also salts and detergents present in the sample solution as well as contaminations arising from the solvent system or the matrix compound influence the crystallization process and the subsequent UV laser-based desorption/ionization process. Therefore the development and evaluation of an efficient and fast sample purification/desalting procedure is of great importance for all MALDI MS based analysis.

Although MALDI-TOF MS provides in principle an unlimited accessible m/z range, several practical limitations, such as low detector efficiencies and enhanced fragmentation induced by the high laser irradiations, set boundaries to the application of MALDI-TOF MS for the characterization of intact high molecular mass molecules. A recently developed analytical method based on the determination of the analytes electrophoretic mobility diameter (EMD) at atmospheric pressure, called gas phase electrophoretic macromolecular mobility analyzer (GEMMA) [7], can overcome these limitations and extend the m/z range in the Mega- to Gigadalton range. Multiply charged macromolecular ions are generated via nano ESI and charge reduced by a bipolar atmosphere generated by a ^{210}Po source to obtain neutral and positive as well as negative singly charged molecules (particles). These ions are size separated according to their EMD using a nano differential mobility analyzer (nDMA) and detected by means of a condensation particle counter (µCPC) based on a direct optical principle. The nano ESI GEMMA approach allows fast and sensitive analysis and size determination of analytes in a range from the low kDa to high GigaDa, such as proteins [8], protein complexes [9], polymers [10] or intact viruses [8]. Similar to MALDI-TOF MS, nano ESI GEMMA provides singly charged molecular ions (in contrast to ESI mass spectrometry with the domination of multiply charged molecules), thus facilitating the easy data interpretation. Nevertheless, as a stable nano ESI process in the cone-jet mode is required for generation of the molecular ions/charged particles and therefore for the acquisition of GEMMA spectra, high amounts of salts and detergents present in the sample have to be removed, due to their destabilizing effects on the nano ESI process and its negative effect on the EMD determination.

References

[1] Lottspeich F. and Zorbas H., Bioanalytik. Heidelberg, Berlin: Spektrum Akademischer Verlag; 1998.

[2] Hillenkamp F., Karas M., Beavis R.C. and Chait B.T., Matrix-assisted laser desorption/ionization mass spectrometry of biopolymers. Analytical Chemistry 1991; **63:** 1193A-1203A.

[3] Zaluzec E.J., Gage D.A. and Watson J.T., Matrix-assisted laser desorption/ionization mass spectrometry: applications in peptide and protein characterization. Protein Expression and Purification 1995; **6:** 109-123.

[4] Harvey D.J., Analysis of carbohydrates and glycoconjugates by matrix-assisted laser desorption/ionization mass spectrometry: an update covering the period 2001-2002. Mass Spectrometry Reviews 2008; **27:** 125-201.

[5] Fenselau C. and Demirev P.A., Characterization of intact microorganisms by MALDI mass spectrometry. Mass Spectrometry Reviews 2001; **20:** 157-171.

[6] Montaudo G., Samperi F. and Montaudo M.S., Characterization of synthetic polymers by MALDI-MS. Progress in Polymer Science 2006; **31:** 277-357.

[7] Kaufman S.L., Skogen J.W., Dorman F.D. and Zarrin F., Macromolecule analysis based on electrophoretic mobility in air: globular proteins. Analytical Chemistry 1996; **68:** 1895-1904.

[8] Bacher G., Szymanski W.W., Kaufman S.L., Zollner P., Blaas D. and Allmaier G., Charge-reduced nano electrospray ionization combined with differential mobility analysis of peptides, proteins, glycoproteins, noncovalent protein complexes and viruses. Journal of Mass Spectrometry 2001; **36:** 1038-1052.

[9] Loo J.A., Berhane B., Kaddis C.S., Wooding K.M., Xie Y., Kaufman S.L. and Chernushevich I.V., Electrospray ionization mass spectrometry and ion mobility analysis of the 20S proteasome complex. Journal of the American Society for Mass Spectrometry 2005; **16:** 998-1008.

[10] Ku B.K., De la Mora F.J., Saucy D.A. and Alexander J.N., Mass distribution measurement of water-insoluble polymers by charge-reduced electrospray mobility analysis. Analytical Chemistry 2004; **76:** 814-822.

1.1 Matrix-assisted laser desorption/ionization mass spectrometry

Since the 1970s laser irradiation is used to generate ions for mass spectrometric analysis [1-3]. Laser desorption ionization (LDI) is based on the direct energy transfer to the sample by absorption of the analyte molecule. Due to the different spectral absorptions at the applied laser wavelength only highly absorbing molecules could be detected, whereas ionization of none or less absorbing molecules was accompanied by extensive fragmentation. Furthermore, the thermal degradation did not allow desorption and ionization of larger molecules as intact entities, therefore the accessible molecular mass range of LDI was below 2 kDa.

In the 1980s Hillenkamp [4] as well as Tanaka [5] were able to overcome these limiting factors by embedding the analyte molecules into a highly UV absorbing matrix. Using the matrix as energy mediator controllable and efficient energy transfer was obtained and thermal degradation of the analyte molecules caused by excessive energy could be avoided mainly due the short time frame (low picoseconds range) of the laser pulse. Nowadays this technique, called vacuum matrix-assisted laser desorption/ionization mass spectrometry (MALDI MS), is widely used for the characterization of biopolymers, proteins and peptides [6-9], as well as oligosaccharides [10, 11], synthetic polymers [12-14] and nucleic acids [15, 16]. Recently new applications for MALDI MS are investigated, e.g. classification of intact micro-organisms (bacteria, fungi) [17-19] and profiling and imaging mass spectrometry of tissue sections [20-22].

1.1.1 The MALDI matrix

Since the introduction of MALDI MS numerous matrix compounds were investigated. Beside universal characteristics, low molecular weight, lack of chemical reactivity, solubility in analyte compatible solvents and vacuum stability, MALDI matrices provide several essential functions [23]. The most important one is the high spectral absorption of the exciting laser wavelength, allowing controllable and efficient energy transfer to the analyte and thus optimizing the desorption/ionization process. Furthermore the matrix separates the analyte molecules preventing analyte aggregation and clustering.

Nearly all matrix substances suitable for UV-MALDI MS are small aromatic molecules. The most prominent group are aromatic carbonic acids, including cinnamic acid derivatives, e.g. α-cyano-4-hydroxycinnamic acid, 3-methoxy-4-hydroxycinnamic acid (ferulic acid), 3,5-dimethoxy-4-hydroxycinnamic acid (sinapic acid) and benzoic acid derivatives, e.g. 2,5-dihydroxybenzoic acid. Other commonly applied matrices are 2,6-dihydroxyacetophenone, 2,4,6-trihydroxyacetophenone and 1,8,9-trihydroxyanthracene (dithranol). Not all MALDI matrix systems consist of one matrix substance, it is reported that mixtures of different types of matrices enhance the performance of MALDI MS experiments [24, 25]. Beside the above mentioned solid matrix substances, also liquid matrix systems (4-nitroaniline and 3-nitrobenzylalcohol), metal powders (nano Co particles) or inorganic salts in glycerol forming light absorbing dispersions and ionic liquids, such as salts of the common acidic MALDI matrix substances with organic cations, are applied for UV-MALDI MS.

1.1.2 The MALDI sample preparation

In general, the analyte as well as the matrix substance are dissolved in identical or at least compatible solvents, in most cases mixtures of organic solvents, e.g. acetonitrile, ethanol and methanol, with water or 0.1 % trifluoroacetic acid. As mentioned above separation of the individual analyte molecules is crucial for acquiring good MALDI mass spectra. To meet this demand typically a 10^3 to 10^4 times molar excess of matrix molecules compared to analyte molecules is applied.

In case of solid matrix substances embedding of the analyte into the matrix crystals has to be achieved using several different ways of sample preparation techniques [26, 27], e.g. thin layer, sandwich, dried droplet and mixed volumes technique. For the thin layer technique matrix solution is applied onto the MALDI target forming a thin layer of matrix crystals and the sample solution is applied on top of this dried layer. The upper matrix layer is dissolved in the sample solution facilitating the embedding of the sample into the top matrix layer. The application of another matrix layer on top of the thin layer preparation, thus forming a matrix-sample-matrix sandwich is therefore referred to as sandwich preparation technique. Beside the deposition of the sample solution onto pre-formed matrix crystal layers, the application of mixtures of sample and matrix solutions onto the MALDI target can be used as sample preparation technique. Directly mixing of sample and matrix solution on the MALDI target facilitates a more evenly embedding of the analyte into the

matrix crystals, thus homogeneously distributed matrix/analyte crystal layers are formed. An even easier and faster sample preparation can be obtained by pre-mixing the sample and matrix solution in a tube and applying an aliquot of this mixture onto the MALDI target, referred to as mixed volumes technique.

1.1.3 The MALDI process

Ion formation during the MALDI process occurs within a few femtoseconds. For UV-lasers, typical pulse durations range from 0.5 to 10 ns, laser spot diameters on the sample are in the range of 30 to 150 μm and laser penetration depth into the sample in the range of 50 to 300 nm [23]. Dependent on the used matrix system, the applied sample preparation technique and the laser properties, e.g. wavelength, spot diameter, the threshold irradiances for ion generation varies. Generally threshold irradiances of 1×10^6 to 5×10^7 W/cm^2 are observed.

Even though MALDI MS is a widely used analytical method, until now there is no generally valid model for the MALDI desorption/ionization process. The currently discussed models divide ion formation into two steps, primary and secondary ionization [28]. First primary ionization generates ionic species from neutral molecules or ion pairs, whereas secondary ionization is based on ion-molecule reactions which take place in the MALDI plume and generate secondary ions. These secondary ions, mainly protonated molecular ions, reach to a certain extent after crossing the mass analyzer finally the detector.

Primary ionization

Multiphoton ionization

A straightforward explanation for ion generation with laser excitation of an absorbing organic molecule is the single molecule multiphoton ionization, leading to a matrix radical cation.

$$M \xrightarrow{n(h\nu)} M^{+\circ} + e^-$$
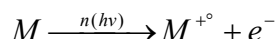
Due to the observation of free electrons emitted from the sample and the fact that matrix radical cations are observed for many commonly used MALDI matrices, this process was considered to be the key to most other MALDI ions. Nevertheless this process is rather unlikely, because the calculated ionization potentials for commonly used MALDI matrices

are too high for a two-photon step and the possibility of a three-photon ionization is too low due to the used laser irradiances.

Energy pooling and multicenter models

Another possibility to generate matrix radical cations or highly excited matrix molecules is that two or more separately excited matrix molecules pool their energy.

$$MM \xrightarrow{2h\nu} M^*M^* \longrightarrow M + M^{+\circ} + e^-$$

$$M^*M^* + A \longrightarrow MM + A^{+\circ} + e^-$$
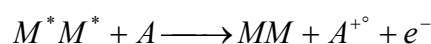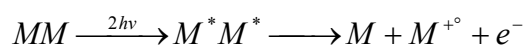
It is statistically more likely that a neighboring molecule of an excited molecule absorbs a photon rather than that the already excited molecule will be hit by a second photon. Thus the energy pooling mechanism will be favored, if it can occur.

Excited-state proton transfer (ESPT)

A very attractive though speculative ionization model, because it requires only one photon, is ESPT. It is based on the presumption of enhanced acidity of excited matrix molecules. Acting as proton donor, neighboring analyte or ground state matrix molecules become protonated and the excited matrix molecule relaxes.

$$M + h\nu \longrightarrow M^*$$

$$M^* + A \longrightarrow (M - H)^- + AH^+$$

$$M^* + M \longrightarrow (M - H)^- + MH^+$$
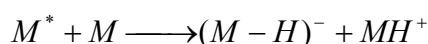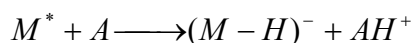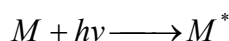
Disproportionation reactions

Some matrices will function in positive and as well in negative ion mode, thus it may seem that positive and negative matrix signals are correlated and that the disproportionation reaction model may be an active ionization mechanism.

$$2M \xrightarrow{nh\nu} (MM)^* \longrightarrow (M - H)^- + MH^+$$
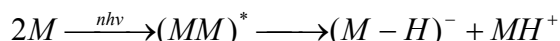
Further primary ionization mechanisms are the desorption of preformed ions or thermal ionization. The model of desorption of preformed ions is based on the presumption that ions are already present in the solid sample and are released by the laser pulse. However, this mechanism has to be restricted to intrinsically ionic compounds such as "tagged"

species (e.g. quaternary ammonium or phosphonium derivatives of peptides), molecules that form strong metal-ion complexes (e.g. crown ethers, metal-binding proteins) and highly acidic analytes. For two-phase matrix systems (graphite particles in glycerol) thermal ionization is a possible ionization mechanism.

Secondary ionization

Due to molecular dynamics simulations the MALDI plume [29] can be seen as a very rapid explosive solid-to-gas phase transition. The large excess of neutral matrix molecules present in the MALDI plume is the ideal prerequisite for a wide range of ion-molecule collisions/reactions involving proton transfer reaction, cationization reactions and electron transfer reactions.

Matrix-matrix proton transfer reactions of matrix radical cations provide intermediates which are able to protonate neutral analyte molecules by matrix-analyte proton transfer reactions. Cationized molecules, e.g. adduct ions with sodium or potassium, are mainly generated through ion-molecule reactions in the gas phase.

1.1.4 The Time-of-flight Analyzer

After successful desorption and ionization of the analyte, the ions have to be accelerated and separated by a mass analyzer. Several different types of mass analyzers are applied for MALDI mass spectrometry, e.g. quadrupole ion trap – time-of-flight (QIT-TOF), quadrupole – time-of-flight (Q-TOF), triple quadrupoles (QqQ), linear ion traps (LIT) and Fourier transform ion cyclotron resonance – time-of-flight (FTICR-TOF). However the most frequently applied approach is a coupling of MALDI with a time-of-flight (TOF) analyzer.

Mass analysis by a TOF analyzer is based on the fact that the time the ions need to pass the drift tube and reach the detector is directly correlated with their mass to charge (m/z) ratio, mathematically described in equations 1 to 3.

$$E_{kin} = \frac{mv^2}{2} = ze_0U \quad \text{(equation 1)}$$

The kinetic energy E_{kin} of an accelerated ion is dependent on mass m and velocity v. Furthermore E_{kin} can be described as a function of the applied acceleration voltage U and the number of charges of the ion z. The elementary electric charge is termed as e_0 (equ. 1).

$$v = \frac{s}{t} \qquad \text{(equation 2)}$$

The velocity *v* can be calculated by dividing the length of the drift zone *s* by the time *t* the ion needs to pass this zone and reach the detector (equ. 2). Substitution of equation 1 in equation 2 provides equation 3, yielding the obtained *m/z* ratio as a function of the applied acceleration voltage, the time the ions need to reach the detector and the length of the drift zone.

$$\frac{m}{z} = \frac{2Ut^2}{s^2} \qquad \text{(equation 3)}$$

A TOF spectrum is obtained by recording the signal intensity as a function of time. The corresponding m/z ratios can be calculated from the equation above and the conversion of the spectrum's x-axis from time to m/z ratio is performed by an empirically determined calibration function.

MALDI ion formation occurs within a few ps after the laser pulse and thereof the starting point for TOF mass analysis can be precisely timed. The obtained molecular ions are accelerated towards the detector by an electric field, which is applied by a high potential difference (typically 3-40 keV) between the sample target and a grid or lens system (3-15 mm distance). After leaving the electrical field the ions pass a field free drift zone applied between the acceleration grid and the detector, which is commonly 0.1 - 3 m long.

Compared to other mass analyzers, such as quadrupole or ion trap systems, application of the TOF mass analyzer has two main advantages. First, a TOF mass analyzer theoretically has no limit of the accessible m/z range. Nevertheless, practical limitations result from low detector efficiencies and decreasing resolutions for high mass molecular ions and the enhanced fragmentation induced by the high laser irradiations and elevated acceleration voltages. Secondly, almost all generated molecular ions are detected, hence no scanning function is required and therefore mass spectra acquisition can be performed much faster than with other mass analyzers (i.e. practical no duty cycle).

Based on an ideal model, all ions of the same mass and charge state are detected at the same time, thus infinite small signals can be obtained. Nevertheless in reality identical ions reach the detector at slightly different times, yielding Gaussian shaped signals. Several processes arising from the desorption/ionization process [30] contribute to this signal broadening. Due to the finite duration of the laser pulse ions are generated at various times. Furthermore a number of effects influence the kinetic energy. Variations of the initial velocities of ions with identical mass, spatial distribution resulting from ionization at

different locations within the expanding MALDI plume and collisions of matrix and analyte ions during the early acceleration phase cause a certain distribution of the kinetic energy. It is possible to enhance the mass spectrometric resolution by applying a reflectron (or even multiturn TOFs) or utilize pulsed or time delayed extraction technique.

A very effective and elegant way of reducing the energy spread is the application of an electrostatic energy mirror, referred to as reflectron [31]. In the reflectron the ions are decelerated and reflected under a small angle to a second detector. Ions possessing a higher kinetic energy than ions with identical mass but lower kinetic energy penetrate the applied electrical field more deeply. Therefore faster ions take a longer way to the detector, than slower ions. Optimization of the reflectrons geometry and voltages allows spatial and time focusing of the ions, leading to an increase in mass spectrometric resolution.

Further reduction of the peak broadening can be achieved with time delayed extraction, first reported in 1990 [32] but based on principles already stated in 1955 by Wiley and McLarren [33]. An intermediate plate is applied between the sample holder and the final grid/lens. For time delayed extraction the same overall voltage is applied to the sample holder and the intermediate grid, thus no extraction field is applied during the laser pulse, whereas a high potential difference is applied between the intermediate grid and the final grid/lens. After an appropriate time delay the extraction field is applied by a high voltage pulse to the intermediate grid. According to the rather long time delays compared to the laser pulse duration it is assumed that ion formation is finished before the ion extraction, thus the effect of the initial time spread is compensated. Furthermore the expansion of the MALDI plume can occur without interference of the extraction field, leading to less matrix-analyte collisions and therefore to a reduction of the kinetic energy distribution. Spatial distribution is compensated by space focusing. Ions with higher initial velocities are able to move further away from the sample slid and gain therefore less kinetic energy when the extraction field is applied. Through optimizing delay time and extraction field force the kinetic energy distribution can be compensated at least across a certain m/z range.

1.1.5 The optimization of the MALDI sample preparation for different kinds of analytes

MALDI mass spectrometry exhibits a number of advantages which make it dedicated for the characterization of a wide range of analytes, such as peptides [6-8], (glyco)proteins [10, 11],

intact micro-organisms [17-19], synthetic polymers [13, 14]. MALDI MS mostly provides singly charged ions facilitating data interpretation over a wide mass range, thus m/z information can be obtained relative easily. Furthermore it offers a high tolerance against salts and detergents (particularly compared to ESI) as well as speed, accuracy and the possibility of automatization. Nevertheless, for different types of analytes the MALDI MS setup has to be optimized, namely sample purification, MALDI matrix system and MALDI sample preparation technique. Depending on the analyte different types of MALDI matrices are favored. Matrices commonly applied for the analysis of proteins and peptides are α-cyano-4-hydroxycinnamic acid [34], 2,5-dihydroxybenzoic acid [35], 3,5-dihydroxy-4-cinnamic acid (sinapic acid) [36] and 3-methoxy-4-hydroxycinnamic acid (ferulic acid) [36]. 2,4,6-trihydroxyacteophenone is used for the analysis of glycoproteins [37]. For the analysis of synthetic polymers 2,5-dihydroxybenzoic acid [12] and 1,8,9-trihydroxyenthracene (dithranol) [13] are used. Also mixtures of two to several matrix substances can be applied as MALDI matrices. The mixture of 2,5-dihydroxybenzoic acid and 2-hydroxy-5methoxybenzoic acid, referred to as super DHB [25], is applied for the analysis of oligosaccharides and synthetic polymers, whereas the mixture of 2,5-dihydroxybenzoic acid and α-cyano-4-hydroxycinnamic acid is said to enhance the analysis of proteins and peptides [24]. As mentioned above analyte as well as matrix substance are dissolved in identical or at least compatible solvents, in most cases mixtures of water or 0.1 %TFA with acetonitrile, acetone, methanol or ethanol. Prior to the selection of the solvent system two points have to be considered. First, the matrix substance has to be dissolvable in the selected solvent system and secondly, degradation of the analyte has to be prevented. Accompanied with the selection of the matrix system is the choice of the MALDI sample preparation technique, which should ensure a proper embedding of the analyte into the matrix crystal. To obtain useful mass spectra from thin layer technique formation of a thin homogeneous matrix crystal layer is required, only provided by matrix systems consisting of highly volatile organic solvents, e.g. acetone or chloroform, thus ensuring fast evaporation. Applying thin layer technique to matrix compounds only soluble in mixtures of organic solvents and water or 0.1 % TFA results in formation of larger crystals irregularly distributed throughout the whole spot. After application of the sample solution on top of such a layer, embedding of the analyte into the matrix crystal will also occur irregularly, forming so called "sweet" spots. If data acquisition is done manually, one can search for these "sweet" spots and obtain significant and mostly reproducible mass spectra. Contrary, if data acquisition is done automatically via rastering the sample spot decreased

mass spectral quality in terms of decreased signal-to-noise ratio is observed. A possibility to overcome this irregular distribution of matrix/analyte crystals is the application of another matrix layer on top of the thin layer preparation, referred to as sandwich technique. Due to the dissolving and recrystallisation step a more homogeneously distributed crystal layer is formed. Another commonly used sample preparation technique based on mixing the sample and matrix solution directly on the MALDI target is the dried droplet technique, yielding a quite homogeneous crystal layer. The more evenly embedding into the matrix crystal layer allows a more homogeneously desorption/ionization of the analyte, thus yielding highly reproducible mass spectra. Another sample preparation technique based on mixing sample and matrix solution is referred to as mixed volumes technique, whereof sample and matrix are pre-mixed in a tube prior to application onto the MALDI target. Directly mixing of sample and matrix solution on the MALDI target is always accompanied with some handling inaccuracies, e.g. droplet position, time frame between sample deposition and addition of matrix solution, which can lead to less reproducible mass spectra. Hence, application of a pre-mixed sample/matrix solution minimizes these inaccuracies. Obviously a homogeneous crystallization is essential for acquisition of significant and reproducible mass spectra. Beside matrix substances, solvent system and applied sample preparation technique also higher amounts of salts and/or detergents present in the sample solution can influence the crystallization behavior. A commonly used and fast approach to remove salts and detergents are miniaturized chromatographic beds fixed in a pipette tip. Several types of chromatographic stationary phases can be utilized to purify and concentrate small amounts of sample solution, e.g. reversed phase material (C_4 and C_{18} alkyl surface groups) and hydrophilic interaction materials. Other methods for sample purification and concentration are e.g. miniaturized size exclusion chromatography, ultrafiltration and drop dialysis.

References

[1]   Vastola F.J., Mumma R.O. and Pirone A.J., Analysis of organic salts by laser ionization. Organic Mass Spectrometry 1970; **3:** 101-104.

[2]   Hillenkamp F., Unsold E., Kaufmann R. and Nitsche R., Laser microprobe mass analysis of organic materials. Nature 1975; **256:** 119-120.

[3]   Posthumus M.A., Kistemaker P.G., Meuzelaar H.L. and Ten Noever de Brauw M.C., Laser desorption-mass spectrometry of polar nonvolatile bio-organic molecules. Analytical Chemistry 1978; **50:** 985-991.

[4]   Karas M. and Hillenkamp F., Laser desorption ionization of proteins with molecular masses exceeding 10,000 daltons. Analytical Chemistry 1988; **60:** 2299-2301.

[5]   Tanaka K., Waki H., Ido Y., Akita S., Yoshida Y., Yoshida T. and Matsuo T., Protein and polymer analysis up to m/z 100 000 by laser ionization time-of-flight mass spectrometry. Rapid Communication in Mass Spectrometry 1988; **2:** 151-153.

[6]   Chaurand P., Luetzenkirchen F. and Spengler B., Peptide and protein identification by matrix-assisted laser desorption/ionization (MALDI) and MALDI-post-source decay time-of-flight mass spectrometry. Journal of the American Society for Mass Spectrometry 1999; **10:** 91-103.

[7]   Hillenkamp F., Karas M., Beavis R.C. and Chait B.T., Matrix-assisted laser desorption/ionization mass spectrometry of biopolymers. Analytical Chemistry 1991; **63:** 1193A-1203A.

[8]   Zaluzec E.J., Gage D.A. and Watson J.T., Matrix-assisted laser desorption/ionization mass spectrometry: applications in peptide and protein characterization. Protein Expression and Purification 1995; **6:** 109-123.

[9]   Vestal M. and Hayden K., High performance MALDI-TOF mass spectrometry for proteomics. International Journal of Mass Spectrometry 2007; **268:** 83-92.

[10]   Harvey D.J., Analysis of carbohydrates and glycoconjugates by matrix-assisted laser desorption/ionization mass spectrometry: an update covering the period 2001-2002. Mass Spectrometry Reviews 2008; **27:** 125-201.

[11]   Dell A. and Morris H.R., Glycoprotein structure determination by mass spectrometry. Science 2001; **291:** 2351-2356.

[12]   Bahr U., Deppe A., Karas M. and Hillenkamp F., Mass Spectrometry of synthetic polymers by UV-matrix-assisted laser desorption/ionization Analytical Chemistry 1992; **64:** 2866-2869.

[13]   Nielen M.W.F., MALDI time-of-flight mass spectrometry of synthetic polymers. Mass Spectrometry Reviews 1999; **18:** 309-344.

[14]   Montaudo G., Samperi F. and Montaudo M.S., Characterization of synthetic polymers by MALDI-MS. Progress in Polymer Science 2006; **31:** 277-357.

[15]   Hillenkamp F., Mass spectrometry of polynucleotides by matrix-assisted laser desorption/ionization (MALDI-MS). Biomedical and Health Research 1995; **8:** 198-205.

[16]   Miketova P. and Schram K.H., Mass spectrometry of nucleotides and oligonucleotides. Molecular Biotechnology 1997; **8:** 249-253.

[17]   Fenselau C. and Demirev P.A., Characterization of intact microorganisms by MALDI mass spectrometry. Mass Spectrometry Reviews 2001; **20:** 157-171.

[18]   Holland R.D., Wilkes J.G., Rafii F., Sutherland J.B., Persons C.C., Voorhees K.J. and Lay J.O., Rapid identification of intact whole bacteria based on spectral patterns using matrix-assisted laser desorption/ionization with time-of-flight mass spectrometry. Rapid Communication in Mass Spectrometry 1996; **10:** 1227-1232.

[19]   Valentine N.B., Wahl J.H., Kingsley M.T. and Wahl K.L., Direct surface analysis of fungal species by matrix-assisted laser desorption/ionization mass spectrometry. Rapid Communication in Mass Spectrometry 2002; **16:** 1352-1357.

[20]   Cornett D.S., Reyzer M.L., Chaurand P. and Caprioli R.M., MALDI imaging mass spectrometry: molecular snapshots of biochemical systems. Nature Methods 2007; **4:** 828-833.

[21]   Chaurand P., Norris J.L., Cornett D.S., Mobley J.A. and Caprioli R.M., New developments in profiling and imaging of proteins from tissue sections by MALDI mass spectrometry. Journal of Proteome Research 2006; **5:** 2889-2900.

[22]   Reyzer M.L. and Caprioli R.M., MALDI-MS-based imaging of small molecules and proteins in tissues. Current Opinion in Chemical Biology 2007; **11:** 29-35.

[23]   Dreisewerd K., The desorption process in MALDI. Chemical Reviews 2003; **103:** 395-426.

[24]   Laugesen S. and Roepstorff P., Combination of two matrices results in improved performance of MALDI MS for peptide mass mapping and protein analysis. Journal of the American Society for Mass Spectrometry 2003; **14:** 992-1002.

[25]   Karas M., Ehring H., Nordhoff E., Stahl B., Strupat K., Hillenkamp F., Grehl M. and Krebs B., Matrix-assisted laser desorption/ionization mass spectrometry with additives to 2,5-dihydroxybenzoic acid. Organic Mass Spectrometry 1993; **28:** 1476-1481.

[26]   Kussmann M., Nordhoff E., Rahbek-Nielsen H., Haebel S., Rossel-Larsen M., Jakobsen L., Goborn J., Mirgorodskaya E., Kroll-Kristensen A., Palm L. and Roepstorff P., Matrix-assisted laser desorption/ionization mass spectrometry

sample preparation techniques designed for various peptide and protein analytes. Journal of Mass Spectrometry 1997; **32:** 593-601.

[27]   Krause J., Stoeckli M. and Schlunegger U.P., Studies on the selection of new matrices for ultraviolet matrix-assisted laser desorption/ionization time-of-flight mass spectrometry. Rapid Communication in Mass Spectrometry 1996; **10:** 1927-1933.

[28]   Knochenmuss R., Ion formation mechanisms in UV-MALDI. The Analyst 2006; **131:** 966-986.

[29]   Knochenmuss R. and Zenobi R., MALDI ionization: the role of in-plume processes. Chemical Reviews 2003; **103:** 441-452.

[30]   Guilhaus M., Mlynski V. and Selby D., Perfect Timing: Time-of-flight Mass Spectrometry. Rapid Communication in Mass Spectrometry 1997; **11:**

[31]   Mamyrin B.A., Time-of-flight mass spectrometry (concepts, achievements and prospects). International Journal of Mass Spectrometry 2001; **206:** 251-266.

[32]   Spengler B. and Cotter R.J., Ultraviolet laser desorption/ionization mass spectrometry of proteins above 100,000 daltons by pulsed ion extraction time-of-flight analysis. Analytical Chemistry 1990; **62:** 793-796.

[33]   Wiley W.C. and McLarren H.I., Time-of-flight mass spectrometer with improved resolution. Review of Scientific Instruments 1955; **26:** 1150-1157.

[34]   Beavis R.C., Chaudhary T. and Chait B.T., Alpha-cyano-4-hydroxycinnamic acid as a matrix for matrix-assisted laser desorption mass spectrometry. Organic Mass Spectrometry 1991; **27:** 156-158.

[35]   Strupat K., Karas M. and Hillenkamp F., 2,5-Dihydroxybenzoic acid: a new matrix for laser desorption-ionization mass spectrometry. International Journal of Mass Spectrometry and Ion Processes 1991; **111:** 89-102.

[36]   Beavis R.C. and Chait B.T., Cinnamic acid derivatives as matrices for ultraviolet laser desorption mass spectrometry of proteins. Rapid Communication in Mass Spectrometry 1989; **3:** 432-435.

[37]   Belgacem O., Buchacher A., Pock K., Josic D., Sutton C., Rizzi A. and Allmaier G., Molecular mass determination of plasma-derived glycoproteins by ultraviolet matrix-assisted laser desorption/ionization time-of-flight mass spectrometry with internal calibration. Journal of Mass Spectrometry 2002; **37:** 1118-1130.

1.2 Gas phase electrophoretic macromolecular mobility analyzer

In the beginning mass spectrometry was focused on the analysis of small molecules. A prerequisite for the applied ionization techniques, such as electron impact ionization [1], chemical ionization [2] and photo-ionization [3], were gaseous molecules. The high thermal energy required for vaporizing high mass molecules results rather in thermal degradation and fragmentation than in desorption and ionization. The development of new desorption/ionization techniques, such as field desorption [4], plasma desorption [5], fast atom bombardment [6] and liquid secondary ion mass spectrometry [7] allowed the desorption and ionization of larger molecules as intact entities in one step. Subsequently first successes in the characterization of intact polymers and biopolymers could be achieved. Nevertheless, high backgrounds and decreasing ion currents with increasing molecular weights as well as the development of improved desorption/ionization techniques prevented a widespread application of these approaches. Nowadays, vacuum matrix-assisted laser desorption/ionization mass spectrometry (MALDI MS) [8] and electrospray ionization mass spectrometry (ESI MS) [9] are the most prominent mass spectrometric approaches applied for the characterization of intact high mass molecules, such as synthetic polymers and biopolymers, as DNA or proteins. Even though mass spectrometric approaches allow fast and accurate molecular weight determination of large molecules a number of disadvantages are associated with these analytical methods. Difficulties in the determination of the charge state of multiply charged ions in the high mass range can arise. Detectors based on secondary electron emission, such as a micro channel plate detector, are velocity dependent, thus they lose sensitivity for higher molecule masses. In the case of MALDI MS sample preparation and laser irradiation conditions have to be optimized for each individual matrix/analyte combination, whereas in the case of ESI MS more or less salt free samples are required.

To overcome these disadvantages a recently developed analytical method based on the determination of the analytes electrophoretic mobility diameter (EMD), called gas phase electrophoretic macromolecular mobility analyzer (GEMMA) can be applied (instrument setup see Figure 1.1). Multiply charged macromolecular ions are generated via nano electrospray (nES) and charge reduced by a bipolar atmosphere generated by a Polonium-210 source to obtain neutral and singly charged ions/particles. These ions are size

separated according to their EMD using a nano differential mobility analyzer (nDMA) and detected by means of a condensation particle counter (µCPC). Analytes in the mass range from kDa to higher GDa can be analyzed and characterized according to their size, e.g. proteins [10], protein complexes [10-12], polymers [13, 14], bacteriophages [15], viruses [10] and inorganic particles [16].
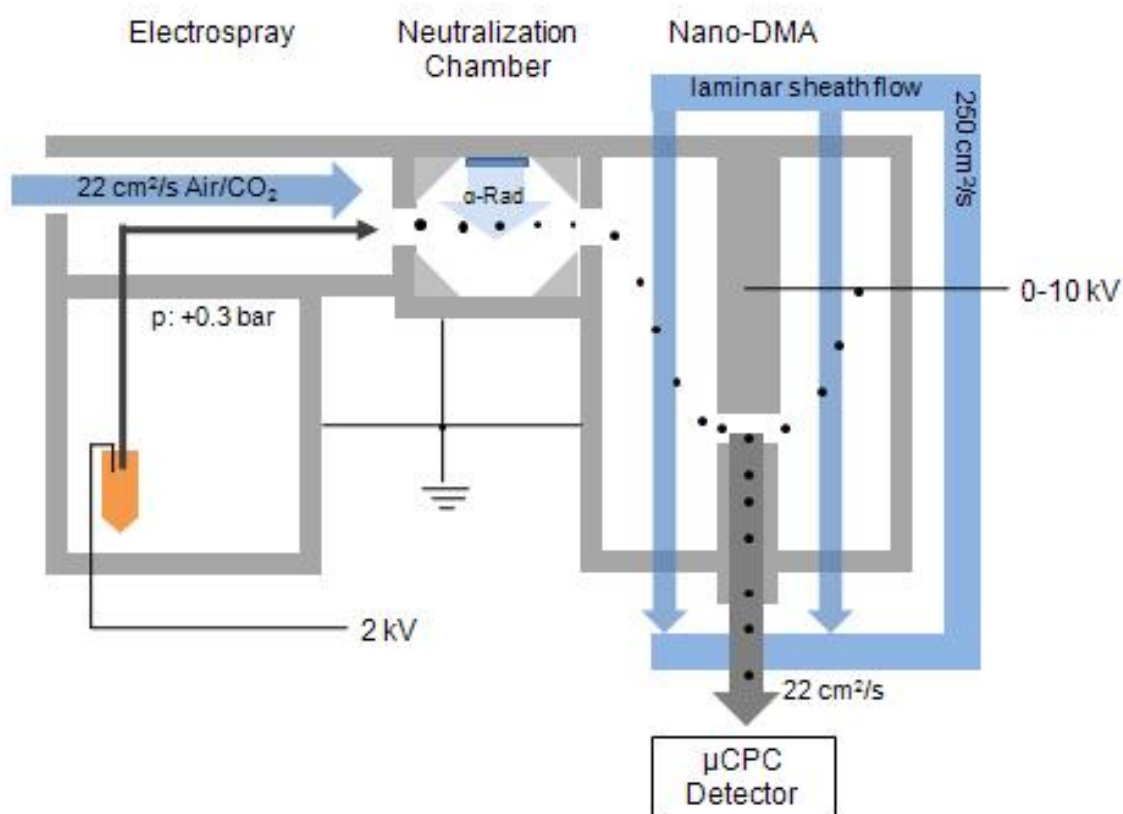
Figure 1.1: Schematic illustration of the applied GEMMA instrument.

1.2.1 Generation of charged particles

Electrospray ionization

Electrospray ionization of liquids is based on the application of a high voltage (few kV) between the conductive liquid in the capillary and an orifice plate mounted opposite the capillary exit. The applied electrical field induces charge separation at the surface of the liquid and thus net charging of the droplet. Depending on various influencing parameters [17], e.g. applied voltage, capillary diameter and liquid properties, several working modes

25

can be distinguished [18]. Due to stability and formation of small highly charged droplets the most commonly used functional mode in GEMMA systems is the cone-jet mode [19].
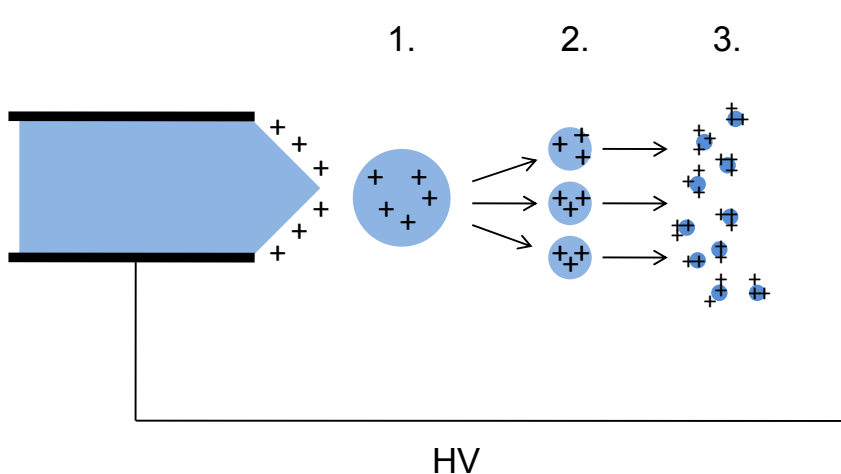
1. Primary ions, 1.5 μm diameter and approx. 60 000 charges
2. Offspring droplets, 0.1 μm diameter and 500 charges
3. Final evaporation/fission step, 0.003 μm diameter and 250 charges

Figure 1.2: *Scheme of the droplet fission cascade with charge and diameter values stated in literature [20]*

At a certain field strength, the electrostatic force equals the surface tension and a perfect cone at the tip of the capillary referred to as Taylor-cone[20], is formed. Further increase of the applied voltage leads to the release of small and uniform droplets. According to the solvent evaporation the diameter of these primary droplets decreases, till the repulsive Coulomb force equals the surface tension, referred to as the Rayleigh-limit. Further solvent evaporation leads to Coulomb fission [21], forming a set of smaller offspring droplets. After several solvent evaporation and Coulomb fission cycles very small droplets containing a low number of analyte molecules are formed. Two different models for the final process leading to the generation of gas-phase ions are stated in literature, namely the charge residue model (CRM) and the ion evaporation model (IEM). The CRM proposed by Dole [22] and Röllgen [23] states that solvent evaporations and Coulomb fissions proceed until the analyte molecule remains and takes up the excess charges of the host droplet which holds true for large and polar molecules. The main focus of the IEM proposed by Iribarne and Thomson [24] is that the field on the surface of very small highly charged droplets becomes strong enough to enable the analyte molecules to overcome to solvation forces and escape

the droplet. This model is valid mainly for small molecules and singly charged ions. In case of the "so-called" con jet mode primary droplets of uniform size (already in the nanometer size range) are generated in the form of pearls on a linear string. This mode is used for the subsequent charge reduction process via the Polonium-210 source described below.

Nano electrospray and neutralizer unit

The sample solution is infused via a nano electrospray (nES) device, typically sample concentrations in the range of a few mg/mL in 20 mM ammonium acetate buffer with the desired pH and flow rates from 50 to 100 nL/min are applied. The nES unit is operated in the cone-jet mode leading to the formation of very small and highly charged droplets. Subsequently the droplets are moving through the laminar air/CO_2 flow towards the neutralizing chamber, where a bipolar environment is generated by α-irradiation provided by a 5 µC ^{210}Po source. The presence of the high concentration of bipolar ions and cluster ions leads to predominantly neutral and positive as well as negative singly charged analyte molecular ions supported by continuous solvent evaporation. The charged particles pass from the neutralizer into the nDMA.

1.2.2 Size separation based on the electrophoretic mobility diameter

Definition of the particle electrical mobility

A particle carrying n elementary charges e (ion) encounters an electric field with field strength E, where the constant electrostatic force F_{el} drags this particle through the gas medium (equ. 4). As the particle accelerates, frictional force F_D caused by viscosity and inertia increases until a steady state is reached, where frictional and electrostatic force are equaled and the terminal velocity v_{TE} of the particle can be calculated (equ. 6) Due to the small dimensions of aerosol particles (large ions) the frictional force can be described by the Stoke´s law containing the Cunningham slip correction factor [25] (equ. 5); v, the velocity, η, the viscosity of the medium, D_P, the particle diameter and C_C, the Cunningham slip correction factor.

$$F_{el} = neE \qquad\qquad \text{equation 4}$$

$$F_D = \frac{3\pi\eta v D_P}{C_C} \qquad\qquad \text{equation 5}$$

$$neE = \frac{3\pi\eta v D_P}{C_C} \; ; \qquad v_{TE} = \frac{neEC_C}{3\pi\eta D_P} \qquad\qquad \text{equation 6}$$

The electrophoretic mobility Z is now a resulting parameter of a charged aerosol particle linked to equation 6, describing the particles terminal velocity due to the electrical field strength (equ. 7).

$$Z = \frac{v_{TE}}{E} = \frac{neC_C}{3\pi\eta D_P} \qquad\qquad \text{equation 7}$$

The electrical mobility of aerosol particles offers a way to characterize aerosols with electrical fields. Furthermore a connection between electrical mobility and the particle diameter is possible and therefore aerosol characterization according to size measurements is enabled.

The nano differential mobility analyzer (nDMA)

The applied nDMA (see Figure 2.1) contains two concentric metal cylinders, referred to as the central electrode and the housing cylinder. For size separation of the incoming charged aerosol particles (ions) a voltage and a laminar sheath gas flow is applied between these two cylinders. The aerosol inlet flow is introduced through a small circular slit, thus narrowing the starting region of the aerosol particles movement towards the central electrode. The aerosol particles encounter an electric field with increasing field strength towards the central electrode. According to their electrical mobility the aerosol particles follow an individual trajectory towards the central electrode, but only particles within a narrow range of electrical mobility are able to exit the nDMA via a small slit at the end of the central electrode. Contrary, aerosol particles with too low mobilities cannot pass the sheath gas in time and aerosol particles with too high mobilities collide with the central electrode before they reach the exit slit. By scanning the voltage applied between the two cylinders and therefore changing the mobility required for the aerosol particles to pass the exit slit, a mobility spectrum of the charged aerosol particles can be achieved.

1.2.3 Particle detection

The condensation particle counter detector (CPC)

A commonly used approach for determination of the charged particle (large ion) concentration leaving the nDMA is the condensation particle counter. First, the entering

aerosol flow is saturated with butanol vapor and secondly, the aerosol flow is cooled resulting in a supersaturation of the butanol vapor, which subsequently begins to condensate on the charged particles in the aerosol flow. Every particle/ion forms a small butanol droplet, which is detected by scattering the light, which is emitted by a laser diode. The vapor-supersaturations applied by commonly used butanol-based CPCs (e.g. TSI Mod. 3025) are high enough to activate droplet formation of particles with a diameter of 3 nm or higher.

1.2.4 Optimizing sample preparation for GEMMA analysis

To obtain a stable nES cone-jet mode a 20 mM ammonium acetate solution adjusted to the desired pH with ammonia or acetic acid should be used as buffer system for optimal conductivity [26]. High amounts of salts and detergents interfering with the nES process have to be removed prior to application to the GEMMA. Due to the high sensitivity of the GEMMA analysis (low pico mole range) in some cases dilution of the sample yields a sufficient reduction of the unwanted contaminations (i.e. high enough purification/desalting efficiency). Nevertheless, application of commonly used desalting methods as size exclusion chromatography, membrane centrifugation, and dialysis is often necessary prior to GEMMA analysis. Due to the low sample amounts/volumes required for GEMMA measurement (in the nL range) miniaturized desalting approaches are recommended. Care has to be taken in the case of membrane-based desalting devices, such as membrane centrifugation or dialysis, because unspecific adsorption can result in sample loss and thus no useful GEMMA spectra from precious samples can be obtained.

References

[1]   Nier A.O., Mass spectrometer for isotope and gas analysis. Review of Scientific Instruments 1947; **18:** 398-411.

[2]   Munson B., Development of chemical ionization mass spectrometry. International Journal of Mass Spectrometry 2000; **200:** 243-251.

[3]   Reid N.W., Photoionization in mass spectrometry. International Journal of Mass Spectrometry 1971; **6:** 1-37.

[4]   Robertson A.J.B., Field ionization mass spectrometry. Journal of Physics 1974; **7:** 321-327.

[5]   Macfarlane R.D., 252Cf-plasma desorption mass spectrometry. I - A Historical perspective. Biological Mass Spectrometry 1993; **22:** 677-680.

[6]   Rinehardt K.L.J., Fast atom bombardment mass spectrometry. Science 1982; **218:** 254-260.

[7]   Gaskell S.J., Liquid secondary ion MS: an emerging technique. Trends in Pharmacological Sciences 1988; **9:** 119-120.

[8]   Karas M. and Hillenkamp F., Laser desorption ionization of proteins with molecular masses exceeding 10,000 daltons. Analytical Chemistry 1988; **60:** 2299-2301.

[9]   Smyth W.F., The use of electrospray mass spectrometry in the detection and determination of molecules of biological significance. Trends in Analytical Chemistry 1999; **18:** 335-346.

[10]   Bacher G., Szymanski W.W., Kaufman S.L., Zollner P., Blaas D. and Allmaier G., Charge-reduced nano electrospray ionization combined with differential mobility analysis of peptides, proteins, glycoproteins, noncovalent protein complexes and viruses. Journal of Mass Spectrometry 2001; **36:** 1038-1052.

[11]   Mouradian S., Skogen J.W., Dorman F.D., Zarrin F., Kaufman S.L. and Smith L.M., DNA analysis using an electrospray scanning mobility particle sizer. Analytical Chemistry 1997; **69:** 919-925.

[12]   Loo J.A., Berhane B., Kaddis C.S., Wooding K.M., Xie Y., Kaufman S.L. and Chernushevich I.V., Electrospray ionization mass spectrometry and ion mobility analysis of the 20S proteasome complex. Journal of the American Society for Mass Spectrometry 2005; **16:** 998-1008.

[13]   Ku B.K., De la Mora F.J., Saucy D.A. and Alexander J.N., Mass distribution measurement of water-insoluble polymers by charge-reduced electrospray mobility analysis. Analytical Chemistry 2004; **76:** 814-822.

[14]   Saucy D.A., Ude S., Lenggoro I.W. and De la Mora F.J., Mass analysis of water-soluble polymers by mobility measurement of charge-reduced ions generated by electrosprays. Analytical Chemistry 2004; **76:** 1045-1053.

[15]   Wick C.H. and McCubbin P.E., Characterization of purified MS2 bacteriophage by the physical counting methodology used in the integrated virus detection system (IVDS). Toxicology Methods 1999; **9:** 245-252.

[16]   Laschober C., Kaufman S.L., Reischl G., Allmaier G. and Szymanski W., Comparison between an unipolar corona charger and a polonium-based bipolar

neutralizer for the analysis of nanosized particles and biopolymers. Journal of Nanoscience and Nanotechnology 2006; **6:** 1474-1481.

[17]   Juraschek R., Pulsation phenomena during electrospray ionization. International Journal of Mass Spectrometry 1998; **177:** 1-15.

[18]   Cloupeau M. and Prunet-Foch B., Electrohydrodynamic spraying functioning modes: a critical review. Journal of Aerosol Science 1994; **25:** 1021-1036.

[19]   Fenn J.B., Mann M., Chin K.M. and Shek F.W., Electrospray ionization - principles and practice. Mass Spectrometry Reviews 1990; **9:** 37-70.

[20]   Taylor G., Disintegration of water drops in electric field. Proceedings of the Royal Society of London Series A 1964; **280:** 383-397.

[21]   Cole R.B., Some tenets pertaining to electrospray ionization mass spectrometry. Journal of Mass Spectrometry 2000; **35:** 763-772.

[22]   Dole M., Mack L.L., Hines R.L., Mobley R.C., Ferguson L.D. and Alice M.B., Molecular beams of macroions. Journal of chemical Physics 1968; **49:** 2240-2249.

[23]   Schmelzeisen-Redeker G., Bütfering L. and Röllgen F.W., Desolvation of ions and molecules in thermospray mass spectrometry. International Journal of Mass Spectrometry and Ion Processes 1989; **90:** 139-150.

[24]   Iribarne J.V. and A. T.B., On the evaporation of small ions from charged droplets. Journal of chemical Physics 1976; **64:** 2287-2294.

[25]   Cunningham E., On the velocity of steady fall of sperical particles through fluid medium. Proceedings of the Royal Society of London Series A 1910; **83:** 357-365.

[26]   Kaufman S.L., Analysis of biomolecules using electrospray and nanoparticle methods: the gas-phase electrophoretic mobility molecular analyzer (GEMMA). Journal of Aerosol Science 1998; **29:** 537-552.

2 Comparing standard and microwave assisted staining protocols for SDS-PAGE of glycoproteins followed by subsequent PMF with MALDI MS

Jasmin Hirschmann[1], Martina Marchetti-Deschmann[1*], Christian Reichel[2], Günter Allmaier[1]

[1] Institute of Chemical Technologies and Analytics, Vienna University of Technology, Vienna, Austria
[2] Austrian Research Centers GmbH - ARC, Seibersdorf, Austria

Abstract

The detection of glycoproteins on SDS-PAGE gels is a very challenging task as glycan moieties can inhibit the protein-dye interaction or protein-silver reaction and therefore slow down or even completely prevent the staining process. Additionally the applied staining procedure can influence the total number of detected peptides after *in-gel* digestion. Three in SDS-PAGE commonly used staining procedures (silver nitrate, CBB R250 and colloidal CBB G250) for glycoproteins and proteins were evaluated in terms of duration, sensitivity and obtainable sequence coverage after PMF. The staining procedures were performed with and without the assistance of microwave irradiation.

Microwave treatment resulted in comparable band intensities and sensitivities as obtained by the original staining protocols, but staining duration was significantly reduced, to 30 min for silver nitrate and to 1.5 h for CBB and cCBB staining method. PMF analysis by vacuum MALDI mass spectrometry was not affected by the microwave treatment. It was found that the total number of detected tryptic peptides has increased when applying microwave irradiation during the staining process.

Microwave supported silver-staining turned out to be the most time saving procedure (30 min), with the highest absolute sensitivity (50 ng) and highest sequence coverage (up to 76 %) in case of PMF.

Introduction

One aspect of proteomics is the profiling of proteins expressed in cells, tissues or organisms. For this purpose large-scale protein identification is performed, so changes in the expression pattern of proteins can be correlated with physiological changes in cells or organisms. After successful protein identification the next step is the characterisation of possible PTMs, as frequently biological activities arise from them. There are more than 100 different types of PTMs and the most common one is glycosylation [1]. Therefore the detection of glycoproteins and subsequent elucidation of the structures of glycan moieties is a main target in proteomics research. The heterogeneity of carbohydrate structures significantly increases the complexity of a glycoprotein and complicates the correlation of specific protein expression pattern with diseases [2-4].

For identifying glycoproteins most frequently 1-D and 2-D PAGE followed by tryptic *in-gel* digestion and subsequent analysis of the derived proteolytic peptides by MS and multistage mass spectrometry (MS^n, n = 2 − 6) is used. For visualisation of the gel separated glycoproteins many different staining procedures can be used, e.g. periodic acid-Schiff [5] and fluorescent dyes [6, 7], but also commonly used silver precipitation [8] and CBB [9]. Especially for glycoproteins this is a critical and further time-consuming step, because staining efficiency primarily depends on the protein structure. CBB dye molecules interact with the hydrophobic amino acid side chains whereas reduction of silver nitrate to elemental silver ions is performed near proteins amide bonds [10]. Carbohydrate moieties considerably inhibit the protein-dye interaction due to restricted access of the dye molecules to the protein cores and subsequently slow down the staining process significantly or decrease its sensitivity [11]. The second problem during protein identification/characterisation of glycoproteins is the high variation of the total number of resulting peptides after *in-gel* digestion and therefore the obtained sequence coverage for the intact protein. Dependent on the glycan content of the protein and the staining procedure the access for the enzyme to the proteolytically interesting peptide bonds is hindered.

In this work we try to solve the problem of long time-consumption of staining protocols, thereby focusing on the most common organic stain, namely CBB, and silver. Silver staining protocols [12] are far more sensitive than most organic dyes, but their gel to gel reproducibility is not always satisfying. Moreover some protocols are not compatible with PMF, due to the application of cross-linking agents like glutaraldehyde which fixes the protein in the gel matrix and makes the extraction of proteolytic peptides for further analysis impossible. So CBB staining is preferred in many situations [13], due to easy handling, high reproducibility and better compatibility to PMF. However the detection limit of CBB staining (10-40 ng) is a great draw back which in some cases can only be reached after incubation of the gels with the dye solution for 10 to 14 hours. In addition to conventional CBB staining a colloidal CBB (cCBB) staining procedure [14] was evaluated. This cCBB stain has a detection limit of 1 ng for standard BSA if the gel is again incubated for 10 to 14 hours in the staining solution. Since commercially available BSA is a non-glycosylated protein the determination of the detection limit for glycoproteins was of interest. All these protocols include time-consuming incubation steps to stain glycoproteins sufficiently. A possibility to shorten visualisation steps is the application of microwave irradiation during the staining process, widely used since the 1990s [15]. In 2002, Nesatyy et al [16] studied the effect of microwave treatment on a variety of common staining protocols used for proteins in gels and membranes. In their study they stated that the temperature increase associated with microwave irradiation results in an increase of diffusion rate of the applied solvents and dyes and therefore the incubation duration for each staining step can be shortened significantly. Supporting the staining process with microwave irradiation also favours peptide recovery after *in-gel* digestion and subsequently higher sequence coverage for identified proteins is gained. This can be explained once more by the increase of temperature. The higher temperature causes further denaturation of the protein embedded in the gel matrix, so more cleavages sites are exposed to the digesting enzyme. The additional expansion of the 3D gel matrix results in a higher number of peptides extracted after enzymatic digestion.

Another application of microwave support in proteomics is the proteolytic cleavage of proteins for mass spectrometric analysis [15, 17-21]. The enzymatic digestion protocol used in this study was not evaluated especially for glycoproteins.

So from the biological sample to the identification or even characterisation of glycoproteins many different steps are used and some of them are rather time-consuming.

Materials and methods

Chemicals

Acetone p.a., acetonitrile p.a. (ACN), acetic acid 96 %, ammonium sulphate, ethanol 96 % (EtOH), formaldehyde solution (min 35 %), methanol p.a (MeOH) and water p. a. (conductivity at 25 °C $\leq$ 1 µS/cm) were obtained from Merck (Darmstadt, Germany). CHCA, DTE (min 99.0 %), phosphoric acid 85 % (w/w) solution in water, potassium hexacyanoferrate(III) and silver nitrate were obtained from Sigma-Aldrich (Steinheim, Germany). Ammonium hydrogen carbonate, β-mercapthoethanol, CBB R250, CBB G250, iodoacetamide and sodium carbonate were obtained from Fluka (Buchs, Switzerland). NuPAGE lithium dodecyl sulphate (LDS) – sample buffer (4×) and NuPAGE MES-SDS electrophoresis buffer (20×) were obtained from Invitrogen (Paisley, UK). TFA and sodium thiosulphate pentahydrate were from Riedel de Haën (Seelze, Germany) and trypsin (modified sequencing grade) from Roche Diagnostics (Mannheim, Germany).

Instrumentation

SDS-PAGE was performed on a XCell Sure Lock^{TM} – Novex mini cell connected to a PowerEase 500 power supply (both from Invitrogen). Standard staining protocols were supported by shaking on a platform rotator PS 3D (Grant Bio, Cambridge, UK).

Microwave assisted staining and enzymatic digestion were performed in a household-microwave oven from TCM (Hamburg, Germany) allowing a maximum power of 850 W.

MALDI-RTOF mass spectra were acquired on an AXIMA TOF^2 and/or an AXIMA CFR$^+$ (both Shimadzu Biotech, Manchester, UK), each equipped with a nitrogen laser (λ = 337 nm). Both instruments were operated in the positive ion, reflectron mode using pulsed extraction. Each mass spectrum (representing one peptide mass fingerprint) was acquired by averaging 500 unselected and consecutive laser shots. No smoothing algorithm was used prior to data analysis.

Samples

Recombinant human erythropoietin (rhEPO, ERYPO$^{®}$) was obtained from Janssen-Cilag Pharma (Schaffhausen, Switzerland). One ready-to-use injection (400 µL) contained 4000 I.U. (33.6µg) erythropoietin alpha. Avidin from egg white, α1-acid glycoprotein from

bovine serum and fetuin from fetal calf serum were purchased from Sigma-Aldrich (Steinheim, Germany). Avidin was used at a concentration of 1 μg/μL in water, α1-acid glycoprotein in a solution of 4 μg/μL in water and fetuin in a concentration of 10 μg/μL in water. Human plasma-derived antithrombin III (AT III) and human plasma-derived coagulation factor IX (F IX) were obtained from Octapharma (Vienna, Austria). AT III was used at a concentration of 4 μg glycoprotein/μL and F IX at a concentration of 1 μg glycoprotein/μL.

SDS-PAGE

Different amounts of glycoprotein (1.5, 1.25, 1.00, 0.75, 0.50, 0.25, 0.10, 0.075, 0.050 and 0.010 μg) were prepared by diluting the stock solutions of rhEPO, avidin, α1-acid glycoprotein, fetuin, AT III and F IX with water. Each dilution was mixed in a ratio of 1:4 with 4× LDS sample buffer containing 10 % β-mercaptoethanol, heated at 99°C for 1 min, and cooled down to room temperature. To avoid volume effects during gel electrophoresis 16 μL of each solution were applied onto the gels. Electrophoresis was performed on 4-12 % Bis-Tris, 1 mm × 10 wells NuPage precast mini gels using MES as running buffer (both from Invitrogen). Constant voltage was set to 200 V, after 45 min the separation was stopped.

Staining

Silver staining

The silver staining used for these experiments was performed according to Shevchenko et al. [12] with slight modifications as described. Briefly, directly after electrophoretic separation the gels were fixed (45 % MeOH, 5 % acetic acid in water) for 30 min, then washed (50 % MeOH) for 20 min and subsequently washed in water overnight (14 – 16 h) to remove interfering contaminants. Then the gels were incubated in sensitizing solution (0.02 % sodium thiosulphate) for 1 min, followed by washing with water for 2 min, and subsequent incubation in a silver nitrate solution (0.1 % silver nitrate in water) for 20 min at 4 °C. After washing the gels with water for 2 min, they were put into the developing solution (2 % sodium carbonate, 0.04 % formaldehyde) till the protein bands became visible (10 – 15 min). To terminate the reaction, stopping solution (5 % acetic acid) was

added. All steps with exception of the silver nitrate incubating step were carried out at room temperature.

Step	Solution composition applied	Incubation.without microwave irradiation	Incubation with microwave irradiation (340 W)
Fixing	45 % MeOH 5 % acetic acid	20 min	2 min
Washing	50 % MeOH	10 min	1 min
Washing	100 mM $Na_2S_2O_3$ 30 mM $K_3[Fe(CN)_6]$	-	2 min
Washing	water	overnight (14 – 16 h)	12 min
Sensitizing	0.02 % $Na_2S_2O_3$	1 min	1 min
Washing	water	2 min	2 min
Incubating	0.1 % silver nitrate	20 min (4°C)	1 min
Washing	water	2 min	2 min
Developing	2 % Na_2CO_3 0.04 % formaldehyde	until bands are visible	3 min
Stopping	5 % acetic acid	10 min	1 min
Storing	1 % acetic acid	4°C	4°C
Total staining duration		**17 h 25 min**	**27 min**

Table 2.1: *Staining protocols for silver nitrate staining without and with microwave assistance.*

For microwave assisted staining the silver staining procedure was further modified. All solutions used for standard silver nitrate staining were the same, but incubation durations were shortened as all following steps were carried out in the microwave oven operated at 340 W. For equal distribution of the heat, the gels were removed after half of the irradiation time, mixed vigorously and put back into the microwave oven for the remaining

time. An additional washing step with a mixture of sodium thiosulphate and potassium hexacyanoferrate (1:1) was applied.Briefly, the gels were fixed for 2 min, washed 1 min with 50 % MeOH and incubated in a solution containing 100 mM sodium thiosulphate/30 mM potassium hexacyanoferrate (1:1, $^v/_v$) for 2 min. After washing the gels six times with water for 2 min they were put 1 min into the sensitizing solution and subsequently washed with water for 2 min. Then the gels were incubated for 1 min in the silver nitrate solution and washed with water for 2 min. Finally the gels were put into the developing solution for 2 - 3 min. The reaction was stopped by adding 5 % acetic acid for 1 min. For both procedures the gels were stained in plastic dishes using about 100 mL of each staining solution and finally stored in 1 % acetic acid and at 4 °C. Table 2.1 summarises both staining procedures.

Coomassie Brilliant Blue R250 staining

Step	Solution composition applied	Incubation without microwave irradiation	Incubation with microwave irradiation (170 W)
Fixing	45 % MeOH 5 % acetic acid	30 min	2 min
Staining	0.1 % CBB R 250 45 % MeOH 5 % acetic acid	overnight (14 – 16 h)	5 min MW 60 min RT
Destaining I	40 % MeOH 7 % acetic acid	30 min	5 min MW 20 min RT
Destaining II	5 % MeOH 7 % acetic acid	overnight (14 – 16 h)	-
Storing	water	4 °C	4 °C
Total staining duration		**33 h**	**1 h 32 min**

Table 2.2: *Staining protocols for Coomassie Brilliant Blue R250 staining without and with microwave assistance (MW, microwave; RT, room temperature).*

For CBB R250 staining the gels were fixed (45 % MeOH, 5 % acetic acid in water) for 30 min directly after separation and subsequently stained overnight (14 – 16 h, 0.1 % CBB R250 in 45 % MeOH, 5 % acetic acid in water). Destaining was performed using two solutions: destain solution I (40 % MeOH and 7 % acetic acid in water) for 30 min is used for removing most of the CBB, followed by destain solution II (5 % MeOH and 7 % acetic acid in water) for 14 – 16 h for clearing the background to obtain distinct protein bands. All steps were carried out at room temperature.

The CBB R250 protocol was modified when supporting the staining procedure with microwave irradiation. All solutions for CBB R250 staining were the same, but incubation durations of each step were shortened. All following steps were carried out in the microwave oven operated at 170 W. The gels were fixed for 2 min and subsequently incubated in the CBB R250 solution for 5 min. After removal of the gels from the microwave oven the gels remained in the hot staining solution for 1 hour without further microwave irradiation. For removal of the CBB R250 the gels were put into destain solution I for 5 min. For gaining a clearer background the gels remained in the hot destain solution for additional 20 min without further microwave irradiation. The use of destain solution II was no longer required. In Table 2.2 both protocols are summarised.

Colloidal Coomassie Brilliant Blue G250 staining

For cCBB G250 staining gels were fixed (30 % EtOH, 2 % phosphoric acid in water) for 30 min, washed (2 % phosphoric acid in water) for 20 min and stained (0.12 % CBB G250, 20 % EtOH, 10 % ammonium sulphate, 10 % phosphoric acid in water) overnight (14 – 16 h). Destaining was performed in water until the background was clear, which lasted overnight (14 – 16 h). If not otherwise noted all steps were carried out at room temperature.

Modifications were necessary when supporting the staining procedure with the microwave oven operated at 170 W. The solutions used for cCBB staining remained the same, but incubation duration of each step was reduced. The gels were incubated for 2 min in the fixing solution, 2 min in the washing solution and 5 min in the cCBB G250 solution. After that the gels remained in the hot staining solution for 1 hour without further microwave irradiation and were then destained in water for 5 min. For gaining a clearer background the gels were kept in the hot solution for additional 20 min without further microwave irradiation. Table 2.3 gives a summary of both protocols. Gels were stored in water and at 4 °C.

Step	Solution composition applied	Incubation without microwave irradiation	Incubation with microwave irradiation (170 W)
Fixing	30 % EtOH 2 % phosphoric acid	30 min	2 min
Washing	2 % phosphoric aacid	20 min	2 min
Staining	0.12 % CBB G250 20 % EtOH 10 % phosphoric acid 10 % ammonium sulphate	slightly heating before adding to the gel overnight (14 – 16 h)	5 min MW 60 min RT
Destaining	water	overnight (14 – 16 h)	5 min MW
Storing	water	4 °C	4 °C
Total staining duration		**32 h 50 min**	**1 h 34 min**

Table 2.3: *Staining protocols for colloidal Coomassie Brilliant Blue G250 staining without and with microwave assistance (MW, microwave; RT, room temperature).*

In-gel digestion

From each gel the band containing 750 ng of glycoprotein was excised and cut into small cubes. For removal of contaminants various washing steps were carried out, once with water, two times with ACN/water (1:1), once with 100 % ACN and finally once with ACN/50 mM NH_4HCO_3 pH 8.5 (1:1, v/v), then the gel pieces were dried in a vacuum centrifuge. All washing steps lasted for 15 min. Disulfide bridges were subsequently reduced with 100 mM DTE (15.4 mg/mL in 50 mM NH_4HCO_3 pH 8.5) for 45 min at 56 °C and alkylated with 55 mM iodoacetamide (10.2 mg/mL in 50 mM NH_4HCO_3 pH 8.5) for 30 min at room temperature in the dark. Another washing step with ACN/ 50 mM NH_4HCO_3 pH 8.5 (1:1) was performed and then approximately 10 µL (dependent on the volume of the gel pieces) of digestion solution containing 12.5 ng/µL trypsin were added. To save additionally time the *in-gel* digestion was also supported with microwave treatment [17-20]. The proteins were digested at 170 W for 10 min. Afterwards peptides were extracted from the gel pieces using ACN/NH_4HCO_3 (1:1), ACN/0.1 % TFA (1:1) and 100

% ACN respectively. The first two extraction steps were carried out two times each for 15 min and the extraction with 100 % ACN for 5 min. All extracts were pooled and dried in a vacuum centrifuge.

MALDI MS sample preparation

Prior to mass spectrometric analysis peptides were dissolved in water and desalted using C_{18} ZipTips (Millipore, Billerica, USA). In terms of better peptide clean-up a desalting procedure with a stepwise elution was carried out. The tips were activated with ACN/water (1:1, v/v) and equilibrated with water. After the binding of the sample, salts and detergents were removed by washing the tips five times with water. The first elution was carried out with ACN/water (3:97, v/v), second with ACN/water (15:85, v/v) and third with ACN/water (50:50, v/v). The three fractions were pooled adding up to a total volume of about 4.5 µL, which were directly used for MALDI mass spectrometry. 1 µL CHCA (6 mg/mL acetone) solution was applied on a stainless steel MALDI target (type DE1580ta, Shimadzu Biotech). After evaporation of the acetone at room temperature a thin homogenous layer of matrix crystals was obtained. On top of this layer 1 µL of the peptide mixture was applied and dried in a gentle stream of air.

Evaluation of protein sequences and glycopeptide analysis

For determination of sequence coverage, measured monoisotopic m/z values were searched against the NCBInr and the SWISS-PROT databases using Mascot (Matrix Science, London, UK, http://www.matrixscience.com) and ProteinProspector (University of California San Francisco Mass Spectrometry Facility, http://prospector.ucsf.edu/).

Results and Discussion

All samples investigated in this study are well known glycoproteins with defined glycosylation sites. EPO is a glycoprotein with 4 glycosylation sites (3 N-glycans, 1 O-glycan) giving an average molecular weight of about 30.4 kDa whereof 30 to 40 % result from the very heterogeneous glycan moieties [22, 23]. The unmodified protein has a molecular weight of 18.2 kDa. Avidin has a molecular weight of 14.3 kDa for the unmodified amino acid sequence and an average molecular weight of 16.0 kDa for the glycosylated form

whereof only one N-glycosylation site counts for 10 % of the molecular weight [24, 25]. The unmodified amino acid sequence of α1-acid glycoprotein sums up to a molecular weight of 21.3 kDa resulting in an average molecular weight of 40.8 kDa for the glycoprotein. 5 N-glycosylation sites constitute the major PTMs resulting in a glycosylation degree of approximately 45 % [26]. Fetuin has an average molecular weight of 48.4 kDa, 3 N-glycosylation sites and 4 O-glycosylation sites [27-29], counting for 26 % of the total molecular weight where 36.4 kDa are represented by the unmodified amino acid sequence. Antithrombin III (AT III) has 4 N-glycosylation sites contributing with a carbohydrate content of about 14 % to the average molecular weight of 58 kDa (49.0 kDa for the unmodified amino acid sequence) [30]. 2 O- and 4 N-glycosylation sites are described for coagulation factor IX (F IX) which furthermore contains a number of other PTMs, such as sulphation, phosphorylation and hydroxylation [31]. Its average molecular weight is about 55 kDa (46.5 kDa for the unmodified protein) and the glycosylation degree is 17 % [32]. The average molecular weights as well as the glycosylation degrees of the chosen glycoproteins cover a broad range from 16 to 58 kDa and 1 to 7 different glycosylation sites with glycosylation degrees ranging from 10 % to 45 %.
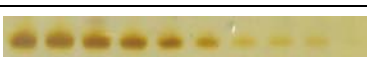
When supporting the staining process with microwave treatment, it is of great importance that the irradiation power can be regulated. For most microwave ovens the down regulation of the power is obtained by variation of the duration of the microwave pulses. These irradiation-free intervals between the maximum power applications are crucial for staining experiments or *in-gel* digestions as they prevent the overheating and therefore melting of the polyacrylamide gel as well as heat denaturation and therefore inactivation of proteolytic enzymes as trypsin. Microwave assisted silver staining was performed at 340 W whereas for CBB R250 and cCBB G250 the irradiation power had to be reduced to 170 W. This was necessary due to the longer incubation durations of the gels in the staining and destaining solutions. It is crucial to avoid boiling of the solutions otherwise the gel loses its smooth character and is more likely to rip in pieces.

For subsequent PMF analysis gel bands containing 750 ng protein were used. A high number of peptides should be received for better comparability of the differing staining procedures. For each staining procedure three PMF analyses were performed.

Recombinant human erythropoietin

<u>Staining duration and sensitivity</u>

Protein	Staining procedure	Total staining duration	Gel	Sensitivity	Sequence coverage
rh EPO	Silver nitrate + MW	27 min		0.050 µg	56.5 %
rh EPO	Silver nitrate – MW	17 h 25 min		0.050 µg	45.4 %
rh EPO	CBB R250 + MW	1 h 32 min		0.25 µg	40.4 %
rh EPO	CBB R250 – MW	33 h		0.25 µg	37.1 %
rh EPO	cCBB G250 + MW	1 h 34 min		0.050 µg	47.4 %
rh EPO	cCBB G250 – MW	32 h 50 min		0.050 µg	37.8 %
Fetuin	Silver nitrate + MW	27 min		0.050 µg	30.9 %
α1-acidic Glycoprotein	Silver nitrate + MW	27 min		0.050 µg	51.0 %
Avidin	Silver nitrate + MW	27 min		0.050 µg	75.9 %
AT III	Silver nitrate + MW	27 min		0.050 µg	49.0 %
F IX	Silver nitrate + MW	27 min		0.050 µg	39.7 %

1.50   1.00   0.50   0.10   0.050
1.25   0.75   0.25   0.075   0.010   } µg

Table 2.4: *Comparison of staining duration and detection limits of silver nitrate, CBB R250 and cCBB G250 staining procedures with (+) and without (-) microwave (MW) irradiation and sequence coverage after in-gel digestion for recombinant human erythropoietin alpha (rh EPO), fetuin, α1-acid glycoprotein, avidin, antithrombin III (AT III) and coagulation factor IX (F IX).*

A gel image related to the three evaluated staining procedures (silver nitrate, CBB R250, cCBB G250) with and without the assistance of microwave irradiation in terms of staining duration and sensitivity is given in Table 2.4. Standard silver nitrate staining resulted in a clear background and protein bands coloured from brown to yellow, a characteristic colouring for glycoproteins. Protein amounts from 1.5 µg (broad brownish band) to 50 ng (narrow yellowish band) could be clearly detected. When supporting the silver nitrate staining with microwave irradiation an additional washing step with a mixture of sodium

43

thiosulphate and potassium hexacyanoferrate (1:1) was applied, commonly used for destaining of silver stained protein spots prior to *in-gel* digestion. In the microwave supported silver staining protocol this mixture replaces the overnight washing step with water performed in the standard procedure. Potassium hexacyanoferrate forms complexes with the contaminants, which are removed during the subsequent washing with water, resulting in a clearer gel background. Even though this additional washing step was applied the gel exhibited no longer a background as clear as with standard silver staining, but was yellowish with brown to orange protein bands. This staining resulted in a lower contrast for the protein bands but nevertheless the same sensitivity range could be obtained, from 1.5 μg (broad brownish band) to 50 ng (narrow orange band). The shortening of the washing step time with water from an overnight procedure to only 15 min by microwave assistance brings a reduction of a total staining duration from 17.5 h to 0.5 h. In terms of absolute staining sensitivity no differences between the standard procedure and the microwave assisted one were observed, in both cases a detection limit of 50 ng for rhEPO was achieved.

Standard CBB R250 staining led to a slightly bluish coloured gel background with distinct protein bands. Due to the long incubation duration with the CBB staining solution, which took 14 – 16 h and resulted in a dark blue gel, a complete destaining of the background was not possible anymore. Therefore the destaining procedure was stopped after 14 – 16 h regardless of a complete destaining of the background. Protein bands from 1.5 μg (distinct bluish band) to 0.25 μg (faint bluish band) could be detected. Supporting the staining procedure with microwave irradiation resulted in an almost transparent gel background after destaining. This advantageous effect can be explained by a temperature increase during microwave treatment causing an increase in diffusion rate for the dye molecules and hence a better destaining efficiency. This efficient background destaining led to more distinct protein bands, which are detectable from 1.5 μg (distinct) to 0.25 μg (faint). Furthermore it has to be mentioned that the protein band at 0.25 μg is easier to detect (better contrast) than in the CBB R250 staining without microwave assistance. The increase in diffusion rate also reduced the duration of the staining and made the second destaining step redundant, which were both performed overnight in the conventional staining. So a reduction of staining duration from 33 h to 1.5 h was obtained. Compared to silver the CBB R250 staining is less sensitive in terms of detection limits. This is also the explanation for the smaller bands observed at higher concentrations after CBB R250 compared to silver staining. Microheterogeneities of glycan moieties, like triantennary

structures compared to diantennary structures or O-glycans attached to a protein result in differences in the molecular weight (about 700-1000 Da) which are already observable by SDS-PAGE. These mass differences are detected but not resolved by gel electrophoresis and can therefore result in broader gel bands as it is observed for rhEPO in Table 2.4. Some of these heterogeneities are present at much lower concentration levels which are furthermore no longer detectable with the less sensitive CBB R250 staining. Therefore the observed protein bands appear narrower in that case and the protein seems to be better focused. Taking a closer look at the detected protein band at 1.5 µg this can already be observed comparing CBB R250 without microwave assistance to CCB R250 with microwave assistance. The latter already exhibits a broader gel band by detecting more glycan microheterogeneities, but it is not as broad as the even more sensitively silver stained analogue.

Standard cCBB G250 staining procedure resulted in an almost transparent background. In contrast to non-colloidal CBB R250 staining, which saturated the gel with dye giving a very intensive staining; the cCBB G250 staining gave a less intensive colouring, which can be removed more easily at room temperature. Distinct protein bands in a brighter blue than obtained with CBB R250 were observed and protein amounts from 1.5 µg to 50 ng were detectable although the gel bands containing 100 ng – 50 ng were hardly visible. When supporting the cCBB G250 staining procedure with microwave irradiation the resulting gel obtained an even clearer background than obtained with the standard procedure. Once more temperature increase during microwave treatment seemed to increase the diffusion rate for a much more effective destaining. Protein bands from 1.5 µg (distinct) to 50 ng (faint) were detectable. By supporting the cCBB G250 staining with microwave irradiation almost the same reduction of staining duration was obtained as it was for the CBB R250 protocol, from 33 h to 1.5 h. The staining as well as the destaining steps could be reduced from overnight incubations to only 1 h.

Using cCBB G250 protocols detection limits comparable to silver nitrate staining can be achieved for non-glycosylated proteins like BSA (1 ng) [14]. These observations could be confirmed for glycosylated proteins. Staining sensitivity for the cCBB G250 protocol was 50 ng independent from microwave treatment. Although the detection limit of cCBB G250 was comparable to silver staining the gel bands were narrower leading to the conclusion that still not all microheterogeneities of glycan moieties could be observed.

In total, the various staining procedures supported by microwave treatment led to significant time savings in all cases – 17 h for the silver nitrate procedure and 31.5 h for

both CBB staining procedures. When comparing the staining procedures for rhEPO it became obvious that the glycoprotein bands after silver nitrate staining were broader and more distinct than they were after CBB staining. So, when using the silver nitrate protocol the total amount of detected protein per gel band was higher and as a consequence a higher amount of protein can be excised for subsequent *in-gel* digestion. No increase in sensitivity was observed for the three staining methods, for silver nitrate and cCBB G250 staining, 50 ng and for CBB R250 0.25 µg protein could be detected with and without microwave treatment.

Peptide recovery and sequence coverage

The staining protocols used in this study were performed with respect to subsequent *in-gel* digestion. Therefore no cross-linking agents for fixing the proteins in the gel matrix to prevent diffusion were used. Gel bands containing 750 ng protein were used for proteolytic digestion and subsequent PMF.

Figure 2.1: *PMF (positive ion MALDI-RTOF mass spectra) of rhEPO after visualization with silver staining protocols with (bottom) and without (top) microwave assistance. Tryptic peptides are indicated with *, all unassigned peaks are background peaks, e.g. tryptic autolysis peptides. (SC, Sequence coverage)*

Figure 2.1 shows the PMF obtained by means of MALDI MS of standard and microwave assisted silver nitrate stained gel bands. Signal-to-noise ratios (S/N) above 10 were

obtained and a number of background peaks, like tryptic autolysis peptides or contaminations from the gel, were observed. Sixteen rhEPO peptides were observed for standard silver staining resulting in a sequence coverage of 45.4 %. For the microwave assisted protocol 18 rhEPO peptides were detected, which led to a higher sequence coverage of 56.5 %. Two additional peptides, m/z 1465 and 2034, were observed. M/z 2034 contributed mainly to the increase in sequence coverage, because it represented a peptide resulting from a missed cleavage and therefore includes m/z 1465, see amino acid positions in Table 2.5.
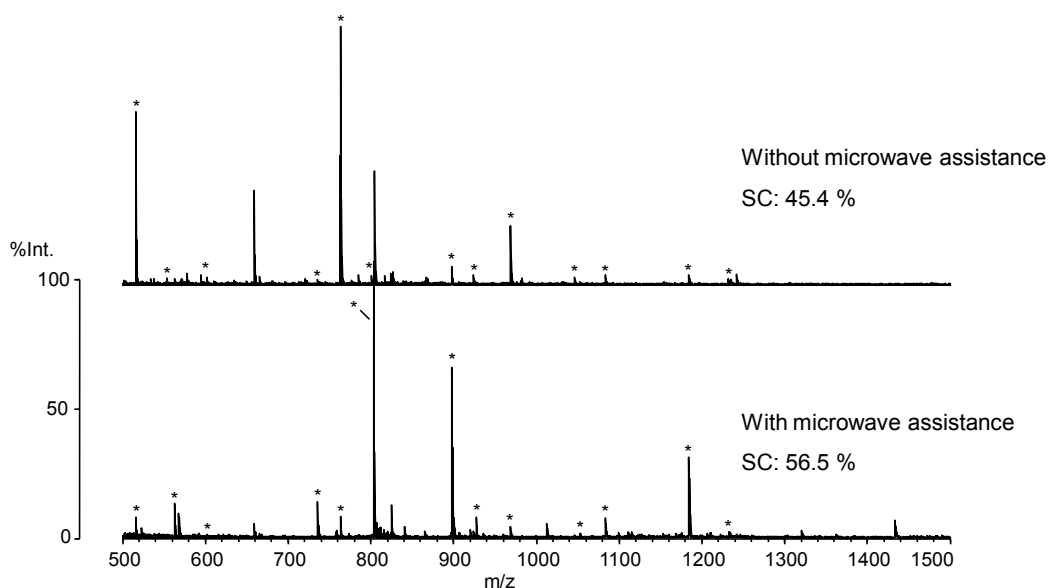

Figure 2.2: *PMF (positive ion MALDI-RTOF mass spectra) of rhEPO after visualization with CBB R250 staining protocols with (bottom) and without (top) microwave assistance. Tryptic peptides are indicated with *, all unassigned peak are background peaks, e.g. tryptic autolysis peptides. (SC, Sequence coverage)*

Mass spectra obtained from PMF analysis after CBB R250 staining are shown in Figure 2.2. Satisfying peak intensities and S/N above 10 were observed, but also an increase in background ions coming from electrophoretic contaminants was noticed, especially in the microwave assisted staining procedure. Despite these peak intensities are low, the effect on database search is tremendous by giving much lower scoring results for protein identification if these unwanted peaks are combined with the correct tryptic peptides, which would indeed be the fact if an unknown protein is investigated. For CBB R250

without microwave assistance in total a lower number of peptides was detected and as a consequence sequence coverage decreased. Microwave assisted staining resulted in 13 rhEPO peptides and 40.4 % sequence coverage and standard CBB R250 staining in 12 rhEPO peptides and 37.1 % sequence coverage. Comparing the observed peptides for the CBB R250 procedures one can see that m/z 602 is only present in mass spectra of microwave treated gels giving a slightly better result for the microwave supported staining protocol.
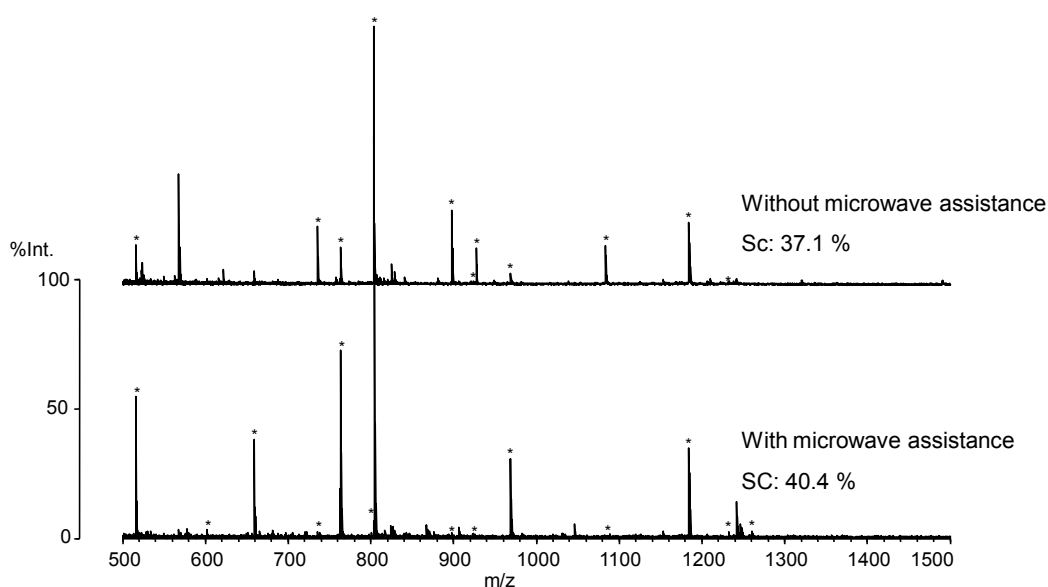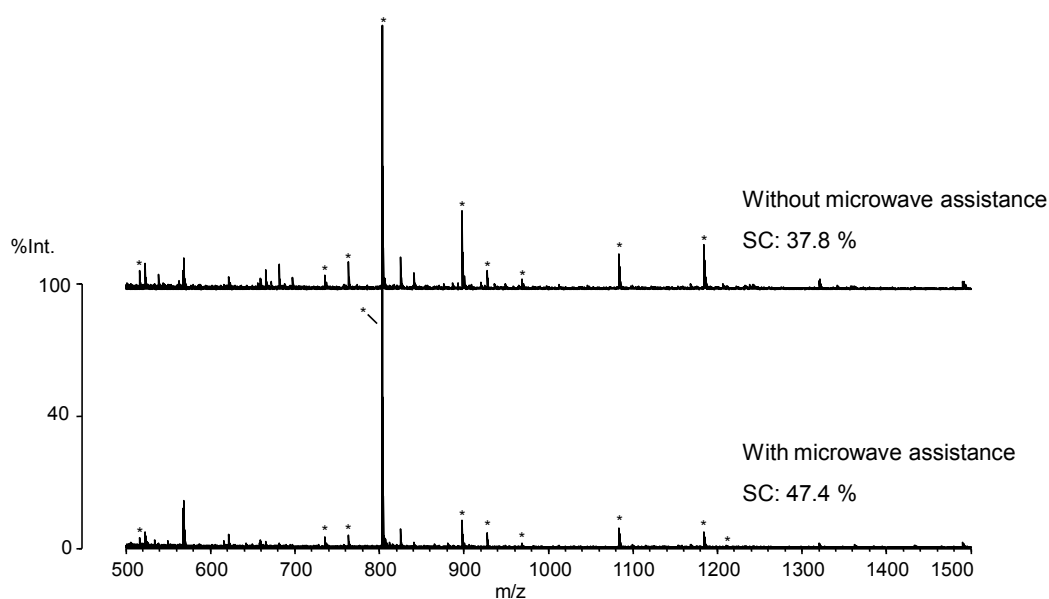

Figure 2.3: *PMF (positive ion MALDI-RTOF mass spectra) of rhEPO after visualization with cCBB G250 staining protocols with (bottom) and without (top) microwave assistance. Tryptic peptides are indicated with *, all unassigned peak are background peaks, e.g. tryptic autolysis peptides. (SC, Sequence coverage)*

Figure 2.3 shows the MALDI mass spectra obtained after cCBB G250 protocols. Comparable peak intensities and number of background peaks to CBB R250 staining could be observed. PMF after microwave assisted staining yielded 15 rhEPO peptides, resulting in a sequence coverage of 47.4 %, whereas the mass spectra of standard staining procedure showed 13 rhEPO peptides and a sequence coverage of 37.8 %. Microwave treatment resulted in two additional peaks, m/z 602 and 1210, both contributing to the higher sequence coverage.

48

Calculated m/z	MC	Position	Modification	Ag +MW	Ag –MW	Found m/z CBB R250 +MW	CBB R250 –MW	cCBB G250 +MW	cCBB G250 +MW
516.13	0	38-41		516.37	516.31	516.28	516.28	516.19	516.35
563.37	1	167-170		563.45	563.42	-	-	-	-
602.36	0	125-130		602.48	602.30	602.46	-	602.21	-
736.42	0	42-47		736.56	736.39	736.47	736.40	736.22	736.43
763.38	0	32-37	Cys-CAM: 34	763.53	763.50	763.36	763.37	763.12	763.44
803.50	0	131-137		803.66	803.58	803.49	803.44	803.21	803.45
898.48	0	171-177		898.67	898.61	898.47	898.51	898.19	898.54
924.48	0	159-166		924.62	924.57	924.37	924.41	924.16	924.71
927.47	0	73-79		927.68	927.59	927.49	927.40	927.18	927.47
969.45	0	182-189	Cys-CAM: 188	969.73	969.59	969.45	969.42	969.14	969.48

Table 2.5: *List of tryptic peptides detected after PMF (CAM, carbamidomethylation; MC, missed cleavage; MW, microwave). All m/z values are monoisotopic.*

Calculated m/z	MC	Position	Modification	Found m/z					
				Ag + MW	Ag − MW	CBB R250 + MW	CBB R250 − MW	cCBB G250 + MW	cCBB G250 + MW
1052.57	1	159-167		1052.67	1052.54	-	-	1052.23	1052.53
1083.59	1	171-179							
1083.57	1	73-80		1083.81	1083.75	1083.61	1083.35	1083.13	1083.53
1184.62	1	28-37	Cys-CAM:34	1184.85	1184.75	1184.63	1184.60	1184.24	1184.59
1210.62	1	180-189	Cys-CAM:188	1210.80	1210.92	-	-	1210.79	-
1233.72	1	38-47		1233.81	1233.51	1233.70	1233.52	1233.90	1233.56
1260.67	1	32-41	Cys-CAM:34	1260.84	1260.43	1260.53	1260.49	1260.31	1260.52
1465.76	0	144-158		1465.81	-	-	-	-	-
2034.10	1	138-158		2034.24	-	-	-	-	-

Table 2.5 continued: *List of tryptic peptides detected after PMF (CAM, carbamidomethylation; MC, missed cleavage; MW, microwave). All m/z values are monoisotopic.*

The performance of microwave assisted staining procedures led in all cases to a higher number of obtained peptides after *in-gel* digestion and finally to higher sequence coverages for rhEPO. Interestingly more intensive background ions after CBB R250 and cCBB G250 staining were detected compared to silver staining, which resulted in less significant protein scores after database search, a problem that might arise in case of unknown glycoprotein samples.

Avidin, α1-acid glycoprotein, and fetuin (standard glycoproteins)
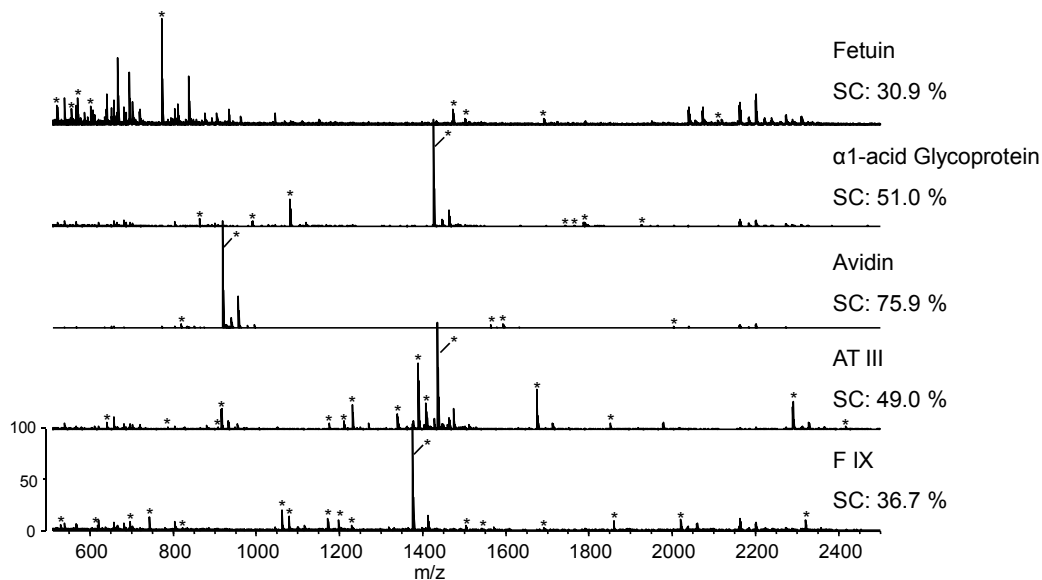
Figure 2.4: *PMF (positive ion MALDI-RTOF mass spectra) of avidin, α1- acid glycoprotein, fetuin, AT III and F IX after visualization with silver staining protocols supported by microwave treatment. Tryptic peptides are indicated with *, all unassigned peak are background peaks, e.g. tryptic autolysis peptides. (SC, Sequence coverage)*

To prove the general applicability of the microwave supported silver nitrate staining procedure, evaluated with rhEPO in terms of time consumption and sequence coverage, it was applied to three well-known glycoproteins, namely avidin, α1-acid glycoprotein and fetuin. For these three mentioned glycoproteins microwave assisted silver nitrate staining resulted in a slightly yellow background of the polyacrylamide gels with yellow to brown

protein bands, which are again characteristic for silver staining of glycoproteins. The reduced degree of glycosylation of these three proteins in comparison to rhEPO was also observed by band shapes which were less broad than the corresponding bands of rhEPO after silver staining. But as observed for rhEPO protein amounts from 1.5 µg (brown) to 50 ng (yellowish) were detected for all three proteins, see Table 2.4. Figure 2.4 compares the PMF of the three glycoproteins. PMF analysis of avidin obtained S/N above 10 containing only few peaks from unwanted background ions in the lower m/z range (m/z < 900) of the mass spectrum. Seven peptides could be detected, which led to a sequence coverage of 75.9 %. This remarkable high sequence coverage can be explained by the low glycosylation degree of about 10 %, represented by only one single N-glycosylation site. Therefore nearly unrestricted access to the enzyme's cleavage sites, arginine and lysine, was given.

Even though more background ions were obtained in the mass spectrum of α1-acid glycoprotein digest, S/N above 20 for the 11 observed peptides was achieved, yielding a sequence coverage of 51.0 %.

For fetuin an unusually high number of background ions in the MALDI mass spectrum especially in the lower m/z range (m/z < 900) was determined. Nevertheless 12 peptides were detected, resulting in a sequence coverage of 30.9 %, a relatively low value compared to avidin and α1-acid glycoprotein. Despite a glycosylation degree of 26 %, a value between α1-acid glycoprotein (45 %) and avidin (10 %), the lowest sequence coverage was obtained. Taking a closer look at the amino acid sequence and the glycosylation sites of fetuin it becomes obvious that the 3 N-glycosylation sites are very close to tryptic cleavage sites. So due to the glycan structures the access to these cleavage sites is blocked and less peptides are generated.

Human antithrombin III and human coagulation factor IX

Finally the microwave supported silver nitrate staining was tested for two plasma-derived blood coagulation glycoproteins, AT III and F IX, to further confirm and evaluate the findings (Table 2.4). Separation of AT III led to a gel with an almost clear background and distinct glycoprotein bands from 1.5 µg (brown) down to 50 ng (brown) which also were quite broad as it was expected for this serum glycoprotein. Even though the gel background after separation of F IX was still a little bit coloured (yellowish) the same limit of detection could be reached, 50 ng. However the background staining made the gel bands

containing lower glycoprotein amounts (in the range 100 to 50 ng) hardly distinguishable, which can in some cases lead to problems during excising these gel bands properly for subsequent tryptic digestion.

In both MALDI mass spectra (Figure 2.4) a high number of unwanted background ions were obtained, but S/N ratios above 10 made the detection of 20 peptides for each glycoprotein possible. This resulted in sequence coverages of 49.0 % for AT III and of 39.7 % for F IX. The slightly reduced sequence coverage for F IX can be explained by its complex mixture of different posttranslational modifications, such as sulphation, phosphorylation and hydroxylation.

Conclusion

Goal of this work was to find a fast and sensitive staining procedure for glycoproteins separated by SDS-PAGE in connection with PMF as well as high sequence coverages. Glycoproteins differing in molecular weight (16 – 48 kDa), number of glycosylated sites (1 – 7), modified by N- as well as O-glycosylation sites and glycosylation degrees between 10 % and 45 % were chosen to cover a wide range of different structural features to prove the unrestricted applicability of this method. Microwave assisted silver nitrate staining turned out to be the most efficient method for characterising glycoproteins. Sensitivity was comparable to conventional MS compatible silver staining (limit of detection for glycoproteins 50 ng). Nevertheless the microwave assisted protocol is much faster (30 min) and led to sequence coverages of about 30 to 75 % for all investigated glycoproteins (750 ng per *in-gel* digest) which is usually sufficient for starting an identification process. The most favourable effect of the application of microwave irradiation for gel staining and *in-gel* digestion is the speed of the protocol allowing the separation, visualisation, *in-gel* digestion and MALDI MS analysis of protein samples within one day.

Acknowledgements

References

[1]   Morelle W., Canis K., Chirat F., Faid V. and Michalski J.C., The use of mass spectrometry for the proteomic analysis of glycosylation. Proteomics 2006; **6:** 3993-4015.

[2]   Helenius A. and Aebi M., Intracellular functions of N-linked glycans. Science 2001; **291:** 2364-2369.

[3]   Rudd P.M., Elliott T., Cresswell P., Wilson I.A. and Dwek R.A., Glycosylation and the immune system. Science 2001; **291:** 2370-2376.

[4]   Varki A., Biological roles of oligosaccharides: all of the theories are correct. Glycobiology 1993; **3:** 97-130.

[5]   Zacharius R.M., Zell T.E., Morrison J.H. and Woodlock J.J., Glycoprotein staining following electrophoresis on acrylamide gels. Analytical Biochemistry 1969; **30:** 148-152.

[6]   Steinberg T.H., Pretty On Top K., Berggren K.N., Kemper C., Jones L., Diwu Z., Haugland R.P. and Patton W.F., Rapid and simple single nanogram detection of glycoproteins in polyacrylamide gels and on electroblots. Proteomics 2001; **1:** 841-855.

[7]   Hokke C.H., Bergwerff A.A., Van Dedem G.W., Kamerling J.P. and Vliegenthart J.F., Structural analysis of the sialylated N- and O-linked carbohydrate chains of recombinant human erythropoietin expressed in Chinese hamster ovary cells. Sialylation patterns and branch location of dimeric N-acetyllactosamine units. European Journal of Biochemistry / FEBS 1995; **228:** 981-1008.

[8]   Merril C.R., Dunau M.L. and Goldman D., A rapid sensitive silver stain for polypeptides in polyacrylamide gels. Analytical Biochemistry 1981; **110:** 201-207.

[9]   Groth S.F.d.S., Webster R.G. and Datyner A., Two new staining procedures for quantitative estimation of proteins on electrophoresis strips. Biochimica et Biophysica Acta 1963; **71:** 377-391.

[10]   Rabilloud T., Proteome research:Two dimensional gel electrophoresis and identification methods. Berlin, Heidelberg, New York: Springer Verlag; 2000.

[11]   Osset M., Pinol M., Fallon M.J., de Llorens R. and Cuchillo C.M., Interference of the carbohydrate moiety in coomassie brilliant blue R-250 protein staining. Electrophoresis 1989; **10:** 271-273.

[12]　Shevchenko A., Wilm M., Vorm O. and Mann M., Mass spectrometric sequencing of proteins silver-stained polyacrylamide gels. Analytical Chemistry 1996; **68:** 850-858.

[13]　Neuhoff V., Arold N., Taube D. and Ehrhardt W., Improved staining of proteins in polyacrylamide gels including isoelectric focusing gels with clear background at nanogram sensitivity using Coomassie Brilliant Blue G-250 and R-250. Electrophoresis 1988; **9:** 255-262.

[14]　Candiano G., Bruschi M., Musante L., Santucci L., Ghiggeri G.M., Carnemolla B., Orecchia P., Zardi L. and Righetti P.G., Blue silver: a very sensitive colloidal Coomassie G-250 staining for proteome analysis. Electrophoresis 2004; **25:** 1327-1333.

[15]　Lill J.R., Ingle E.S., Liu P.S., Pham V. and Sandoval W.N., Microwave-assisted proteomics. Mass Spectrometry Reviews 2007; **26:** 657-671.

[16]　Nesatyy V.J., Dacanay A., Kelly J.F. and Ross N.W., Microwave-assisted protein staining: mass spectrometry compatible methods for rapid protein visualisation. Rapid Communication in Mass Spectrometry 2002; **16:** 272-280.

[17]　Sun W., Gao S., Wang L., Chen Y., Wu S., Wang X., Zheng D. and Gao Y., Microwave-assisted protein preparation and enzymatic digestion in proteomics. Molecular and Cellular Proteomics 2006; **5:** 769-776.

[18]　Pramanik B.N., Mirza U.A., Ing Y.H., Liu Y.H., Bartner P.L., Weber P.C. and Bose A.K., Microwave-enhanced enzyme reaction for protein mapping by mass spectrometry: a new approach to protein digestion in minutes. Protein Science 2002; **11:** 2676-2687.

[19]　Juan H.F., Chang S.C., Huang H.C. and Chen S.T., A new application of microwave technology to proteomics. Proteomics 2005; **5:** 840-842.

[20]　Lin S., Yun D., Qi D., Deng C., Li Y. and Zhang X., Novel microwave-assisted digestion by trypsin-immobilized magnetic nanoparticles for proteomic analysis. Journal of Proteome Research 2008; **7:** 1297-1307.

[21]　Swatkoski S., Gutierrez P., Wynne C., Petrov A., Dinman J.D., Edwards N. and Fenselau C., Evaluation of microwave-accelerated residue-specific acid cleavage for proteomic applications. Journal of Proteome Research 2008; **7:** 579-586.

[22]　Sasaki H., Bothner B., Dell A. and Fukuda M., Carbohydrate structure of erythropoietin expressed in Chinese hamster ovary cells by a human erythropoietin cDNA. Journal of Biological Chemistry 1987; **262:** 12059-12076.

[23]   Stubiger G., Marchetti M., Nagano M., Grimm R., Gmeiner G., Reichel C. and Allmaier G., Characterization of N- and O-glycopeptides of recombinant human erythropoietins as potential biomarkers for doping analysis by means of microscale sample purification combined with MALDI-TOF and quadrupole IT/RTOF mass spectrometry. Journal of Separation Science 2005; **28:** 1764-1778.

[24]   DeLange R.J. and Huang T.S., Egg white avidin. 3. Sequence of the 78-residue middle cyanogen bromide peptide. Complete amino acid sequence of the protein subunit. Journal of Biological Chemistry 1971; **246:** 698-709.

[25]   Bruch R.C. and White H.B., 3rd, Compositional and structural heterogeneity of avidin glycopeptides. Biochemistry 1982; **21:** 5334-5341.

[26]   http://www.expasy.org/uniprot/Q3SZR3, March 2008.

[27]   Christie D.L., Dziegielewska K.M., Hill R.M. and Saunders N.R., Fetuin: the bovine homologue of human alpha 2HS glycoprotein. FEBS Letters 1987; **214:** 45-49.

[28]   Pisano A., Jardine D.R., Packer N.H., Farnsworth V., Carson W., Cartier W., Redmond J.W., William K.L. and Gooley A.A., Identifying sites of glycosylation in proteins. In: Techniques in glycobiology. Townsend R.R. and Hotchkiss A.T.J. (Ed.), New York: Marcel Dekker; 1996.

[29]   Hagglund P., Bunkenborg J., Elortza F., Jensen O.N. and Roepstorff P., A new strategy for identification of N-glycosylated proteins and unambiguous assignment of their glycosylation sites using HILIC enrichment and partial deglycosylation. Journal of Proteome Research 2004; **3:** 556-566.

[30]   Kleinova M., Buchacher A., Heger A., Pock K., Rizzi A. and Allmaier G., Exact molecular mass determination of various forms of native and de-N-glycosylated human plasma-derived antithrombin by means of electrospray ionization ion trap mass spectrometry. Journal of Mass Spectrometry 2004; **39:** 1429-1436.

[31]   Arruda V.R., Hagstrom J.N., Deitch J., Heiman-Patterson T., Camire R.M., Chu K., Fields P.A., Herzog R.W., Couto L.B., Larson P.J. and High K.A., Posttranslational modifications of recombinant myotube-synthesized human factor IX. Blood 2001; **97:** 130-138.

[32]   http://www.expasy.org/uniprot/P00740, March 2008.

3 Evaluation of MALDI preparation techniques for surface characterization of intact *Fusarium* spores by MALDI linear time-of-flight mass spectrometry

Jasmin Hirschmann[1], Martina Marchetti-Deschmann[1], Robert Mach[2], Christian Peter Kubicek[2], Günter Allmaier[1]

[1] Institute of Chemical Technologies and Analytics, Vienna University of Technology, Vienna, Austria

[2] Institute of Chemical Engineering, Vienna University of Technology, Vienna, Austria

Abstract

Classification of mycotoxin producing fungal species is of great relevance in agriculture and food producing industry as well as in the medical field. Recently species specific surface protein profiles of intact fungal spores, such as *Penicillium, Aspergillus and Trichoderma*, were studied with MALDI-TOF MS, thus providing a rapid and straight forward analysis procedure for species identification and characterization. This study focuses on mycotoxin producing *Fusarium* strains common in Austria. To obtain a suitable MALDI matrix system and sample preparation method, thin layer, dried droplet and sandwich method and several commonly used MALDI matrices, CHCA, DHB, FA, SA, THAP dissolved in various solvent mixtures (organic solvents as ACN, MeOH, EtOH and iPrOH and for the aqueous phase water and 0.1 % TFA) were evaluated in terms of mass spectra reproducibility, peak number and peak intensities.

Most significant protein profiles were obtained with a 10 mg FA in 1 mL ACN/0.1 % TFA (7:3, v/v) used as matrix system. Mixing the spores with the matrix solution directly onto the MALDI target (referred to as dried droplet technique) results in an evenly distributed spores/matrix crystal layer, yielding highly reproducible protein profiles from the spores surfaces. Numerous intensive peaks throughout the whole investigated m/z range could be

detected. Differences in the obtained mass spectra (peak number and intensities) allowed the differentiation of various *Fusarium* species. Thus for further investigations on intact *Fusarium* spores this matrix mixture applied with dried droplet technique will be utilized.

Introduction

Classification and identification of whole micro-organisms based on the registration of unique and representative biomarker ions generated by mass spectrometric approaches dates back to the early 1970s[1-3]. First attempts at characterizing micro-organisms by means of mass spectrometric fingerprinting were made by Anhalt and coworkers[4]. They applied pyrolysis mass spectrometry for generating mass spectra of several bacterial species which could be differentiated with respect to the presence of characteristic phospholipids, ubiquinones and menaquinones. Nevertheless, differentiation of bacteria strains belonging to the same species was not possible. Only a limited number of substances could be detected as strong fragmentation during the ionization process (electron impact ionization was used) led to a considerable loss of information on the chemical composition and also the accessible mass range (a quadrupole mass analyzer was used) made the detection of indicative high mass ions impossible. Throughout the 1980s new desorption/ionization techniques were implemented, plasma desorption, laser desorption ionization and fast atom bombardment or liquid secondary ion mass spectrometry, which were then successfully applied to characterize intact micro-organisms[5, 6]. Although less fragmentation was observed using these so-called "soft" ionization techniques the desorption and ionization of larger analytes was still limited. The development of even "softer" ionization techniques as electrospray ionization mass spectrometry (ESI MS)[7-11] and vacuum matrix-assisted laser desorption/ionization mass spectrometry (MALDI MS)[12-14] enabled the desorption and ionization of small as well as large molecular mass compounds from intact micro-organisms. Due to the preferential generation of multiply charged ions of larger compounds in complex mixtures by ESI MS the need of high resolution mass analyzers is indispensible but also cost intensive. In addition data interpretation gets very complex. Therefore ESI MS is of minor relevance for classification of intact micro-organisms up to now. MALDI MS allows generation of singly charged ions covering an extreme broad m/z range, and as a consequence time-of-flight (TOF) mass analyzer is commonly used with MALDI, because it provides (in principle) an unlimited m/z range. The easier data

interpretation caused by the singly or very low charged molecular ions and the providing of m/z data across a large m/z range makes MALDI-TOF MS dedicated for characterization of intact micro-organisms. Furthermore MALDI MS offers high tolerance against salts and detergents, as well as fast and accurate molecular mass determination and the possibility of automation, which makes it a real alternative to microbiological and molecular biological methods often taking several days. An important aspect is that without extensive sample preparation MALDI mass spectrometric analysis of intact micro-organisms can be performed, yielding analyte profiles, unique and representative of an individual species[15, 16].

Lately classification and identification of intact micro-organisms by MALDI-TOF MS is utilized by a number of research groups. Due to the great importance of bacteria in the medical field, homeland security and food industry many research groups focus their work on bacteria[12, 13, 17, 18] and bacterial spores[19, 20]. Only a few groups focus on fungal cells[21], in particular on fungal spores[22-24]. In contrast to bacteria fungal cell walls are mainly composed of different polysaccharides (80 – 90 %), including chitin which adds rigidity and structural stability to the cells, but also proteins, lipids, polyphosphates and inorganic ions are present[25]. The composition of fungal cell walls and therefore also of fungal spores is assumed to be a dynamic structure where qualitative and quantitative differences can occur between different fungal species, but also between different strains of the same fungal species, a prerequisite for classification and differentiation of fungal species by means of MALDI-TOF MS. Especially for the detection of biohazards in food, environment and homeland security rapid detection and identification of fungal species is of great importance. Infection of economic important crop plants, e.g. wheat or maize with plant pathogenic fungal species, e.g. *Fusarium* or *Aspergillus*, results in significant crop losses and therefore profit cuts, too. Furthermore the fungal infection of economic-important plants leads to contamination of aliment and animal feed causing toxication of humans and breeding cattle with mycotoxins, toxic metabolites produced by many fungal species[26-29].

Due to these facts this study concentrates on mycotoxin-producing *Fusarium* species, which are common in Austria and central eastern Europe. Previous studies[21-24] on intact fungal species have shown that the obtainable mass spectrometric information and mass spectra reproducibility are essential requisites for successful classification and identification of fungal species. Various parameters are reported to influence mass spectral data and mass spectra reproducibility, such as the pre-treatment of the fungal sample

(growth media, washing procedure), the applied matrix compound and solvent system and the MALDI sample preparation technique. Therefore a rapid and reproducible MALDI MS sample preparation method for intact *Fusarium* spores was developed and evaluated.

Experimental

Chemicals

Ferulic acid (FA), sinapinic acid (SA), 2,4,6-trihydroxyacetophenone (THAP), aniline and n-butylamine were obtained from Fluka (Buchs, Germany). 2,5-dihydroxybenzoic acid (DHB), α-cyano-4-hydroxycinnamic acid (CHCA) and 2-hydroxy-5-methoxybenzoic acid (MSA) were purchased from Sigma-Aldrich (Steinheim, Germany). Acetonitrile p.a. (ACN), acetone p.a., methanol p.a. (MeOH), ethanol 96 % (EtOH), isopropanol p.a. (iPrOH), formic acid 98 – 100 %, glyerol and water p.a. were obtained from Merck (Darmstadt, Germany). Trifluoroacetic acid (TFA) was obtained from Riedel-de-Haën (Seelze, Germany).

Preparation of *Fusarium* samples

Fusarium fungi (*F. graminearum* pH1, *F. graminearum* CPK 2785, *F. poae* CPK 2786, *F. sporotrichoides* CPK 2787, *F. culmorum* CPK 2789 and *F. cerealis* CPK 2790) provided by C. P. Kubicek were cultivated on solid SNA medium (synthetic nutrient agar)[30]. For spore production, 50 mL of liquid mungbean-medium (20 g mungbean in 1 L water were heated for 20 min and directly used after filtration) were inoculated with abraded mycelium of two fully grown SNA plates. After four days slow shaking (160 rpm) at 28 °C a sufficient amount of spores had been formed. For removal of mycelium and mungbean medium the spores were filtered through a sterile glass funnel containing glass wool and centrifuged at 8000 rpm at 4 °C for 10 min. To avoid degradation during long time storage at − 20 °C the generated spores were mixed with an aqueous solution containing 20 % glycerol. The concentration of spores was determined by spore counting using a light-optical microscope (Nikon Instruments Europe, Amstelveen, The Netherlands).

Sample preparation for MALDI MS

Matrix compounds	Matrix concentration	Solvent Mixture	Mixing ratio
Ferulic acid (FA)	10, 20, 30 mg/mL	ACN/0.1 % TFA	3/7, 1/1, 7/3
		iPrOH/0.1 % TFA	3/7, 1/1, 7/3
Sinapinic acid (SA)	10, 20, 30 mg/mL	ACN/0.1 % TFA	3/7, 1/1, 7/3, 2/1
		iPrOH/0.1 % TFA	3/7, 1/1, 7/3, 2/1
2,5-Dihydroxybenzoid acid (DHB)	10, 20, 30 mg/mL	ACN/0.1 % TFA	3/7, 1/1, 7/3, 2/1, 6/4
		iPrOH/0.1 % TFA	3/7, 1/1, 7/3, 2/1, 6/4
		EtOH/0.1 % TFA	1/9
		iPrOH/0.1 % TFA	1/9
		EtOH/water	1/9
		iPrOH/water	1/9
DHB/2-Hydroxy-5-methoxybenzoic acid (MSA)(9/1)	10, 20, 30 mg/mL	EtOH/0.1 % TFA	1/9
		iPrOH/0.1 % TFA	1/9
		EtOH/water	1/9
		iPrOH/water	1/9
DHB/CHCA (1/1)	10, 20, 30 mg/mL	ACN/5 % formic acid/0.1 % TFA	14/3/3
		iPrOH/5 % formic acid/0.1 % TFA	14/3/3
α-Cyano-4-hydroxycinnamic acid (CHCA)	6 mg/mL	Aceton	-
	10, 20 mg/mL	iPrOH/0.1 % TFA	4/1
2,4,6-trihydroxyacetophenone (THAP)	10, 20, 30 mg/mL	MeOH	-
		iPrOH	-
DHB/Butylamine	30 mg/mL	MeOH	-
DHB/Aniline	10 mg/mL	ACN/water	1/1
CHCA/Butylamine	40 mg/mL	MeOH	-
CHCA/Aniline	10 mg/mL	ACN/0.1 % TFA	1/1

Table 3.1: *Evaluated matrix/solvent combinations for intact spore mass spectrometry of Fusarium species.*

Prior to MALDI MS analysis glycerol had to be removed from the spores. 50 to 100 µL of spores solution were washed 3 times with 100 µL water using Nanosep™ (Pall Corporation, Ann Arbor, MI, USA) centrifugal devices (MWCO 10 kDa) at 10000 rpm for 10 min. The

glycerol free spores were suspended in water to obtain a final spore concentration of 3.5 million spores/µL.

During the optimization of the MALDI MS preparation different matrices and solvents were tested: 12 matrix compounds (see Table 3.1), in different concentrations (6, 10, 20, 30 and 40 mg/mL) and solvent mixtures (15 variations) were valued. For details see Table 3.1 showing all combinations tested.

Three sample preparation techniques[31] were used. Briefly, for thin layer technique 0.5 µL of the matrix mixture were applied on the stainless steel MALDI target (often reused prior to this type of application, DE1580ta, Shimadzu Biotech Kratos Analytical, Manchester, UK), dried in a gentle stream of air and on top of the matrix crystal layer 0.5 µL of the spores solution were applied and dried again in a gentle stream of air. For the sandwich method a second matrix layer of 0.5 µL was applied on top of the dried thin layer preparation resulting in a matrix-sample-matrix sandwich. For the dried droplet technique, first 0.5 µL spores solution were applied on the target and 0.5 µL matrix solution were added by direct mixing on the target by the pipette tip.

The resulting matrix/spore crystal layer were viewed and photographed by a light-optical microscope (Nikon Instruments Europe, Amstelveen, The Netherlands).

Mass spectrometry

MALDI TOF mass spectra of the spores preparations were acquired on an AXIMA TOF^2 and AXIMA CFR$^+$ (both Shimadzu Biotech Kratos Analytical, Manchester, UK), each equipped with a nitrogen laser ($\lambda = 337$ nm). Both instruments were operated in the positive linear ion mode using pulsed extraction (PE) for optimal average resolution (PE setting m/z 5000). Each mass spectrum was acquired by averaging 2500 unselected and consecutive laser profiles (one pulse per profile). Laser power was set to 70 – 110 arbitrary units (relative scale 0 – 180) according to the corresponding threshold laser power required for the applied matrix systems. The ion gate was set to m/z 1000 to blank most of the ions arising from the matrix and other contaminants.

Results and Discussion

With regard to the aim of this study, the generation of peptide and/or protein profiles of the surfaces of intact *Fusarium* spores, acidic matrix compounds (CHCA[32], DHB[33, 34], FA[35],

SA[35], and THAP[36]) and neutral ionic liquid matrix systems (DHB/Butylamine[37], CHCA/Butylamine[38]), all preferred for MALDI MS of isolated peptides and proteins, were utilized. Various solvent systems were used to dissolve the matrix compounds, namely ACN, MeOH, EtOH, iPrOH and acetone. These organic solvents were either used in pure form or they were mixed with plain water or TFA acidified water. Various considerations, such as the ability to dissolve the matrix compound, the evaporation behavior and the exhibited surface tension, the latter two are influencing the crystallization behavior of the matrix, provided the basis for the solvent systems selected. We tested commonly used organic solvents, as ACN, MeOH and EtOH, but also iPrOH which exhibits a higher surface tension and is more hydrophobic, leading to a more localized, hence more concentrated sample application onto the MALDI target, resulting in a different, potentially more efficient crystallization of the matrix/analyte system.
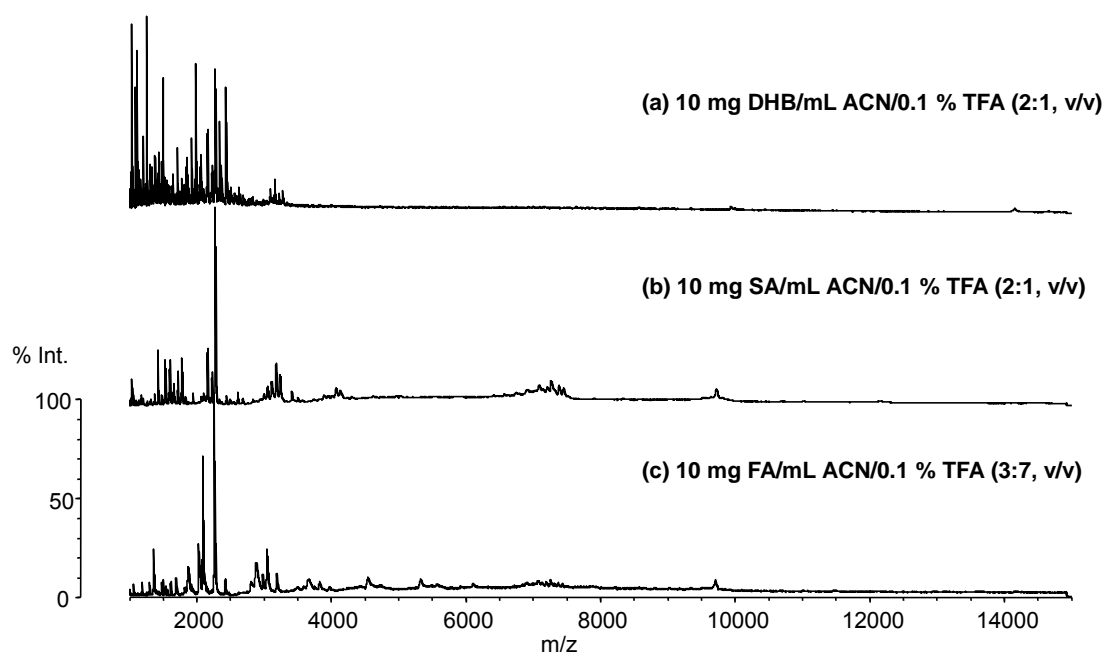
Figure 3.1: *Positive ion MALDI linear TOF mass spectra of intact Fusarium spores (F. graminiearum pH1) Matrix systems applied with dried droplet method were: (a) 30 mg DHB/mL ACN/0.1 % TFA (2:1, v/v), (b) 30 mg SA/mL ACN/0.1 % TFA (2:1, v/v), (c) 10 mg FA/mL ACN/ 0.1 % TFA (3:7, v/v).*

We started the investigations on intact *Fusarium* spores by testing previously published matrix systems suitable for fungal spores (*Penicllilium, Aspergillus, Rhizopus,*

Triochderma, Phanerochaete), (a) 30 mg DHB in 1 mL ACN/0.1 % TFA (2:1, v/v)[24], (b) 30 mg SA in 1 mL ACN/0.1 % TFA (2:1, v/v)[23] and (c) 10 mg FA dissolved in 1 mL ACN/0.1 % TFA (3:7, v/v)[21], applied with dried droplet technique. Figure 3.1, showing the obtained positive ion MALDI mass spectra, illustrates the great influence of the matrix compound and the solvent system on the obtained peptide/protein profiles. Although the mass spectra obtained with matrix SA and FA (Figure 3.1 b and c) show a reasonable number of peaks throughout the whole investigated m/z range, the specific mass spectra of the two preparations were not comparable to each other in terms of peaks detected and their intensities. Contrary, less spectral information was achieved with DHB (Figure 3.1 a), mainly showing peaks in the lower m/z region. Due to differing peptide/protein profiles evaluation of matrix systems is necessary. Investigation of FA as matrix yields the most informative analyte profiles, a high number of peaks exhibiting high intensities could be observed throughout the whole investigated m/z range. Contrary the application of SA, DHB and THAP results in less peaks (mainly peaks in the lower m/z range from m/z 1000 to 3500 are observed) and lower peak intensities. Comparable analyte profiles are achieved from matrix systems consisting of mixtures of matrix substances, namely DHB/CHCA[39] and DHB/MSA[34]. Only very little spectral information could be received from mass spectra generated with CHCA and the selected ionic liquid matrices[37, 40, 41], few peaks with quite low intensities were detected. As mentioned above the mass spectrum generated by means of the matrix FA provided the highest mass spectral information content in terms of peak number and therefore seems to be a quite suitable matrix compound for MALDI-TOF MS of *Fusarium* species. So these results agree with the findings of Valentine *et al* [21] that FA is the matrix of choice when characterizing fungal species due to the enhanced mass spectral information provided. A difference was found for the ratio of the solvent system ACN/0.1 % TFA, which turned out to be more suitable for *Fusarium* spores. The amount of the more hydrophobic solvent ACN in the mixture was increased so that a final ratio of 7:3 (v/v, ACN/0.1 TFA) was used.

Beside the influence of the matrix system, also sample preparation is affecting protein profiles in terms of reproducibility, peak number and intensity. Hence three MALDI preparation techniques were evaluated, thin layer, sandwich and dried droplet techniques.

X10

%Int.
100
0
2000   6000   *m/z*   10000   14000

Thin layer technique; *F. graminearum* pH1

X2

%Int.
100
0
2000   6000   *m/z*   10000   14000

Sandwich technique; *F. graminearum* pH1

%Int.
100
0
2000   6000   *m/z*   10000   14000

Dried droplet technique; *F. graminearum* pH1
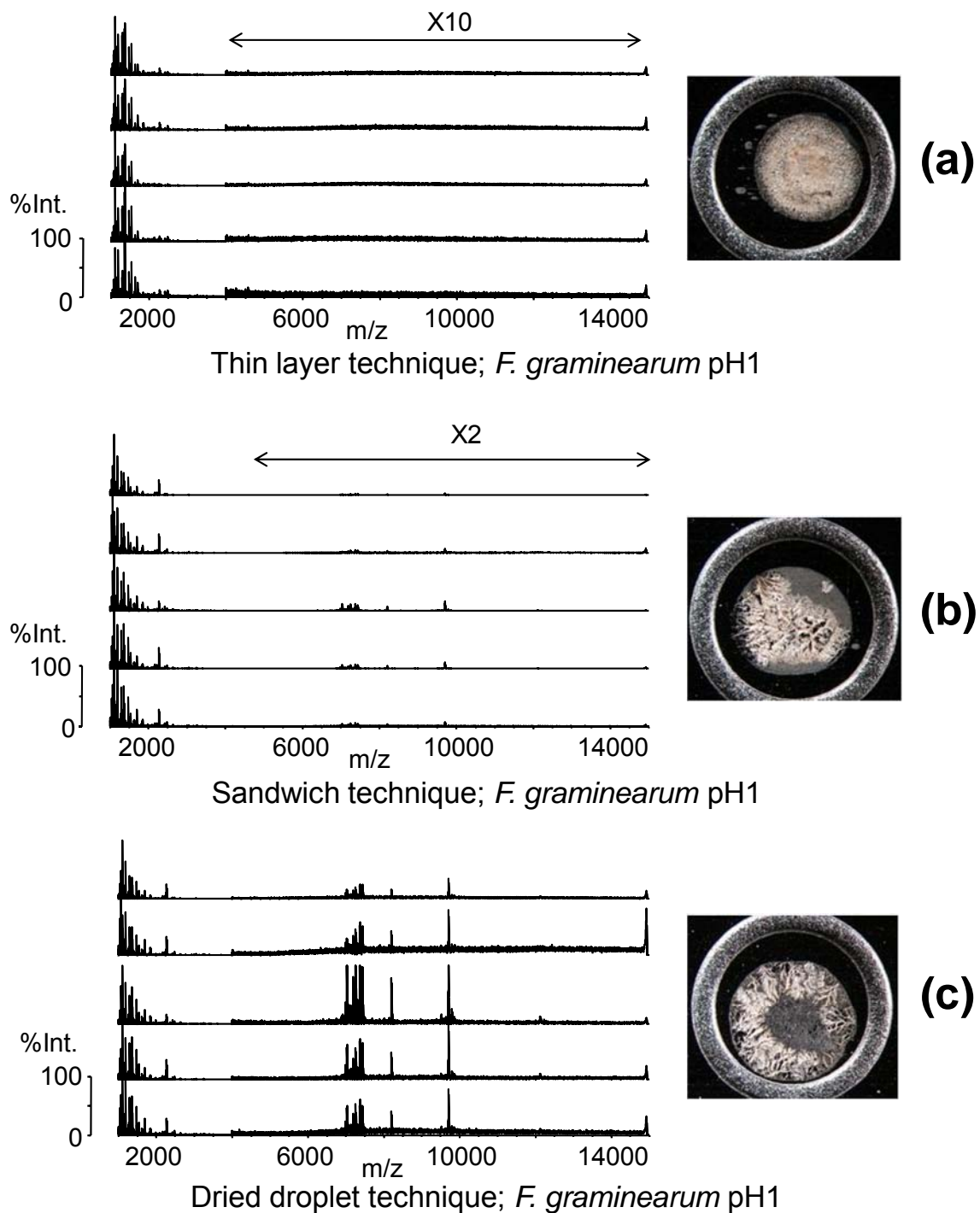
(a)

(b)

(c)

Figure 3.2: *Positive ion MALDI linear TOF mass spectra and corresponding microscopic images of the matrix/sample preparation (ring diameter 2.8 mm) of intact Fusarium spores (F. graminearum pH1) applied with (a) thin layer, (b) sandwich and (c) dried droplet technique. Matrix system used: 10 mg FA/ mL ACN/0.1 % TFA (7:3, v/v).*

Figure 3.2 presents light-optical microscope images showing the crystallization behavior of these three sample preparations and their corresponding mass spectra. *F. graminearum* pH1 was prepared using 10 mg FA in 1 mL ACN/0.1 % TFA (7:3, v/v) as matrix system. The findings in terms of crystallization behavior are generally valid for all investigated matrix systems in this study.

For thin layer technique matrix solution is applied onto the MALDI target forming a thin layer of matrix crystals and the sample solution is applied on top of this layer. The upper matrix layer is dissolved in the sample solution facilitating the embedding of the spores into the matrix layer. Only matrix systems consisting of highly volatile organic solvents, ensuring fast evaporation, result in thin homogeneous matrix crystal layers. In this study only one matrix system, 6 mg CHCA in 1 mL acetone, meets this demand, but results in mass spectra showing very few peaks with low intensity. Even though CHCA in pure acetone is dedicated for application with thin layer technique, no significant peptide/protein profiles could be achieved, indicating that thin layer technique is no suitable matrix/sample preparation method for *Fusarium* spore analysis. Matrix compounds dissolved in mixtures of ACN, EtOH, MeOH, iPrOH with water or aqueous 0.1 % TFA formed larger crystals irregularly distributed throughout the whole spot using thin layer preparation, see Figure 3.2 a. After application of the sample solution on top of such a layer, embedding of the spores into the matrix crystals will also occur irregularly, often forming so called "sweet" spots. If data acquisition is done manually, one can search for these "sweet" spots and obtain significant, but not always reproducible MALDI mass spectra. If data acquisition is done automatically via rastering the sample spot at defined laser energies decreased mass spectral quality in terms of decreased signal-to-noise ratio was observed and no reproducible protein profiles could be obtained (Figure 3.2 a), as only a few "sweet" spots could be localized across the sample spot. Furthermore a lower desorption/ionization efficiency is obtained for thin layer technique, caused by the irregular embedding of the spores into the matrix crystal. A possibility to overcome this irregular distribution of matrix/spore crystals is the application of another matrix layer on top of the thin layer preparation, also referred to as sandwich preparation technique. Due to this dissolving and recrystallisation step a more homogeneously distributed crystal layer should be formed and a better incorporation of the spores into the matrix crystals should occur. Looking at the light-optical microscope images of the sandwich preparation technique one can see two different kinds of crystals, small compact ones and larger branched crystals of the matrix. Even though no uniform preparation was achieved, automatic rastering of the

spot resulted in most cases in reproducible protein profiles (Figure 3.2 b). Nevertheless reproducibility was not satisfying enough. Optimal reproducibility was obtained from the dried droplet technique. Direct mixing of spores and matrix solution on the MALDI target facilitated a more evenly embedding of the spores into the matrix crystals. Small branched crystals growing from the border into the centre of the spot were formed. Even tough no consistent crystal layer is formed throughout the whole spot (the centre of the spot is covered only thinly with crystals), excellent desorption/ionization of the surface peptides/proteins from the spores was obtained, yielding highly reproducible peptide/protein profiles (Figure 3.2 c).
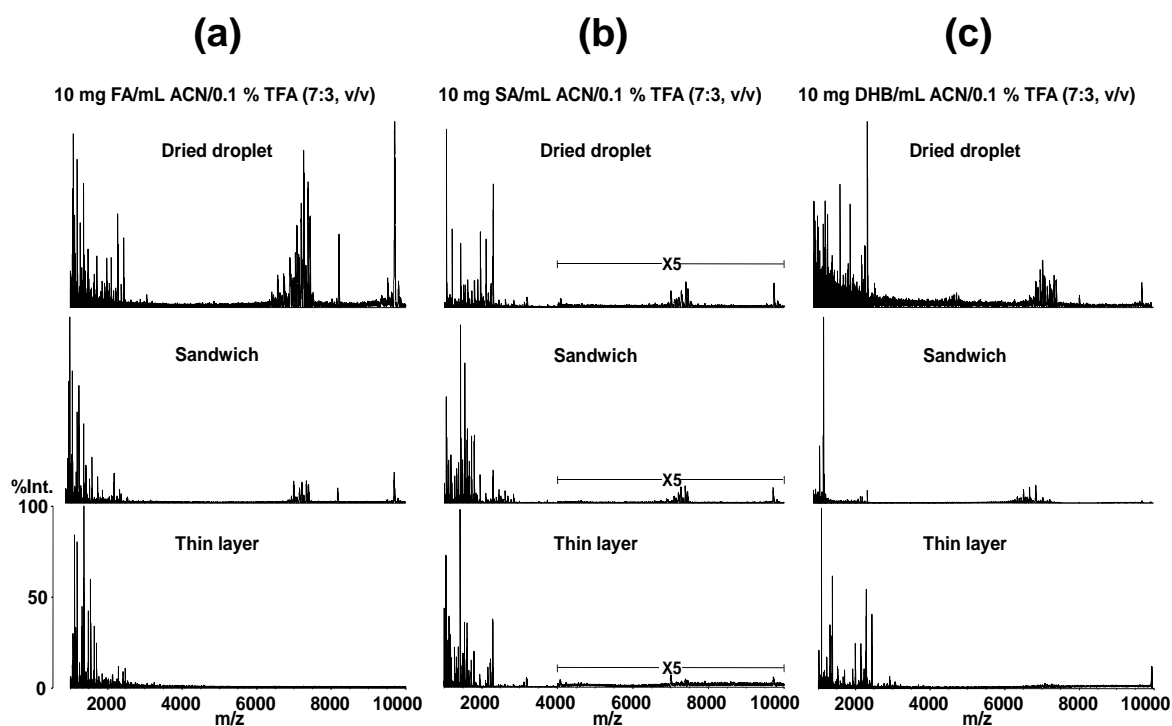
Figure 3.3: *Positive ion MALDI linear TOF mass spectra of intact Fusarium spores (F. graminearum pH1) applied with thin layer, sandwich and dried droplet technique utilizing three different matrix systems, 10 mg (a) FA, (b) SA or (c) DHB dissolved in 1 mL ACN/ 0.1 % TFA (7:3, v/v).*

Figure 3.3 summarizes the effects of the most effective matrix compounds and sample preparation techniques on the obtainable mass spectral information in terms of the complexity of the peak pattern. Beside mass spectra reproducibility also the obtainable protein information generated by the above mentioned sample preparation techniques, thin

layer, sandwich and dried droplet technique, was studied. Figure 3.3 shows MALDI mass spectra obtained from matrix systems consisting of 10 mg FA, SA and DHB dissolved in 1 mL ACN/0.1 % TFA (7:3, v/v) and the following preparation techniques: thin layer, sandwich and dried droplet technique. Beside the variations in the achieved protein profiles due to the different matrix compounds utilized, variations in peak number and intensity could be observed when changing the sample preparation technique. Consistent for all three matrix systems the achieved peptide/protein profiles improve from thin layer to sandwich to dried droplet preparation technique. Thin layer technique results in protein profiles lacking information about higher molecular mass compounds (> 4000 Da), whereas sandwich and dried droplet technique yield peptide/protein profiles containing low as well as high molecular mass compounds. Even though yielding quite similar peptide/protein profiles higher peak intensities could be obtained with dried droplet technique.

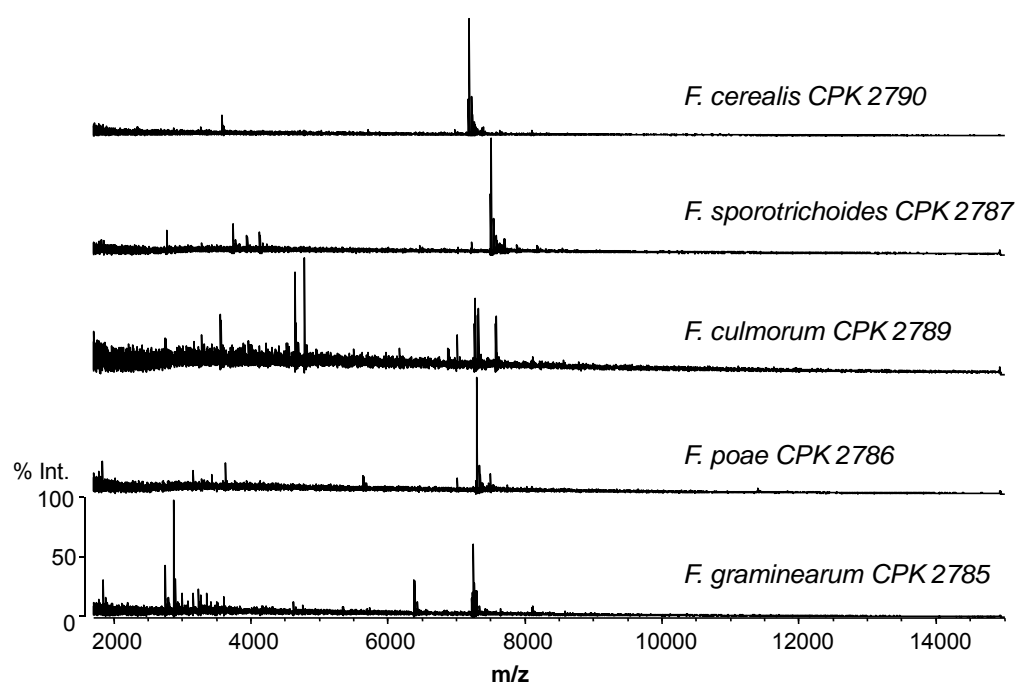**Figure 3.4:** *Positive ion MALDI linear TOF mass spectra of intact Fusarium spores (F. graminearum CPK 2785, F. poae CPK 2786, F. sporotrichoides CPK 2787, F. culmorum CPK 2789 and F. cerealis CPK 2790) Matrix system used: 10 mg FA/ mL ACN/0.1 % TFA (7:3, v/v) applied with dried droplet technique.1.7 million spores were applied onto the MALDI target.*

Combination of the matrix compound FA (10 mg FA dissolved in 1 mL ACN/0.1 % TFA (7:3, v/v)), which generated the most informative analyte profiles, and the dried drop technique, which yielded highly reproducible peptide/protein profiles, resulted in the most valuable peptide/protein profiles (patterns) for *Fusarium* spores. Figure 3.4 shows typical intact spore mass spectrometric profiles with the above mentioned optimized matrix and sample preparation for the following mycotoxin-producing species: *F. graminearum* CKP 2785, *F. poae* CPK 2786, *F. sporotrichoides* CPK 2787, *F. culmorum* CPK 2789 and *F. cerealis* CPK 2790. Numerous intensive peaks throughout the whole investigated m/z range from 1500 to 15000 could be observed, yielding species specific peptide/protein profiles allowing the unambiguously differentiation of these *Fusarium* species. Based on that the development of a database for *Fusarium* species and isolates is feasible and under development.

Conclusion

Aim of this study was to find a MALDI sample preparation method for intact spore mass spectrometry (generation of surface peptide/protein patterns) of intact *Fusarium* spores. Various key issues became apparent during the evaluation of several MALDI sample preparation methods. Homogenous embedding of spores into matrix crystals and evenly distribution of these matrix crystals throughout the whole MALDI target spot enabled homogeneous desorption/ionization, which is essential for acquiring significant peptide/protein patterns of intact spores. On this account dried droplet technique turned out to be the most suitable preparation technique. The matrix and spores are mixed in liquid phase resulting in appropriate embedding of the spores into the matrix crystals and subsequent highly reproducible MALDI mass spectra across a m/z range from 1500 to 15000 could be acquired. The MALDI matrix system and sample preparation technique of choice generating highly reproducible peptide/protein patterns for *Fusarium* spore characterization was the following: the matrix mixture consisting of 10 mg FA in 1 mL ACN/0.1 % TFA (7:3, v/v) applied with dried droplet technique. By means of this approach for the first time a differentiation of various *Fusarium* spores was demonstrated. Future objectives are the characterization, identification and differentiation of mycotoxin-producing *Fusarium* species common in Austria and central eastern Europe via intact spore MS and the development of a database.

Acknowledgements

References

[1]   Simmonds P.G., Whole Microorganisms Studied by Pyrolysis-Gas Chromatography-Mass Spectrometry: Significance for Extraterrestrial Life Detection Experiments. Applied Microbiology 1970; **20:** 567-572.

[2]   Schulten H.R., Beckey H.D., Meuzelaar H.L. and Boerboom A.J., High resolution field ionization mass spectrometry of bacterial pyrolysis products. Analytical Chemistry 1973; **45:** 191-195.

[3]   Meuzelaar H.L. and Kistemaker P.G., A technique for fast and reproducible fingerprinting of bacteria by pyrolysis mass spectrometry. Analytical Chemistry 1973; **45: 587-590.**

[4]   Anhalt J.P. and Fenselau C., Identification of bacteria using mass spectrometry. Analytical Chemistry 1975; **47:** 219-225.

[5]   Heller D.N., Cotter R.J., Fenselau C. and Uy O.M., Profiling of bacteria by fast atom bombardment mass spectrometry. Analytical Chemistry 1987; **59:** 2806-2809.

[6]   Heller D.N., Fenselau C., Cotter R.J., Demirev P., Olthoff J.K., Honovich J., Uy M., Tanaka T. and Kishimoto Y., Mass spectral analysis of complex lipids desorbed directly from lyophilized membranes and cells. Biochemical and Biophysical Research Communications 1987; **142:** 194-199.

[7]   Despeyreux D., Phillpotts R. and Watts P., Electrospray Mass Spectrometry for Detection and Characterization of Purified Cricket Paralysis Virus (CrPV). Rapid Communication in Mass Spectrometry 1996; **10:** 937-941.

[8]   Goodacre R., Heald J.K. and Kell D.B., Characterisation of intact microorganisms using electrospray ionisation mass spectrometry. FEMS Microbiology Letters 1999; **176:** 17-24.

[9]   Vaidyanathan S., Rowland J.J., Kell D.B. and Goodacre R., Discrimination of aerobic endospore-forming bacteria via electrospray-Ionization mass spectrometry of whole cell suspensions. Analytical Chemistry 2001; **73:** 4134-4144.

[10] Furstenau S., Whole virus mass analysis by electrospray ionization. Journal of the Mass Spectrometry Society of Japan 2003; **51:** 50-53.

[11] Bothner B. and Siuzdak G., Electrospray ionization of a whole virus: analyzing mass, structure, and viability. ChemBioChem 2004; **5:** 258-260.

[12] Holland R.D., Wilkes J.G., Rafii F., Sutherland J.B., Persons C.C., Voorhees K.J. and Lay J.O., Rapid identification of intact whole bacteria based on spectral patterns using matrix-assisted laser desorption/ionization with time-of-flight mass spectrometry. Rapid Communication in Mass Spectrometry 1996; **10:** 1227-1232.

[13] Krishnamurthy T. and Ross P.L., Rapid identification of bacteria by direct matrix-assisted laser desorption/ionization mass spectrometric analysis of whole cells. Rapid Communication in Mass Spectrometry 1996; **10:** 1992-1996.

[14] Claydon M.A., Davey S.N., Edwards-Jones V. and Gordon D.B., The rapid identification of intact microorganisms using mass spectrometry. Nature Biotechnology 1996; **14:** 1584-1586.

[15] Welham K.J., Domin M.A., Scannell D.E., Cohen E. and Ashton D.S., The characterization of micro-organisms by matrix-assisted laser desorption/ionization time-of-flight mass spectrometry. Rapid Communication in Mass Spectrometry 1998; **12:** 176-180.

[16] Fenselau C. and Demirev P.A., Characterization of intact microorganisms by MALDI mass spectrometry. Mass Spectrometry Reviews 2001; **20:** 157-171.

[17] Arnold R.J. and Reilly J.P., Fingerprint matching of E. coli strains with matrix-assisted laser desorption/ionization time-of-flight mass spectrometry of whole cells using a modified correlation approach. Rapid Communication in Mass Spectrometry 1998; **12:** 630-636.

[18] Haag A.M., Taylor S.N., Johnston K.H. and Cole R.B., Rapid identification of Haemophilus and other bacteria by matrix-assisted laser desorption ionization time-of-flight mass spectrometry. American Clinical Laboratory 2000; **19:** 20-21.

[19] Ryzhov V., Hathout Y. and Fenselau C., Rapid characterization of spores of Bacillus cereus group bacteria by matrix-assisted laser desorption-ionization time-of-flight mass spectrometry. Applied and Environmental Microbiology 2000; **66:** 3828-3834.

[20] Ullom J.N., Frank M., Gard E.E., Horn J.M., Labov S.E., Langry K., Magnotta F., Stanion K.A., Hack C.A. and Benner W.H., Discrimination between bacterial spore

types using time-of-flight mass spectrometry and matrix-free infrared laser desorption and ionization. Analytical Chemistry 2001; **73:** 2331-2337.

[21]   Valentine N.B., Wahl J.H., Kingsley M.T. and Wahl K.L., Direct surface analysis of fungal species by matrix-assisted laser desorption/ionization mass spectrometry. Rapid Communication in Mass Spectrometry 2002; **16:** 1352-1357.

[22]   Welham K.J., Domin M.A., Johnson K., Jones L. and Ashton D.S., Characterization of fungal spores by laser desorption/ionization time-of-flight mass spectrometry. Rapid Communication in Mass Spectrometry 2000; **14:** 307-310.

[23]   Li T.Y., Liu B.H. and Chen Y.C., Characterization of Aspergillus spores by matrix-assisted laser desorption/ionization time-of-flight mass spectrometry. Rapid Communication in Mass Spectrometry 2000; **14:** 2393-2400.

[24]   Chen H.Y. and Chen Y.C., Characterization of intact Penicillium spores by matrix-assisted laser desorption/ionization mass spectrometry. Rapid Communication in Mass Spectrometry 2005; **19:** 3564-3568.

[25]   Kavanagh K., Fungi - Biology and Applications. Chichester: John Wiley and Sons, Ltd; 2005.

[26]   Sweeney M.J. and Dobson A.D., Mycotoxin production by Aspergillus, Fusarium and Penicillium species. International Journal of Food Microbiology 1998; **43:** 141-158.

[27]   Placinta C.M., D´mello J.P.F. and Macdonald A.M.C., A review of worldwide contamination of cereal grains and animal feed with Fusarium mycotoxins. Animal Feed Science and Technology 1999; **78:** 21-37.

[28]   Bennett J.W. and Klich M., Mycotoxins. Clinical Microbiological Reviews 2003; **16:** 497-516.

[29]   Goswami R.S. and Kistler H.C., Heading for desaster: Fusarium graminearum on cereal crops. Molecular Plant Pathology 2004; **5:** 515-525.

[30]   Nirenberg H.I., Untersuchungen über die morphologische und biologische differenzierung der Fusarium-Sektion Liseola. Mitteilungen der Biologischen Bundesanstalt 1976; **169:** 117pp.

[31]   Kussmann M., Nordhoff E., Rahbek-Nielsen H., Haebel S., Rossel-Larsen M., Jakobsen L., Gobom J., Mirgorodskaya E., Kroll-Kristensen A., Palm L. and Roepstorff P., Matrix-assisted laser desorption/ionization mass spectrometry sample preparation techniques designed for various peptide and protein analytes. Journal of Mass Spectrometry 1997; **32:** 593-601.

[32] Beavis R.C., Chaudhary T. and Chait B.T., Alpha-cyano-4-hydroxycinnamic acid as a matrix for matrix-assisted laser desorption mass spectrometry. Organic Mass Spectrometry 1991; **27:** 156-158.

[33] Strupat K., Karas M. and Hillenkamp F., 2,5-Dihydroxybenzoic acid: a new matrix for laser desorption-ionization mass spectrometry. International Journal of Mass Spectrometry and Ion Processes 1991; **111:** 89-102.

[34] Karas M., Ehring H., Nordhoff E., Stahl B., Strupat K., Hillenkamp F., Grehl M. and Krebs B., Matrix-assisted laser desorption/ionization mass spectrometry with additives to 2,5-dihydroxybenzoic acid. Organic Mass Spectrometry 1993; **28:** 1476-1481.

[35] Beavis R.C. and Chait B.T., Cinnamic acid derivatives as matrices for ultraviolet laser desorption mass spectrometry of proteins. Rapid Communication in Mass Spectrometry 1989; **3:** 432-435.

[36] Thiede B. and von Janta-Lipinski M., Noncovalent RNA-peptide complexes detected by matrix-assisted laser desorption/ionization mass spectrometry. Rapid Communication in Mass Spectrometry 1998; **12:** 1889-1894.

[37] Mank M., Stahl B. and Boehm G., 2,5-Dihydroxybenzoic acid butylamine and other ionic liquid matrixes for enhanced MALDI-MS analysis of biomolecules. Analytical Chemistry 2004; **76:** 2938-2950.

[38] Armstrong D.W., Zhang L.K., He L. and Gross M.L., Ionic liquids as matrixes for matrix-assisted laser desorption/ionization mass spectrometry. Analytical Chemistry 2001; **73:** 3679-3686.

[39] Laugesen S. and Roepstorff P., Combination of two matrices results in improved performance of MALDI MS for peptide mass mapping and protein analysis. Journal of the American Society for Mass Spectrometry 2003; **14:** 992-1002.

[40] Snovida S.I., Chen V.C. and Perreault H., Use of a 2,5-dihydroxybenzoic acid/aniline MALDI matrix for improved detection and on-target Derivatization of glycans: A preliminary report. Analytical Chemistry 2006; **78:** 8561-8568.

[41] Lemaire R., Tabet J.C., Ducoroy P., Hendra J.B., Salzet M. and Fournier I., Solid ionic matrixes for direct tissue analysis and MALDI imaging. Analytical Chemistry 2006; **78:** 809-819.

4   GEMMA and MALDI-TOF MS of pharmaceutical grade reactive PEGs

Jasmin Hirschmann[1], Martina Marchetti-Deschmann[1], Peter Turecek[2], Günter Allmaier[1]

[1] Institute of Chemical Technologies and Analytics, Vienna University of Technology, Vienna, Austria

[2] Baxter Biosciences AG, Vienna, Austria

Abstract

One of the most prominent polymer group applied for drug conjugation is poly(ethylene) glycol. Since drug production is subjected to strict restrictions on the part of the FDA and EMEA, also PEG has to be characterized accurately. Particularly its molecular mass distribution (MMD) and polydispersity can result in unrequested inhomogeneous final products. Therefore evaluation of PEG before applying it to drug conjugation is essential. In this study a new analytical method for size and molecular mass determination based on electrophoretic mobility called GEMMA is used to characterize linear PEG´s with two differing terminating functional groups. To confirm the data acquired by GEMMA a second, well established method for molecular weight determination, MALDI-TOF MS, was applied. Utilizing these two analytical approaches four monomethoxylated PEG-succinimidyl succinate (mPEG-SS) derivatives were investigated in terms of polydispersity and MMD. Although based on differing principles, both analytical methods yield comparable results. Due to the functional limit of the µCPC detector no GEMMA data were achievable for mPEG-SS 2K. GEMMA based MMD maxima of 4.77 kDa (± 4.4 % precision) for mPEG-SS 5K, 9.76 kDa (± 2.6 %) for mPEG-SS 10K and 18.7 kDa (± 1.8 %) for mPEG-SS 20K were obtained. MALDI data yielded MMD maxima of 2.19 kDa (± 0.3 %) for mPEG-SS 2K, 4.87 kDa (± 0.6 %) for mPEG-SS 5K, 10.2 kDa (± 0.9 %) for mPEG-SS 10K and 19.7 kDa (± 1.7 %) for mPEG-SS 20K. All obtained MMD maxima for the mPEG batches lie within the company stated specifications, MMD ± 10 % (based on

MALDI-TOF MS data). For mPEG-SS 2K a polydispersity of 1.02 and for mPEG-SS 5K, 10K and 20K a polydispersity of 1.01 were determined from GEMMA as well as from MALDI-TOF MS data and are also in excellent agreement with the company´s data of 1.05 − 1.1 which are derived from GPC experiments.


Introduction

In modern society polymers are implemented in a wide range of applications. One of the most prominent utilization is their conjugation to peptides and proteins [1, 2]. Nowadays synthetic peptides and recombinant proteins are commonly used as potent and specific therapeutic agents, though their unrestricted application is limited by several intrinsic factors, low stability *in vivo* and thereof short plasma half-life [3, 4] and immunogenicity [5, 6]. Conjugation of peptide/protein-based drugs with polymers, e.g. poly(ethylene) glycol (PEG) [7, 8], dextrans [9, 10] or poly(amino acids) [11], is an increasingly used strategy to overcome these limitations and hence facilitates large-scale application. Polymers suitable for peptide/protein conjugation have to fulfil a variety of criteria [12]. The polymer should be readily biodegradable to avoid progressive accumulation in the body. Its polydispersity should be as close as possible to 1 to yield an acceptable homogeneity of the final drug. Distribution and accumulation in the desired body compartments as well as prolonged action should be given by a sufficient body/compartment-residence time. Finally, the polymer conjugation to the peptide/protein should be obtained via a single reactive group to avoid cross-linking, thus yielding an inhomogeneous product.

Due to its outstanding properties [12, 13], non-toxic, non-immunogenic, non-antigenic, highly soluble in water and many organic solvents, hydrophobic, flexible chain and accepted by the FDA and EMEA for human use, PEG is the most prominent polymer used for polymer-drug conjugation nowadays. The solubility in water and in numerous organic solvents allows PEGylation of peptides/proteins under mild physiological conditions. The combination of the highly flexible chain and the high hydrophobicity (PEG binds 2-3 water molecules per ethylene oxide unit) is suggested to be responsible for the PEG´s ability to reduce immunogenicity and antigenicity [5] and to prevent due to steric hindrance enzymatic degradation [14] of peptides/proteins. Another important property concerning the pharmaceutical usage of PEG is its low polydispersity, M_w/M_n 1.01 (PEG < 5000 Da) to 1.1 (PEG > 50 kDa) [13]. Considering the requirements of a polymer applied for drug

conjugation, PEG seems to be the most suitable choice. Covalent coupling of PEG to proteins overcomes most of the limiting intrinsic factors mentioned above [15, 16], immunogenicity [5, 17-19] and antigenicity [20-22] are decreased, body-residence time [23, 24] and stability towards metabolic enzymes [25] are increased. Beside the obvious advantages, PEG-protein conjugation is also accompanied by some undesirable effects, as the loss of biological activity. For example, PEG-interferon α2a (Pegasys®) retains only 7 % of the antiviral activity of the native protein, but due to the improved pharmacokinetics it still obtains a better performance [26]. Since the introduction of protein PEGylation by Davis and Abuchowski [5, 25] in the 1970´s a great number of PEG-drug conjugates came on the market, e.g. PEG-adenosine deaminase (Adagen®) [27], PEG-granulocyte colony-stimulating factor (Neulasta®) [28], PEG-growth hormone receptor antagonist (Somavert®) [29], PEG-interferon α2a (Pegasys®) [26], PEG-interferon α2b (PEG-Intron®) [30], PEG-asparaginase (Oncaspar®) [31], and more PEG-proteins are currently in clinical trial phases [11, 32]. Further pharmaceutical applications of PEG are the conjugation to smaller drugs, like antitumor drugs, peptides, or oligonucleotides [11, 33] and the use as drug delivery systems [34, 35] or diagnostic carrier [36].

Because drug production is subjected to strict controls, reactive PEG batches applied to drug conjugation have to be evaluated in detail. In general, monomethoxylated PEG´s (mPEG) are used, which are synthesised by anionic ring opening polymerization initiated with methoxide ions [13]. Due to the presence of trace amounts of water during polymerization, commercially available mPEG can contain a considerable amount of diol PEG (up to 15 %), leading to unrequested cross-linked co-products and varying degree of coupling groups. A mPEG batch is commonly composed of molecules built up by different numbers of monomers, thus yielding in ideal cases a Gaussian shaped molecular mass distribution (MMD). Possible consequences are drug conjugates with varying biological properties, e.g. body-residence time, immunogenicity. So to avoid unwanted cross-linked products and to determine the polydispersity it is recommended to evaluate mPEG batches prior to the conjugation process with different analytical techniques, GPC [37-40] and/or DLS [41-43].
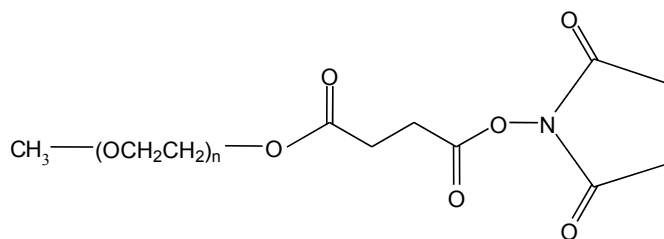
Sample	Number of ethylenglycol monomers (n)	Calculated molecular weight (average)
mPEG-SS 2K	40	1991
mPEG-SS 5K	108	4987
mPEG-SS 10K	222	10009
mPEG-SS 20K	449	20009

Figure 4.1: *Structure and calculated molecular weight of methoxylated poly(ethylene glycol) succinicmidyl succinate derivatives (mPEG-SS).*

In this study four monomethoxy PEG-succinimidyl succinate (mPEG-SS) derivatives, structures and calculated exact molecular masses shown in Figure 4.1, were characterized according to MMD and polydispersity. Therefore a new method based on the determination of the analytes electrophoretic mobility diameter (EMD), called gas phase electrophoretic mobility macromolecular analyzer (GEMMA) was used [44, 45]. Multiply charged macromolecular ions are generated via nano electrospray (nES) and charge reduced by a bipolar atmosphere generated by a Polonium-210 (alpha-particles) source to obtain neutral and singly charged positive and negative ions. These ions are size separated according to their EMD using a nano differential mobility analyzer (nDMA) and detected by means of a condensation particle counter (μCPC), which is a direct optical (laser-based) detector allowing counting single particles. Based on the correlation of EMD to molecular weight of well defined globular proteins [46] the MMD of four mPEG-SS derivatives can be determined. To confirm and complement the data achieved with GEMMA matrix-assisted laser desorption/ionization time-of-flight mass spectrometry (MALDI-TOF MS) of the reactive PEG derivatives was applied. MALDI MS in combination with a linear TOF analyzer, mainly used for accurate molecular weight determination of proteins, carbohydrates and oligonucleotides is also a well established method for characterization of polymers [47-50]. Prerequisite for MALDI-TOF MS analysis is the embedding of the

analyte into a matrix substance, which exhibits a high spectral absorption of the exciting laser wavelength and therefore enables desorption and ionization of intact analyte ions. Mass analysis of these (high mass molecular) ions is performed often by a linear TOF analyzer and is based on the fact that the time the ions need to pass a field free drift region applied between the ion source and the secondary electron multiplier detector is directly correlated with their mass to charge (m/z) ratio. The resulting signals are recorded as a function of time; the conversion of the spectrum´s x-axis from time to m/z ratio is performed by an empirically determined calibration function characteristic for a particular instrument.

Materials and Methods

Chemicals

2,5-dihydroxybenzoic acid (DHB) and 2-hydroxy-5-methoxybenzoic acid (MSA) were purchased from Sigma-Aldrich (Steinheim, Germany). Sodium chloride, ammonium acetate, ethanol 96 % (EtOH) and water p.a (conductivity at 25 °C ≤ 1μS/cm) were obtained from Merck (Darmstadt, Germany).

PEG samples

Four linear PEG samples (methoxy PEG-succinimidyl succinates) dedicated for pharmaceutical applications from SunBio (Anyang City, South Korea) were investigated, namely mPEG-SS 2K, mPEG-SS 5K, mPEG-SS 10K and mPEG-SS 20K.

Sample preparation for GEMMA and MALDI-TOF MS

For GEMMA analysis all four PEG´s were dissolved in ammonium acetate buffer (pH 6.8; 20 mM) resulting in a concentration of 1 mg/mL. A concentration series (0.5, 0.25, 0.1, 0.025, 0.01 and 0.005 mg/mL) was prepared by diluting the stock solutions of the four mPEG-SS derivatives.

For MALDI-TOF MS analysis the PEG´s were dissolved in water, resulting in a concentration of 1 mg/mL for mPEG-SS 2K and 10 mg/mL for mPEG-SS 5K, 10K and 20K. Three matrix systems based on DHB dissolved in water/EtOH (9:1, v/v) were evaluated in terms of optimal mass spectrometric resolution [51, 52]. Matrix system A

consisted of 10 mg DHB dissolved in 1 mL water/EtOH (9:1, v/v). 2 µL PEG solution and 1 µL matrix solution were directly mixed on the stainless steel MALDI target. Matrix system B consisted of superDHB, a mixture of DHB and MSA (9:1, w/w) in water/EtOH (9:1, v/v); PEG solution and matrix solution were pre-mixed (1:4, v/v) in an Eppendorf tube and two times 1.5 µL of this mixture (separated by a drying step) were applied onto the target. Finally the so obtained spot was recrystallized with 0.8 µL EtOH. For matrix system C superDHB (DHB/MSA (9:1, w/w) in 1 mL water/EtOH (9:1, v/v)), PEG solution and 0.1 M NaCl solution were pre-mixed in an Eppendorf tube in a mixing ratio of 1:1:6 (v/v/v). Two times 1.5 µL of this mixture (separated by a drying step) were applied onto the target. Finally the generated sample spot was recrystallized with 0.8 µL EtOH.

Nano electrospray GEMMA

The GEMMA system consists of a nano electrospray (nES) unit (TSI model 3480), a nano differential mobility analyzer (nDMA; TSI model 3080) and an ultrafine condensation particle counter (µCPC; TSI model 3025A) as detector (all parts from TSI Inc, Shoreview, MN, USA). Multiply charged ions are generated by the electrospray process and charge reduced to yield neutral and singly charged molecules. The ions are size separated according to their electrophoretic mobility diameter (EMD) in the nDMA and detected with the µCPC. For determination of the PEG´s size and the derived molecular weight, EMD of several well defined globular standard proteins were determined and used as calibrants. Based on the resulting correlation between EMD and molecular mass of the nanoobject unknown polymers can be characterized [46]. The settings of the nES source were 2 kV and 0.3 L/min CO_2 (99.995 %, Air Liquide, Schwechat, Austria)/1 L/min compressed air (generated by compressor type Hobby Star 200W, ARGE, Garsten – St. Ulrich, Austria) were applied to operate the instrument in a stable cone-jet mode for the used ammonium acetate buffer (pH 6.8; 20 mM). A fused silica capillary with an inner diameter of 150 nm was used and the tip of the spray needle exhibited an angle of 75°. The electrospray process was operated in the positive ion mode. Ten scans (120 s per scan) were averaged for each final size GEMMA spectrum presented in this paper.

MALDI-TOF mass spectrometry

MALDI-TOF mass spectra of polymer samples were acquired on an AXIMA TOF² (Shimadzu Biotech Kratos Analytical, Manchester, UK) equipped with a nitrogen laser (λ

= 337 nm). The instrument was operated in positive ion, linear as well as reflectron mode using pulsed extraction optimised by the company-supplied algorithm for optimal resolution (set on 2000, 5000, 10000 and 20000 for the corresponding mPEG-SS derivatives). Each mass spectrum was acquired by averaging 80 to 800 unselected and consecutive laser shots. Prior to data analysis the mass spectra were smoothed with Savitsky-Golay algorithm.

Calculation of the polydispersity

Calculation of polydispersity values from GEMMA data was performed without software support. M_n (number average-molecular weight) was calculated as $M_n = \sum n_i M_i / \sum n_i$, n_i representing the number of polymer molecules having mass M_i, and M_w (weight-averaged molecular weight) was calculated as $M_w = \sum n_i M_i^2 / \sum n_i M_i$. Polydispersity was calculated as M_w/M_n. Calculation of polydispersity values from MALDI-TOF MS data was supported by MALDI-MS application software (Shimadzu Biotech Launchpad 2.7, Shimadzu Biotech Kratos Analytical, Manchester, UK).

Results and Discussion

The method used for determination of the size and the derived molecular mass of PEG´s containing one reactive group (reacting particular with amino groups of lysine) was GEMMA.
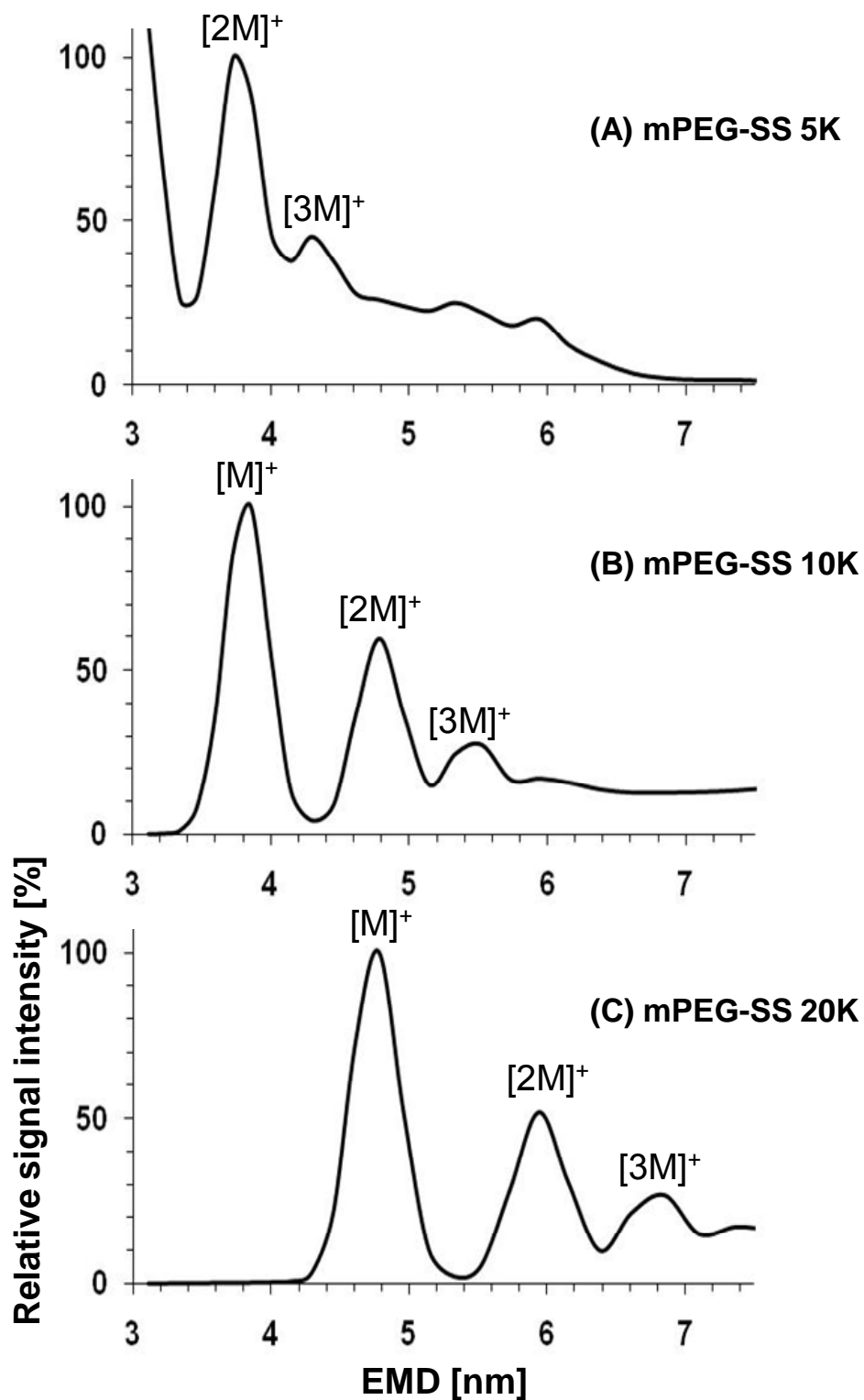
Figure 4.2: *GEMMA spectra of mPEG-SS 5K (A), 10K (B) and 20K (C).*

Figure 4.2 shows the obtained GEMMA spectra of three of the four investigated PEG´s.
Two to three peaks can be observed in each GEMMA spectrum, corresponding to aerosol

droplets containing unimers, one singly charged polymer chain, di- or trimers, two or three polymer chains building a cluster carrying one charge. All EM diameter values and corresponding maxima of the MMD are summarized in Table 4.1.

	Unimer		Dimer		Trimer	
	EMD [nm]	MW [Da]	EMD [nm]	MW [Da]	EMD [nm]	MW [Da]
mPEG-SS 5K	-	-	3.72	9100	4.29	13910
mPEG-SS 10K	3.85	10080	4.78	19210	5.52	29540
mPEG-SS 20K	4.78	19210	5.94	36790	6.85	56380

Table 4.1: *Electrophoretic mobility diameter (EMD) and derived maxima of molecular mass distribution of GEMMA spectra obtained from droplets containing one (unimer), two (dimer) or three (trimer) polymer chains of mPEG-SS 5K, 10K and 20K.*

Due to the functional limit of the µCPC analyzer at a particle diameter of 3 nm no GEMMA data could be obtained for mPEG-SS 2K. By the same reason detection of mPEG-SS 5K unimers was not possible, nevertheless di- and trimers of mPEG-SS 5K were detectable at EM diameters of 3.72 nm and 4.29 nm. The GEMMA spectrum of mPEG-SS 10K exhibits unimers (3.85 nm) as well as di- (4.78 nm) and trimers (5.52 nm). mPEG-SS 20K yields unimers with an EM diameter of 4.78 nm, dimers of 5.94 nm and trimers of 6.85 nm. The formation (and its abundance) of dimers and trimers is directly correlated with the sample concentration, which is shown in Figure 4.3 exhibiting GEMMA spectra of various concentrations of mPEG-SS 20K.
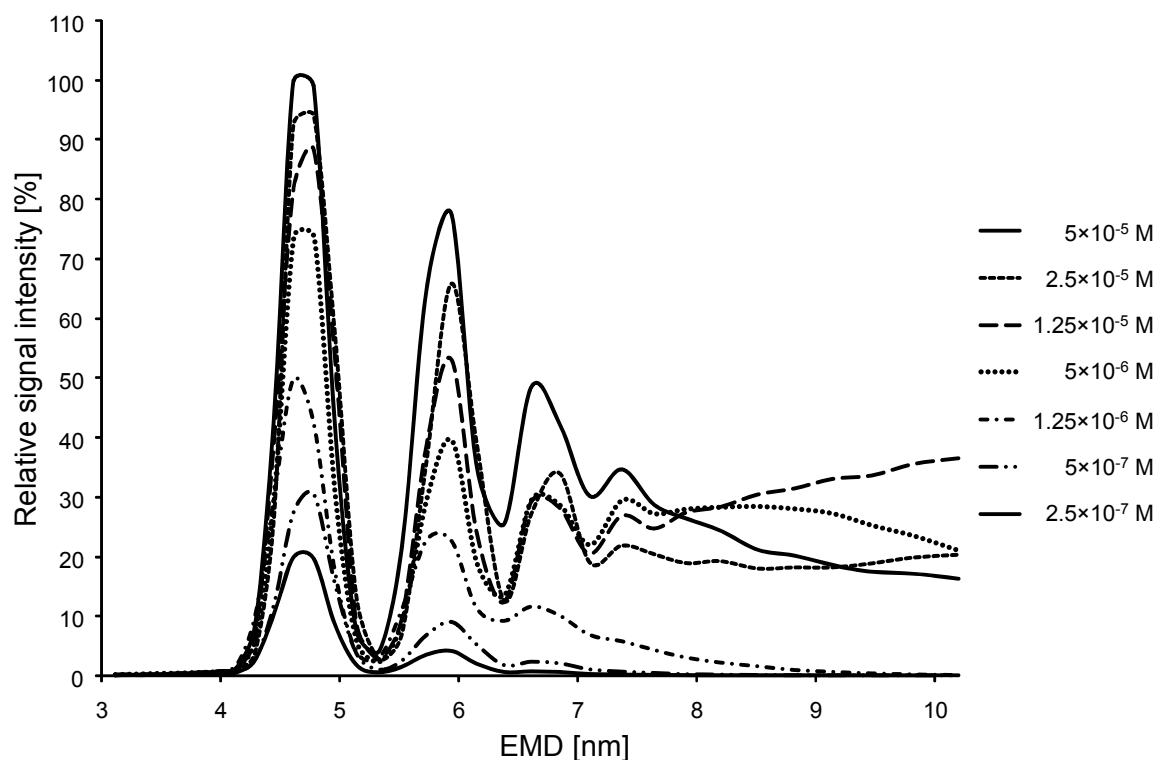
Figure 4.3: *GEMMA spectra of mPEG-SS 20K at different sample concentrations showing the correlation of the formation of di- and trimers to the sprayed sample concentration.*

With increasing sample concentration (2×10^{-4} M to 1×10^{-6} M) not only unimers but also di- and trimers and at higher concentrations (2×10^{-4} M to 2×10^{-5} M) even tetramers can be detected. From concentrations below 1×10^{-6} M only unimers can be detected. For determination of the MMD the detection of these multimer clusters is desirable, because these clusters consist of individual molecules having their own mass distribution, which is combined when forming such clusters, thus a relative narrowing of the mass distribution is achieved. Saucy et al used this relative narrowing of the mass distribution obtained by the clustering process to characterize various PEG standards [45]. Based on the formed multimer clusters the maxima of the MMD were determined, yielding 4.77 kDa for mPEG-SS 5K, 9.76 kDa for mPEG-SS 10K and 18.70 kDa for mPEG-SS 20K. Precision of the GEMMA analysis increased from mPEG-SS 5K (± 4.4 %) to mPEG-SS 20K (± 1.8 %). All MMD maxima data are summarized in Table 4.2. During the acquisition of the 10 scans required for one GEMMA spectrum a total volume of 1.34 µL sample solution is consumed (based on a measured sample solution flow of 67 nL/min this is related to a consumption of 1.34 µg). Application of the above mentioned concentration series showed that sample concentrations from the micro-mole to the nano-mole range can be detected with the

83

GEMMA instrument, thus only a small amount of mPEG-SS derivatives is required to obtain significant GEMMA spectra.

Maximum of molecular mass distribution [Da]			
	Manufacturing company (based on MALDI-TOF MS)	GEMMA	MALDI-TOF MS
mPEG-SS 2K	2000 (± 10 %)	not feasible	2190 (± 0.3 %)
mPEG-SS 5K	5000 (± 10 %)	4770 (± 4.4 %)	4870 (± 0.6 %)
mPEG-SS 10K	10000 (± 10 %)	9760 (± 2.6 %)	10150 (± 0.9 %)
mPEG-SS 20K	20000 (± 10 %)	18700 (± 1.8 %)	19700 (± 1.7 %)

Table 4.2: *Molecular mass distributions (MMD) of the used batches specified by the company and comparison to the measured maxima of the MMDs molecular obtained by GEMMA and MALDI-TOF MS. Values in brackets indicate precision of the determination.*

Three preparation methods all based on the matrix DHB, a commonly used MALDI matrix for characterization of PEG´s [53], were evaluated in terms of obtainable MMD and signal intensity. Generally, DHB dissolved in water/EtOH forms long needle shaped crystals resulting in an inhomogeneous distribution of sample and matrix on the target spot. Acquisition of MALDI-TOF mass spectra with high S/N ratio and mass spectrometric resolution is only possible at so called "sweet spots", where matrix and sample are mixed homogeneously within defined crystal structures. Addition of 10 % MSA [52] and/or recrystallization with EtOH [54] help to overcome the unfavourable crystallization behaviour of DHB. In both cases smaller more evenly distributed crystals are formed, thus leading to increased sensitivity and resolution. Recrystallization may also be accompanied by an appreciated side effect, the removal of salt contaminations. In contrast to MALDI-TOF MS of biopolymers, ionization of synthetic polymers occurs mostly via cationization rather than protonation [50, 53], thus addition of a (inorganic) cationization agent leads to an increase of mass spectrometric sensitivity [47, 55, 56]. Another effect going along with the use of a cationization agent is the suppression of other salt contaminations present in the polymer

sample, matrix or solvents. The consequences of utilization of the above mentioned matrix additive (MSA), cationization agents and recrystallization on the MALDI-TOF mass spectra of mPEG-SS samples were investigated.
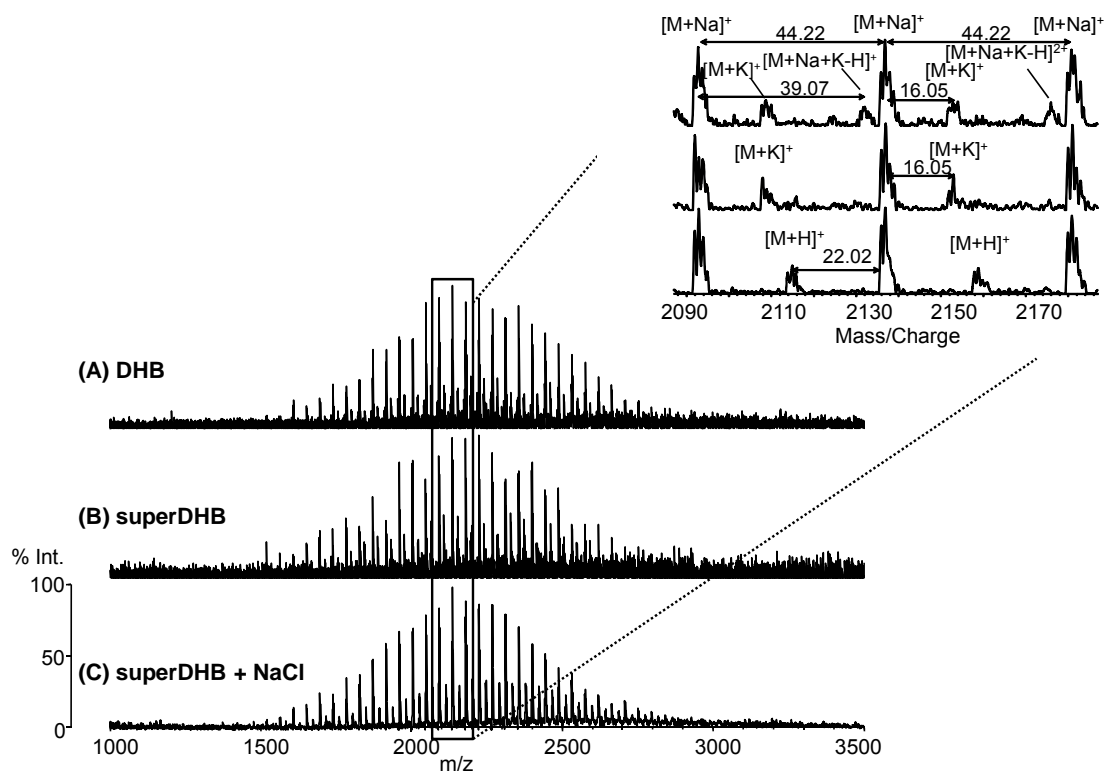

Figure 4.4: *Positive ion MALDI-TOF mass spectra of mPEG-SS 2K in the reflectron mode prepared with the matrix DHB (A), superDHB (B) and superDHB doped with NaCl (C). In the inset a small m/z section of the mass spectra is presented showing the observable molecular ions and the corresponding Δm values.*

Figure 4.4 shows the MALDI-TOF mass spectra of mPEG-SS 2K prepared by the mentioned techniques (DHB, superDHB and super DHB with NaCl) and acquired in the reflectron mode. The inset of the Figure 4.4 shows a small m/z range of the mass spectra in detail with the observable molecular ions and the corresponding Δm values. In all three mass spectra the Na-adduct ions are the most prominent species. Even the plain preparation with DHB without any additives shows 3 groups of ions at 44 Da intervals, respectively Na-adduct ions (most intensive species), K-adduct ions (Δm 38 Da or to the Na-adduct ion Δm 16 Da) and a third signal resulting from [M+Na+K-H]$^+$ (Δm 39 Da to the Na-adduct

85

ion). By use of superDHB, also MALDI-TOF mass spectra containing Na- (most intensive) and K-adduct ions were determined, but the signal from $[M+Na+K-H]^+$ is not observable anymore. Most likely this adduct ion was removed by recrystallization with EtOH. Third matrix solution was superDHB mixed with NaCl acting as cationization agent. Only now it was possible to determine protonated molecular ions of mPEG-SS 2K, but still the Na-adduct ions were the more prominent peaks, whereas no K-adduct ions could be observed. SuperDHB containing NaCl yields less complex MALDI-TOF mass spectra, showing the protonated molecular ions as well as the still dominating Na-adduct ions. Analysis of the mass spectra showed a MMD from m/z 1477 going up to m/z 2797. SuperDHB containing NaCl was used for MALDI-TOF mass spectrometric analysis of the other polymer samples, mPEG-SS 5K, 10K and 20K. The obtained mass spectra are shown in Figure 4.5.
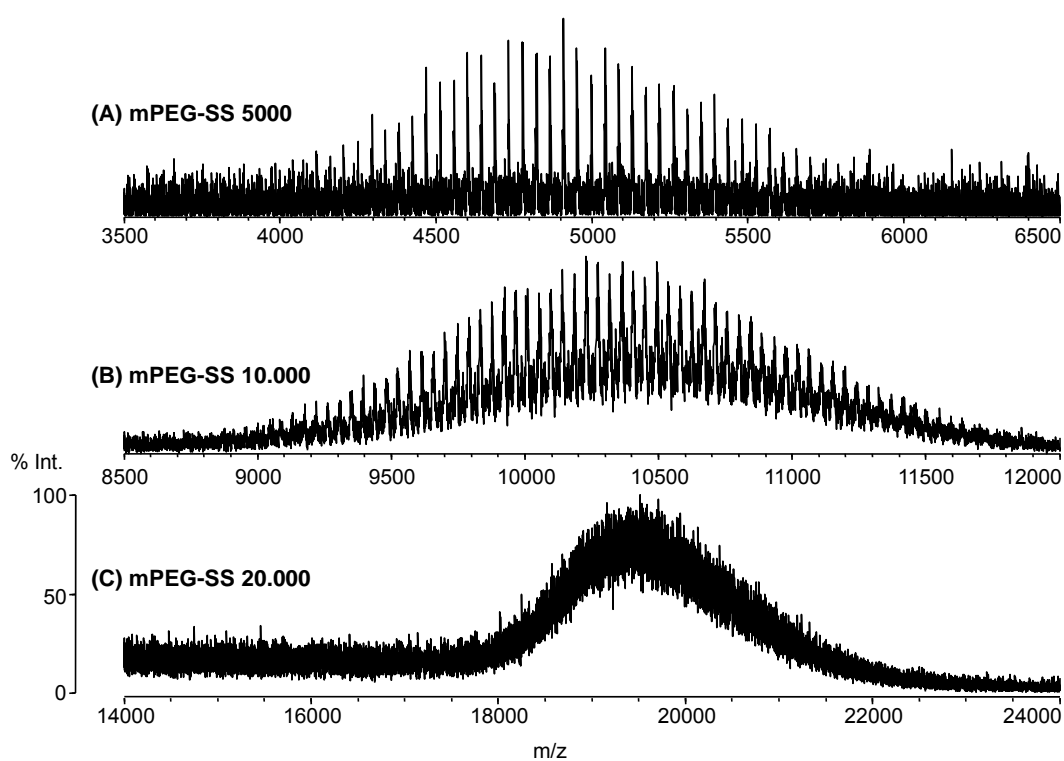

Figure 4.5: *Positive ion MALDI-TOF mass spectra of mPEG-SS 5K, 10K and 20K. Mass spectrum of mPEG-SS 5K was acquired in the reflectron mode (A) whereas mass spectra of mPEG-SS 10K (B) and 20K (C) were acquired in the linear mode.*

The positive ion MALDI mass spectrum of mPEG-SS 5K acquired in the reflectron mode shows a Na-adduct ion distribution starting at m/z 4075 and going up to m/z 5703 with a mass difference of 44 Da between adjacent polymer molecular ions. No K-adducts or protonated molecular ions were observed. Unlike mPEG-SS 2K and 5K which were analysed with the reflectron mode, mass spectrum of mPEG-SS 10K was acquired in the linear operation mode, resulting in a series of Na-adduct ions with 44 Da difference. The molecular ion distribution of the polymer species ranges from m/z 8950 to m/z 11590. MALDI-TOF mass spectrometric analysis of mPEG-SS 20K was also performed in the linear operation mode and yielded a resolved signal starting at m/z 17800 and ending at m/z 21450. In this m/z region the achievable mass spectrometric resolution was not sufficient anymore to resolve the individual molecular ions of the polymer species (which are just 44 Da apart). Table 4.2 summarizes the maxima of the MMD obtained by MALDI-TOF MS. Following MMD maxima were obtained, for mPEG-SS 2K 2190 Da, mPEG-SS 5K 4870 Da, mPEG-SS 10K 10150 Da and for mPEG-SS 20K 19700 Da. These values differ from the calculated average molecular masses listed in Figure 4.1; mPEG-SS 2K yields a difference of +199 Da, mPEG-SS 5K of -117 Da, mPEG-SS 10K of +141 Da and mPEG-SS 20K of -309 Da. Due to decreasing resolution of the linear TOF analyzer, precision of the MALDI-TOF mass spectrometric analysis decreased from mPEG-SS 2K (± 0.3 %) up to mPEG-SS 20K (± 1.7 %).

Comparing the maxima of the MMD of the investigated mPEG-SS derivatives it becomes obvious that the precision of the two methods (GEMMA and MALDI-TOF MS) tend to opposite directions. Precision of GEMMA analysis of polymers increases and the precision of MALDI-TOF MS decreases with increasing MMD. Precision decrease of MALDI-TOF MS is based on the decreasing resolution of the TOF mass analyzer. Increasing GEMMA precision is based on the detection of the multimer clusters, containing one to three PEG chains, which yield a relative narrowing of the MMD, see [45]. So for PEG´s with a low MMD more significant data can be obtained utilizing MALDI-TOF MS, whereas for analysis of PEG´s with higher MMD GEMMA is the more suitable method. Nevertheless both methods yield MMD maxima lying within the specifications stated by the company, MMD ± 10%, yielded via MALDI-TOF MS. The MMD data were provided via the product data sheet and information about the applied methods was obtained from the internet (www.sunbio.com). So the MMD maxima obtained by MALDI-TOF MS (2190 Da) lies within the stated specifications of 1800 to 2200 Da for mPEG-SS 2K. As mentioned above, no MMD maximum for mPEG-SS 2K could be obtained via GEMMA

analysis, due to the functional limit of the µCPC detector at a particle diameter of 3 nm. MMD maxima of 4770 Da (GEMMA) and 4870 Da (MALDI-TOF MS) for mPEG-SS 5K also fulfil the company´s specifications from 3600 to 4400 Da. For mPEG-SS 10K maxima of 9760 Da for GEMMA analysis and 10150 Da for MALDI-TOF analysis were achieved, perfectly fitting to MMD from 9000 to 11000 Da. Also MMD maxima acquired for mPEG-SS 20K, 18700 Da (GEMMA) and 19700 (MALDI-TOF MS) were lying within the specifications of 18000 to 22000 Da. All MMD maxima data are summarized in Table 4.2.

Polydispersity			
	Manufacturing company (based on GPC)	GEMMA	MALDI-TOF MS
mPEG-SS 2K	1.05 – 1.1	not feasible	1.02
mPEG-SS 5K	1.05 – 1.1	1.01	1.01
mPEG-SS 10K	1.05 – 1.1	1.01	1.01
mPEG-SS 20K	1.05 – 1.1	1.01	1.01

Table 4.3: *Polydispersity of the used batches specified by the company and compared to the values calculated from obtained GEMMA and MALDI-TOF MS data.*

Second parameter for characterization of the mPEG-SS derivatives was the polydispersity, data are summarized in Table 4.3. Polydispersity stated by the company is based on MALDI-TOF MS data as well as on GPC data, given specifications are 1.05 – 1.1. Calculation of the polydispersity on basis of MALDI-TOF data was supported by MALDI-MS application software (Shimadzu Biotech Launchpad 2.7, Shimadzu Biotech Kratos Analytical, Manchester, UK), whereas calculation based on GEMMA data was performed by using the equations stated previously. For mPEG-SS 2K polydispersity was only calculated from MALDI data, because no GEMMA data could be achieved due to functional limits of the µCPC (GEMMA detector). MALDI-TOF MS yielded a polydispersity of 1.02. For mPEG-SS 5K, 10K and 20K polydispersity could be calculated from MALDI-TOF as well as from GEMMA data, yielding a polydispersity of 1.01 consistent through both methods and all experiments. All calculated polydispersity values

are in agreement with the company data, they even are lower than the stated limits. So all mPEG-SS samples exhibit a very low MMD indicated by the low polydispersity value (very narrow distribution).

Conclusion

Strict controls of national and international regulatory agencies force accurate characterization of reactive PEG polymer batches applied for PEGylation in drug production (e.g. recombinant proteins). Due to non homogenous final products, especially the determination of MMD and the polydispersity is of great relevance. In this study four mPEG-SS batches were analysed via MALDI-TOF MS and GEMMA, two instruments based on different physico-chemical principles. Molecular mass determination via MALDI-TOF MS analysis is based on the determination of the time-of-flight and the correlated m/z values whereas GEMMA analysis acts on the electrophoretic mobility diameter and the derived molecular mass. Obtained maxima of the MMD of the mPEG-SS batches lie within the specifications stated by the company, MMD ± 10 %, no further conclusions on the data quality achieved via GEMMA or MALDI-TOF could be drawn, due to the lack of more detailed product information, e.g. exact MMD maximum achieved by the company. Polydispersity values of 1.02 for mPEG-SS 2K and 1.01 for mPEG-SS 5K, 10K and 20K were calculated from GEMMA as well as MALDI-TOF data, indicating that the mPEG-SS derivatives exhibit a low MMD, hence fulfil the desired criteria to be utilized for conjugation to proteins and peptides.

Acknowledgement

References

[1]   Vicent M.J. and Duncan R., Polymer conjugates: nanosized medicines for treating cancer. Trends in Biotechnology 2006; **24:** 39-47.

[2]   Khandare J. and Minko T., Polymer-drug conjuagtes: Progress in polymeric prodrugs. Progress in Polymer Science 2006; **31:** 359-397.

[3] Werle M. and Bernkop-Schnurch A., Strategies to improve plasma half life time of peptide and protein drugs. Amino Acids 2006; **30:** 351-367.

[4] Shechter Y., Mironchik M., Saul A., Gershonov E., Precido-Patt L., Sasson K., Tsubery H., Mester B., Kapitkovsky A., Rubinraut S., Vachutinski Y., Fridkin G. and Fridkin M., New Technologies to Prolong Life-time of Peptide and Protein Drugs In vivo. International Journal of Peptide Research and Therapeutics 2006; **13:** 105-117.

[5] Abuchowski A., van Es T., Palczuk N.C. and Davis F.F., Alteration of immunological properties of bovine serum albumin by covalent attachment of polyethylene glycol. The Journal of Biological Chemistry 1977; **252:** 3578-3581.

[6] Veronese F.M., Caliceti P. and Schiavon O., Branched and linear poly(ethylene glycol): influence of the polymer structure on enzymological, pharmacokinetic and immunological properties of protein conjugates. Journal of Bioactive and Compatible Polymers 1997; **12:** 196-207.

[7] Veronese F.M. and Pasut G., PEGylation, successful approach to drug delivery. Drug Discovery Today 2005; **10:** 1451-1458.

[8] Pasut G., Sergi M. and Veronese F.M., Anti-cancer PEG-enzymes: 30 years old, but still a current approach. Advanced Drug Delivery Reviews 2008; **60:** 69-78.

[9] Torchilin V.P., Voronkov Y.I. and Mazaev A.V., The use of immobilized streptokinase. (Streptodekaza) for the therapy of thromboses. Therapeutic Archieves (Russia) 1982; **54:** 21-25.

[10] Mehvar R., Recent trends in the use of polysaccharides for improved delivery of therapeutic agents: pharmacokinetic and pharmacodynamic perspectives. Current Pharmaceutical Biotechnology 2003; **4:** 283-302.

[11] Langer C.J., CT-2103: a novel macromolecular taxane with potential advantages compared with conventional taxanes. Clinical Lung Cancer 2004; **6 Suppl 2:** S85-88.

[12] Pasut G. and Veronese F.M., Polymer-drug conjugation, recent achievements and general strategies. Progress in Polymer Science 2007; **32:** 933-961.

[13] Roberts M.J., Bentley M.D. and Harris J.M., Chemistry for peptide and protein PEGylation. Advanced Drug Delivery Reviews 2002; **54:** 459-476.

[14] Working P.K., Newman S.S., Johnson J. and Cornacoff J.B., Saftey of poly(ethylene glycol) derivatives. In: Poly(ethylene glycol) Chemistry and

Biological Applications. Harris J.M. and S. Z. (Ed.), Washington, DC: ACS Books; 1997.

[15] Bailon P. and Berthold W., Polyethylene glycol-conjugated pharmaceutical proteins. Pharmaceutical Science and Technology Today 1998; **1:** 352-356.

[16] Caliceti P. and Veronese F.M., Pharmacokinetic and biodistribution properties of poly(ethylene glycol)-protein conjugates. Advanced Drug Delivery Reviews 2003; **55:** 1261-1277.

[17] Katre N.V., Immunogenicity of recombinant IL-2 modified by covalent attachment of polyethylene glycol. Journal of Immunology 1990; **144:** 209-213.

[18] Kamisaki Y., Wada H., Yagura T., Matsushima A. and Inada Y., Reduction in immunogenicity and clearance rate of Escherichia coli L-asparaginase by modification with monomethoxypolyethylene glycol. Journal of Pharmacology and Experimental Therapeutics 1981; **216:** 410-414.

[19] Nucci M.L., Olejarczyk J. and Abuchowski A., Immunogenicity of polyethylene glycol-modified superoxide dismutase and catalase. Journal of Free Radicals in Biology and Medicine 1986; **2:** 321-325.

[20] Davis S., Abuchowski A., Park Y.K. and Davis F.F., Alteration of the circulating life and antigenic properties of bovine adenosine deaminase in mice by attachment of polyethylene glycol. Clinical and Experimental Immunology 1981; **46:** 649-652.

[21] Tsuji J., Hirose K., Kasahara E., Naitoh M. and Yamamoto I., Studies on antigenicity of the polyethylene glycol (PEG)-modified uricase. International Journal of Immunopharmacology 1985; **7:** 725-730.

[22] He X.H., Shaw P.C., Xu L.H. and Tam S.C., Site-directed polyethylene glycol modification of trichosanthin: effects on its biological activities, pharmacokinetics, and antigenicity. Life Sciences 1999; **64:** 1163-1175.

[23] Knauf M.J., Bell D.P., Hirtzer P., Luo Z.P., Young J.D. and Katre N.V., Relationship of effective molecular size to systemic clearance in rats of recombinant interleukin-2 chemically modified with water-soluble polymers. The Journal of Biological Chemistry 1988; **263:** 15064-15070.

[24] Satake-Ishikawa R., Ishikawa M., Okada Y., Kakitani M., Kawagishi M., Matsuki S. and Asano K., Chemical modification of recombinant human granulocyte colony-stimulating factor by polyethylene glycol increases its biological activity in vivo. Cell Structure and Function 1992; **17:** 157-160.

[25] Abuchowski A., McCoy J.R., Palczuk N.C., van Es T. and Davis F.F., Effect of covalent attachment of polyethylene glycol on immunogenicity and circulating life of bovine liver catalase. The Journal of Biological Chemistry 1977; **252:** 3582-3586.

[26] Bailon P., Palleroni A., Schaffer C.A., Spence C.L., Fung W.J., Porter J.E., Ehrlich G.K., Pan W., Xu Z.X., Modi M.W., Farid A., Berthold W. and Graves M., Rational design of a potent, long-lasting form of interferon: a 40 kDa branched polyethylene glycol-conjugated interferon alpha-2a for the treatment of hepatitis C. Bioconjugate Chemistry 2001; **12:** 195-202.

[27] Levy Y., Hershfield M.S., Fernandez-Mejia C., Polmar S.H., Scudiery D., Berger M. and Sorensen R.U., Adenosine deaminase deficiency with late onset of recurrent infections: response to treatment with polyethylene glycol-modified adenosine deaminase. Journal of Pediatrics 1988; **113:** 312-317.

[28] Wong S.S., Chemistry of Protein Conjugation and Cross-Linking. Boca Raton: CRC Press; 1991.

[29] Trainer P.J., Drake W.M., Katznelson L., Freda P.U., Herman-Bonert V., van der Lely A.J., Dimaraki E.V., Stewart P.M., Friend K.E., Vance M.L., Besser G.M., Scarlett J.A., Thorner M.O., Parkinson C., Klibanski A., Powell J.S., Barkan A.L., Sheppard M.C., Malsonado M., Rose D.R., Clemmons D.R., Johannsson G., Bengtsson B.A., Stavrou S., Kleinberg D.L., Cook D.M., Phillips L.S., Bidlingmaier M., Strasburger C.J., Hackett S., Zib K., Bennett W.F. and Davis R.J., Treatment of acromegaly with the growth hormone-receptor antagonist pegvisomant. The New England Journal of Medicine 2000; **342:** 1171-1177.

[30] Wang Y.S., Youngster S., Grace M., Bausch J., Bordens R. and Wyss D.F., Structural and biological characterization of pegylated recombinant interferon alpha-2b and its therapeutic implications. Advanced Drug Delivery Reviews 2002; **54:** 547-570.

[31] Graham M.L., Pegaspargase: a review of clinical studies. Advanced Drug Delivery Reviews 2003; **55:** 1293-1302.

[32] Duncan R., Coatsworth J.K. and Burtles S., Preclinical toxicology of a novel polymeric antitumour agent: HPMA copolymer-doxorubicin (PK1). Human and Experimental Toxicology 1998; **17:** 93-104.

[33] Bonora G.M., Polymer-conjugated bioactive oligonucleotides. Journal of Bioactive and Compatible Polymers 2002; **17:** 375-389.

[34]   Cammas-Marion S., Okano T. and Kataoka K., Functional and site-specific macromolecular micelles as high potential drug carrier. Colloides and Surfaces B: Biointerfaces 1999; **16:** 207-215.

[35]   Sinha V.R., Aggarwal A. and Trehan A., Biodegradable PEGylated microspheres and nanospheres. American Journal of Drug Delivery 2004; **2:** 157-171.

[36]   Duewell S., Wuthrich R., von Schulthess G.K., Jenny H.B., Muller R.N., Moerker T. and Fuchs W.A., Nonionic polyethylene glycol-ferrioxamine as a renal magnetic resonance contrast agent. Investigative Radiology 1991; **26:** 50-57.

[37]   Hagelin G., Arukwe J.M., Kasparkova V., Nordbo S. and Rogstad A., Characterization of Low Molecular Weight Polymers by Matrix-assisted Laser Desorption/Ionization Mass Spectrometry. A Comparison with Gel Permeation Chromatography. Rapid Communication in Mass Spectrometry 1998; **12:** 25-27.

[38]   Lou X., van Dongen J.L. and Meijer E.W., Off-line size-exclusion chromatographic fractionation-matrix-assisted laser desorption ionization time-of-flight mass spectrometry for polymer characterization. Theoretical and experimental study. Journal of Chromatography A 2000; **896:** 19-30.

[39]   Miller K.E., Bramanti E., Prazen B.J., Prezhdo M., Skogerboe K.J. and Synovec R.E., Multidimensional analysis of poly(ethylene glycols) by size exclusion chromatography and dynamic surface tension detection. Analytical Chemistry 2000; **72:** 4372-4380.

[40]   Simekova M. and Berek D., Studies on high-performance size-exclusion chromatography of synthetic polymers. I. Volume of silica gel column packing pores reduced by retained macromolecules. Journal of Chromatography A 2005; **1084:** 167-172.

[41]   Nordmeier E.H., Characterization of polymers in solution with light scattering. Critical Reviews of Optical Science and Technology 1997; **CR 69:** 43-73.

[42]   Mendichi R. and Giacometti A., Use of a multi-detector size exclusion chromatography system for the characterization of complex polymers. Current Trends in Polymer Science 2001; **6:** 17-32.

[43]   Saunders G. and Meehan E., Polymer characterization by GPC with light scattering detection. Chromatography and Separation Technology 2002; **24:** 12-13.

[44]   Kaufman S.L., Skogen J.W., Dorman F.D. and Zarrin F., Macromolecule Analysis Based on Electrophoretic Mobility in Air: Globular Proteins. Analytical Chemistry 1996; **68:** 1895-1904.

[45] Saucy D.A., Ude S., Lenggoro I.W. and Fernandez de la Mora J., Mass analysis of water-soluble polymers by mobility measurement of charge-reduced ions generated by electrosprays. Analytical Chemistry 2004; **76:** 1045-1053.

[46] Bacher G., Szymanski W.W., Kaufman S.L., Zollner P., Blaas D. and Allmaier G., Charge-reduced nano electrospray ionization combined with differential mobility analysis of peptides, proteins, glycoproteins, noncovalent protein complexes and viruses. Journal of Mass Spectrometry 2001; **36:** 1038-1052.

[47] Bahr U., Deppe A., Karas M. and Hillenkamp F., Mass Spectrometry of Synthetic Polymers by UV-Matrix-Assisted Laser Desorption/Ionization Analytical Chemistry 1992; **64:** 2866-2869.

[48] Völcker N.H., Klee D., Hanna M., Höcker H., Bou J.J., Martinez de Ilarduya A. and Munoz-Guerra S., Synthesis of heterotelechelic poly(ethylene glycol)s and their characterization by MALDI-TOF-MS. Macromolecular Chemistry and Physics 1999; **200:** 1363-1373.

[49] Jackson A.T., Green M.R. and Bateman R.H., Generation of end-group information from polyethers by matrix-assisted laser desorption/ionisation collision-induced dissociation mass spectrometry. Rapid Communication in Mass Spectrometry 2006; **20:** 3542-3550.

[50] Montaudo G., Samperi F. and Montaudo M.S., Characterization of synthetic polymers by MALDI-MS. Progress in Polymer Science 2006; **31:** 277-357.

[51] vanRooij G.J., Duursma M.C., Heeren R.M.A., Boon J.J. and deKoster C.G., High resolution end group determination of low molecular weight polymers by matrix-assisted laser desorption/ionization on an external ion source fourier transform ion cyclotron resonance mass spectrometer. Journal of American Society of Mass Spectrometry 1996; **7:** 449-457.

[52] Karas M., Ehring H., Nordhoff E., Stahl B., Strupat K., Hillenkamp F., Grehl M. and Krebs B., Matrix-assisted laser desorption/ionization mass spectrometry with additives to 2,5-dihydroxybenzoic acid. Organic Mass Spectrometry 1993; **28:** 1476-1481.

[53] Nielen M.W.F., MALDI time-of-flight mass spectrometry of synthetic polymers. Mass Spectrometry Reviews 1999; **18:** 309-344.

[54] Harvey D.J., Matrix-assisted laser desorption/ionization mass spectrometry of carbohydrates. Mass Spectrometry Reviews 1999; **18:** 349-450.

[55] Rashidzadeh H., Wang Y. and Guo B., Matrix effects on selectivities of poly(ethylene glycol)s for alkali metal ion complexation in matrix-assisted laser desorption/ionization. Rapid Communication in Mass Spectrometry 2000; **14:** 439-443.

[56] Shimada K., Matsuyama S., Saito T., Kinugasa S., Nagahata R. and Kawabata S., Conformational effects on cationization of poly(ethylene glycol) by alkali metal ions in matrix-assisted laser desorption/ionization time-of-flight mass spectrometry. International Journal of Mass Spectrometry 2005; **247:** 85-92.

5   Nano electrospray gas phase electrophoretic macromolecular mobility analysis and MALDI linear time-of-flight mass spectrometry of recombinant von Willebrand factor

Jasmin Hirschmann[1], Martina Marchetti-Deschmann[1], Roland Müller[1], Peter Turecek[2], Günter Allmaier[1]

[1]Institute of Chemical Technologies and Analytics, Vienna University of Technology, Vienna, Austria

[2] Baxter Biosciences AG, Vienna, Austria

Abstract

Von Willebrand factor (vWF), an adhesive glycoprotein with an approximate molecular weight (MW) of the monomer of 260 kDa, circulates in the human blood plasma as a series of multimers ranging in size from 450 kDa to 20.000 kDa, thus the determination of accurate MW of the monomer is of great importance and due to its high mass challenging. In this study accurate MW determination of intact recombinant vWF monomer (rvWF) was performed with GEMMA and MALDI TOF MS. Three rvWF preparations with differing buffer systems and glycoprotein concentrations were analyzed. First investigations by means of CGE-on-the-chip with a laser-induced-fluorescence detector under reducing conditions revealed two compounds (MW of 277 kDa (migration time 44.3 s) and 341 kDa (migration time 49.5 s)) present in each sample at varying extent, namely mature and pro-rvWF. The MALDI MS analysis in the linear positive ion mode allowed the detection of mature rvWF with a MW of 256.1 kDa (± 0.8 %) and pro-rvWF with a MW of 349.8 kDa (± 0.8 %). Two samples containing pro-rvWF in very minor concentration resulted in GEMMA detection of the mature rvWF with a MW of 227.4 kDa (± 2.5 %), corresponding to a size of 10.9 nm. For one sample containing both rvWF species in almost equal

concentrations no differentiation of the two species was possible with GEMMA analysis. Due to its lower resolution only a peak representing a mixture of both species at 11.8 nm could be observed, yielding a MW of 298.8 kDa (± 1.6 %).

Introduction

Von Willebrand factor (vWF) is an adhesive complex glycoprotein with a molecular mass of the monomer of approx. 260 kDa (determined by SDS agarose gel electrophoresis) [1-3] circulating in human plasma as dimer and a series of oligomers ranging in molecular mass from 450 kDa to 20.000 kDa [2, 4, 5]. Synthesized in endothelial cells [6, 7] and megakaryocytes [8] the precursor polypeptide, pre-pro-vWF, consists of a 22-amino acid residue signal peptide, a 741-residue pro-peptide and a 2050-residue polypeptide [9]. After *in vivo* removal of the signal peptide two pro-vWF units are linked via disulfide bonds forming dimers, the building blocks for mature vWF multimers [10, 11]. Prior to plasma release the pro-peptide is cleaved off and the remaining part contains several post translational modifications, namely glycosylation [9, 12-14] and sulfation [15]. The final mature vWF carries 12 N- and 10 O-glycans, whereof specific N-glycans are further modified by sulfation [16]. The carbohydrate moiety contributes to several specific properties of vWF, e.g. physiological activity, receptor binding, clearance from plasma circulation and structural stability [17, 18]. After biosynthesis mature vWF is either released into the blood circulation system or it is stored in the Weibel-Palade body [19]. In human plasma vWF serves a dual purpose in hemostasis. In case of vascular injury it mediates adhesion of platelet glycoproteins, e.g. collagen to vascular subendothelium [20]. Furthermore vWF builds a non-covalent complex with blood coagulation factor VIII (FVIII) avoiding its rapid clearance from plasma, thus normal thrombin generation can take place [21].

Inherited defects on vWF cause von Willebrand Disease (vWD), one of the most common bleeding disorders in humans [22]. Symptoms of vWD are abnormal platelet function leading to constant nose bleeding, unexplained bruising or prolonged bleeding after injury. Due to the reduced level of vWF vWD is commonly accompanied by a decrease of FVIII procoagulant activity. Depending on the severity of the vWF defect several degrees of vWD occur. Patients with mild vWD have reduced vWF plasma levels and are treated by administration of desmopressin, which temporarily increases the vWF level [23]. Patients suffering from more severe forms of vWD have to be treated with human plasma derived

concentrates or cryoprecipitates, containing both FVIII and vWF [24, 25]. However, this replacement therapy is accompanied by some limitations [26]. Human plasma derived vWF concentrates show varying vWF and FVIII levels and ratios, depending on the donor´s pool. Furthermore due to proteolytic degradation during the isolation and purification (manufacturing) process, the multimer composition of the plasma derived vWF concentrates varies and no high molecular mass multimers, exhibiting the highest hemostatical activity, can be found. The use of recombinant vWF (rvWF) produced by fermentation of transformed cells would overcome these limitations [27]. Absence of plasma proteases avoids rvWF degradation and the risk of virus transmission is nearly eliminated. *In vivo* and *in vitro* evaluations have confirmed that structure and properties of rvWF are comparable to plasma derived vWF [28].

Due to the high molecular mass of the rvWF monomers and the multimeric composition characterization of rvWF is a quite challenging task and was to our knowledge never performed by the three techniques, namely nano ES (electrospray) gas phase electrophoretic macromolecular mobility analyzer (GEMMA), a particular kind of ion mobility spectrometer, vacuum matrix-assisted laser desorption ionization (MALDI) mass spectrometry (MS) and additionally capillary gel electrophoresis-on-the-chip (CGE-on-the-chip). Contrary to the commonly used approach, SDS-polyacrylamide [29] and -agarose gel electrophoresis [30], in this study determination of the exact molecular size, sample heterogeneity and exact molecular mass of three rvWF preparations was performed by nano ES GEMMA, MALDI-linear TOF (time-of-flight) MS as well as CGE-on-the-chip. Nano ES GEMMA analysis is based on generating multiply charged molecular ions by means of a nano ES process in the cone-jet mode followed by charge reduction via Polonium-210, thus yielding neutral and singly charged positive and negative ions. These ions are size separated according to their electrophoretic mobility diameter (EMD) using a nano differential mobility analyzer (nDMA) and detected by means of a condensation particle counter (μCPC) based on an indirect optical detection [31-33]. Based on the excellent correlation (r = 0.998) of the EMD to the molecular mass of well defined globular proteins the molecular mass of glycoproteins can be determined[34]. The second method used for characterization of rvWF was positive ion MALDI MS applying a linear TOF system with a standard detector[35]. The well-established "soft" desorption/ionization technique MALDI generates mainly singly up to triply charged molecular ions, shows a high salt and detergent tolerance and requires low amounts of samples, which makes MALDI-TOF MS to the dedicated technique for accurate molecular mass determination of intact high mass

proteins [36]. Prior to detailed characterization via nano ES GEMMA and MALDI TOF MS the rvWF samples were investigated with CGE-on-the-chip, yielding a first overview of the three samples in terms of homogeneity and approximate molecular mass within a reasonable time span (60 s of separation time).

Materials and Methods

Chemicals

Ammonium acetate, acetic acid 96 %, acetonitrile p.a. (ACN), methanol p.a. (MeOH), formic acid 98 – 100 % (FA) and water p.a. (conductivity at 25 °C $\leq$ 1 µS/cm) were purchased from Merck (Darmstadt, Germany). Coomassie Brilliant Blue R250 (CBB), sodium dodecyl sulphate (SDS) and 2,4,6 trihydroxyacetophenone monohydrate (THAP) were obtained from Fluka (Buchs, Switzerland). Lithium dodecyl sulphate (LDS) and 1,4-dithiothreitol (DTT, min 99.0 %) were obtained from Sigma-Aldrich (Steinheim, Germany). NuPage LDS sample buffer (4×), NuPage Tris-Acetate SDS running buffer (20×), HiMark unstained high molecular weight protein standard and Invitromass high molecular weight mass calibration kit were purchased from Invitrogen (Carlsbad, CA, USA). Trifluoroacetic acid (TFA) was obtained from Riedel de Haën (Seelze, Germany).

Recombinant von Willebrand factor (rvWF)

Three non-commercial rvWF preparations were produced from Baxter Biosciences (Vienna, Austria). Sample A contained 0.67 mg/mL rvWF dissolved in a buffer system consisting of 5.25 g/L L-glycin, 5.25 g/L L-lysin-hydrochlorid, 5.25 g/L trisodium-citrat × $2H_2O$, 0.62 g/L $CaCl_2$ × $2H_2O$ and 2.2 g/L NaCl (pH 6.8). Sample B contained 0.49 mg/mL rvWF and sample C 0.54 mg/mL rvWF; both samples were dissolved in the following buffer system consisting of 20 mM HEPES, 150 mM NaCl and 0.5 % saccharose (pH 7.4).

Capillary gel electrophoresis-on-the-chip for evaluation of sample homogeneity

CGE-on-the-chip experiments were carried out using the 2100 Bioanalyzer and the Protein P200 plus assay (Agilent Technologies, Waldbronn, Germany) with a non-commercial set-

up. The instrument was operated and the obtained results were integrated and evaluated with the aid of the 2100 Expert software v.B.02.02.SI238.

All chips (Agilent Technologies, Waldbronn, Germany) were prepared according to the manufacturer´s instruction. Briefly, 4 µL of the rvWF sample solutions were mixed with 2 µL of the provided denaturing solution containing 0.0052 mg/mL DTT, heated on 95 °C for 5 min and finally the mixture was diluted with 84 µL water. 6µL of the final sample solution were applied into the designated sample wells on the CGE-chip and electrokinetically injected. For molecular mass determination a protein ladder consisting of well defined proteins (provided in the Agilent Technologies kit) was treated in the same way.

SDS-PAGE for optimization of salt/detergent removal

For analysis of protein samples under reducing conditions 6 µL sample solution, 3 µL NuPage LDS sample buffer (4×) and 3 µL 0.1 M DTT were mixed, incubated for 1 min at 99 °C and cooled down to room temperature. 10 µL of the resulting mixture were applied directly onto the slab gel. For molecular mass estimation the HiMark protein standard mixture was applied onto the gel additionally. A mixture containing 6 µL HiMark protein standard, 3 µL LDS sample buffer (4×) and 3 µL water were directly applied onto the gel. Electrophoresis was performed on a 3-8 % Tris-Acetate, 1mm × 10 wells NuPage precast mini gel (Invitrogen, Carlsbad, CA, USA) using freshly prepared Tris-Acetate SDS running buffer. Constant voltage was set to 150 V, after 70 min the separation was stopped. Directly after the separation the gel was placed in a fixing solution (45 % MeOH, 5 % acetic acid) for 30 min and subsequently stained with a Coomassie staining solution (0.1 % CBB R250, 45 % MeOH, 9 % acetic acid) for 45 min. Finally the gel was placed in a destaining solution (45 % MeOH, 9 % acetic acid) for 45 min, within this time frame the gel background became completely clear and distinct protein bands became visible.

Sample preparation methods for nano ES GEMMA analysis

Due to the differing buffer compositions containing a high amount of salts, additives and detergents the three rvWF samples had to be desalted/purified prior to application to the nano ES GEMMA device. Three different desalting approaches were evaluated, membrane centrifugation, size exclusion chromatography and dialysis with a starting volume of 300 µL. For membrane centrifugation Nanosep™ centrifugal devices with a MW cut off of

3000 Da (Pall Corporation, Ann Arbor, MI, USA) were used. 300 µL rvWF sample solution were spinned down 20 min at 5000 rpm, the residue was washed once with 100 µL 20 mM ammonium acetate buffer (pH 6.8) and resuspended in 300 µL 20 mM ammonium acetate buffer (pH 6.8). Size exclusion chromatography was performed with MicroSpin™ G-25 columns (GE Healthcare, Little Chalfont, UK). The volume applied onto the MicroSpin™ column is limited, thus two 150 µL aliquots rvWF solution were desalted. Both aliquots were desalted twice for 2 min at 2000 rpm, each time using a new spin column. Prior to application to the GEMMA the aliquots were combined again, resulting in approx. 300 µL. Dialysis of rvWF preparations was performed in Slide-A-Lyzer® dialysis cassettes with a MW cut off of 10.000 Da (Pierce, Rockford, IL, USA). 300 µL rvWF solution were diluted to a volume of 1.5 mL and filled into the dialysis cassette, which remained floating approximately 24 h in the dialysis solution (20 mM ammonium acetate, pH 6.8). Possible rvWF loss monitoring during desalting/purifying procedure was done by means of the described SDS-PAGE method.

Prior to accurate molecular mass determination of rvWF monomers by nano ES GEMMA analysis reduction of the disulfide bonds (which are responsible for the dimer and multimer formation in the native state) was necessary.

Recombinant vWF sample solutions were finally once desalted with MicroSpin™ G-25, and afterwards 2 % (w/v) SDS and 0.15 % (w/v) DTT were added followed by incubation for 1 min at 99 °C (reduction process). Prior to the GEMMA analysis SDS and DTT was removed by further two MicroSpin™ G-25 desalting steps.

Nano ES GEMMA

The nano ES GEMMA system (TSI 3980) consists of a nano ES charge reduction unit (TSI 3480), a nano differential mobility analyzer (nDMA; TSI 3080) and an ultrafine condensation particle counter (µCPC; TSI 3025A) as detector (all parts from TSI Inc, Shoreview, MN, USA). Multiply charged ions are generated by the nano electrospray unit and charge reduced by a bipolar atmosphere generated by means of Polonium-210 to yield neutral and singly positive and negative charged molecules. The molecular ions are size separated according to their electrophoretic mobility diameter (EMD) within a flow of particle-free air in the nDMA and detected with the µCPC. For molecular mass determination of rvWF first the EMD of several well defined standard proteins were determined and correlated with their molecular mass. Based on the resulting relationship

between EMD and molecular mass, the size of unknown biomolecules as the rvWF were determined and subsequently the molecular mass was derived [34, 37].

The settings of the nano ES source were 2 kV spray voltage and 0.3 L/min CO_2 (99.995 %, Air Liquide, Schwechat, Austria)/1 L/min compressed air (generated by compressor type Hobby-Star 200W, AGRE, Garsten-St. Ulrich, Austria) were applied to operate the instrument in a stable cone-jet mode for the used ammonium acetate buffer (20 mM, pH 6.8). A fused silica capillary with an inner diameter of 150 nm was used and the tip of the spray needle exhibited an angle of 75°. The ES process was operated in the positive ion mode. Ten to twenty scans (120 s per scan) across the whole size range were averaged for each final nano ES GEMMA spectrum presented in this paper.

Sample preparation for MALDI mass spectrometry

For reduction of the disulfide bridges of the rvWF dimers and multimers 10 µL original sample solution were mixed with 0.5 µL 10 % LDS (w/v) and 1 µL 1 M DTT. The resulting mixture was vortexed thoroughly, spinned down and incubated at 99 °C for 1 min. Afterwards sample desalting/purification was performed with ZipTip™ pipette tips containing a hydrophilic HPL resin (Millipore, Bedford, MA, USA). First 10 µL solution A (ACN/ 0.1 % FA, 9:1, v/v) were mixed with the sample solution. For wetting the HPL stationary phase 10 µL of solution B (ACN, 0.1 % FA, 1:1, v/v) were aspirated and dispensed to waste. Equilibration of the resin was obtained by aspirating and dispensing plain solution A three times. The sample was bound to the resin by aspirating and dispensing the sample solution seven times. To remove all interfering salts, additives and detergents the tip was washed with plain solution A ten times. Finally the protein was eluted with 2 to 4 µL MALDI matrix solution (10 mg THAP dissolved in 1 mL 0.1 % TFA/ACN (1:1, v/v) solution). For MALDI MS analysis 0.5 µL of the resulting sample/matrix solution were applied onto the often used as well as washed stainless steel MALDI target. Calibration was performed externally by using the Invitromass high molecular weight mass calibration kit. The calibration kit was applied according to the manufacturer´s instructions.

MALDI mass spectrometry

All MALDI TOF MS experiments were carried out on an AXIMA TOF² (Shimadzu Biotech Kratos Analytical, Manchester, UK) equipped with a nitrogen laser ($\lambda = 337$ nm).

The instrument was operated in positive ion, linear mode without using pulsed extraction. Each mass spectrum was acquired by averaging 50 to 200 unselected and consecutive laser shots. Prior to data analysis the mass spectra were smoothed with Savitsky-Golay algorithm.
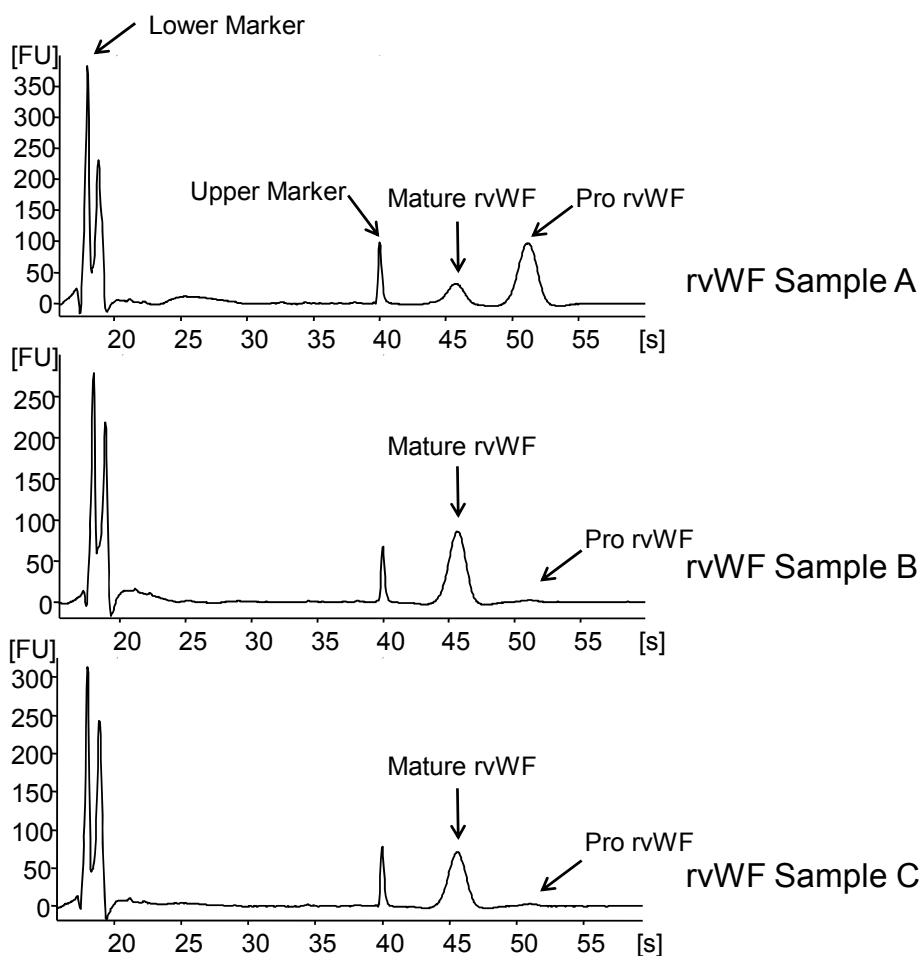
Results and Discussion

Figure 5.1: CGE-on-the-chip electropherogramms of rvWF samples A, B and C under reducing conditions without prepurification. (FU, fluorescence units, s, seconds in migration time).

To obtain first information about the homogeneity of rvWF samples CGE-on-the-chip was utilized. Without any particular sample preparation and within a short time span (60 s run time) data of rvWF samples A, B and C (Figure 5.1) were obtained, revealing that each

sample contains two peaks representing different rvWF species. Based on the determined molecular mass of these peaks, which has to be treated in case of glycoproteins with great caution, mature rvWF with a determined molecular mass of 277 kDa and due to incomplete enzymatic cleavage a varying amount of pro-rvWF with a molecular mass of 341 kDa was determined and assigned. Sample A contained as main component pro-rvWF and to a minor extent mature rvWF (see Figure 5.1, top). But the electropherogramms of sample B and C, two different preparations, exhibited as dominating form mature rvWF and only very low amounts of pro-rvWF. After this first and fast evaluation a more detailed characterization was performed utilizing nano ES GEMMA and MALDI TOF MS.

Due to differing buffer compositions containing high amounts of salts and detergents interfering with the nano ES process rvWF samples had to be desalted prior to nano ES GEMMA analysis. Three different approaches, membrane centrifugation (Nanosep™ 3K), size exclusion chromatography (MicroSpin™ G-25) and dialysis (Slide-A-Lyzer® 10K) were evaluated using rvWF sample A. Glycoprotein recovery after the desalting procedure was monitored with SDS-PAGE under reducing conditions.
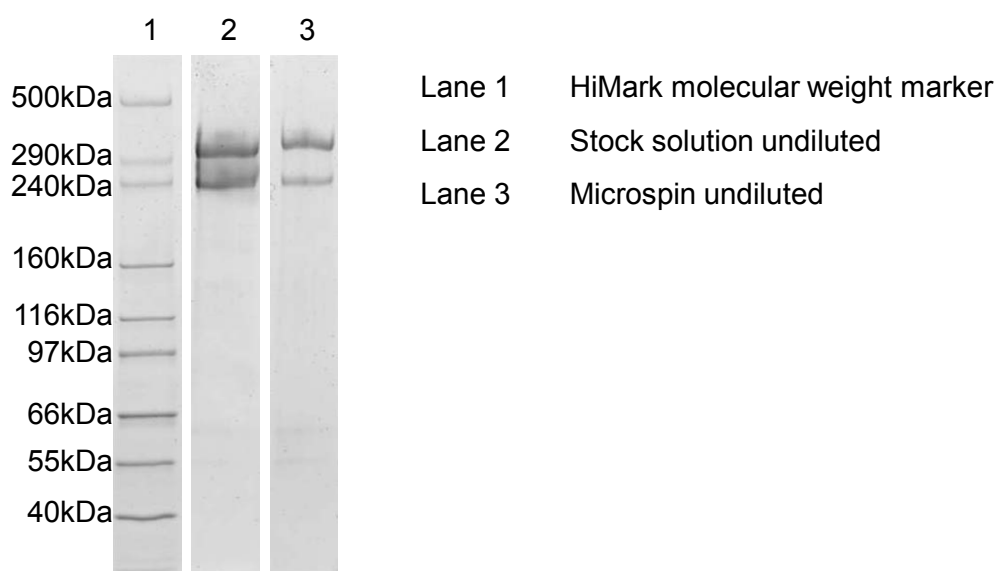

Figure 5.2: SDS-PAGE image of rvWF sample A under reducing conditions without and after MicroSpin™ desalting procedure.

Figure 5.2 shows the SDS-PAGE data comparing rvWF sample A without desalting (lane 2) and desalted two times with Microspin™ G-25 (size exclusion chromatography) columns (lane 3). Untreated rvWF sample A shows two protein bands at approximately 269 kDa and 339 kDa, confirming the data achieved by CGE-on-the-chip. Size exclusion chromatography (MicroSpin™ G-25) of rvWF sample A also yielded two distinct protein bands, slightly fainter than the protein bands obtained from the untreated sample. Dialysis of rvWF samples resulted in extensive sample loss, most likely caused by adsorption of the highly adhesive rvWF to the dialysis membrane. Hardly any analyte loss compared to the untreated sample was obtained by the membrane centrifugation (Nanosep™ 3K) device; two distinct protein bands could be observed again. Due to the faster procedure (4 min) compared particular to the membrane centrifugation and the satisfying desalting/purifying efficiency MicroSpin™ G-25 (size exclusion chromatography) columns were used for further experiments related to the nano ES GEMMA. Even though rvWF sample B and C were provided in a differing buffer system comparable desalting/purifying efficiency could be obtained by utilizing MicroSpin™ G-25 (size exclusion chromatography) columns (data not shown).

Figure 5.3 shows nano ES GEMMA spectra of reduced rvWF samples A to C differing in rvWF concentrations. GEMMA spectra of rvWF sample A (Figure 5.3, top) shows an intensive peak at 11.9 nm (± 1.6 %) corresponding to a molecular mass of 298.8 kDa, whereas rvWF sample B (Figure 5.3, center) and C (Figure 5.3, bottom) yield peaks at 10.9 nm corresponding to a molecular mass of 227 kDa (± 2.5 %). According to CGE-on-the-chip as well as SDS-PAGE data rvWF sample A contains two compounds whereas the high molecular mass compound is the dominating compound (see Figure 5.1, top electropherogramm). In principle, the nano ES GEMMA spectrum should exhibit two peaks, mature rvWF at 11.3 nm and pro-rvWF at 12.7 nm, both values back-calculated from obtained MALDI TOF data. Unfortunately, the resolution of the used nDMA is not high enough to clearly separate both molecular ions (mainly due to the low number of voltage steps in this sizing region). What could be determined was a peak maximum of 11.8 nm, which turned out to be the average value between 10.9 nm (based on GEMMA data of sample B and C) and 12.7 nm (the base for this value were MALDI TOF data). Samples B and C contain mainly mature and practically no pro-rvWF which was also found in their nano ES GEMMA spectra. The concentration of the latter species is negligible as also corroborated by the CGE-on-the-chip data. Nevertheless differences

(peak width and a reproducible fine structure) between samples B and C can be detected and might be indicative for unknown sample differences.
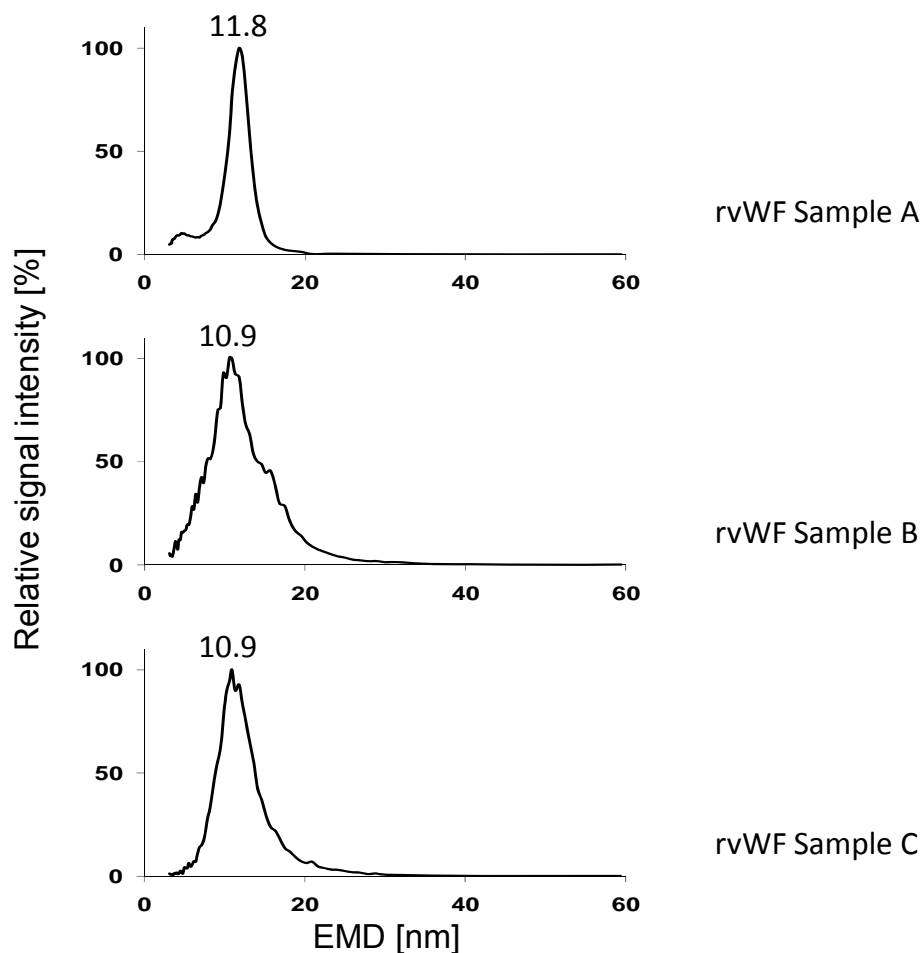

Figure 5.3: *Nano ES GEMMA spectra of rvWF samples A, B and C after reduction of disulfide bridges and desalting with MicroSpin™ devices.*

The second technique for the characterization of the intact glycoprotein rvWF utilized, was MALDI-TOF MS. Due to its relative (compared to nano ES) high tolerance against salts and detergents no extensive sample desalting/purification was necessary in contrast to the nano ES GEMMA method. After reduction of disulfide bonds to obtain the rvWF monomers, salts and detergents were removed by a commonly used ZipTip desalting approach.
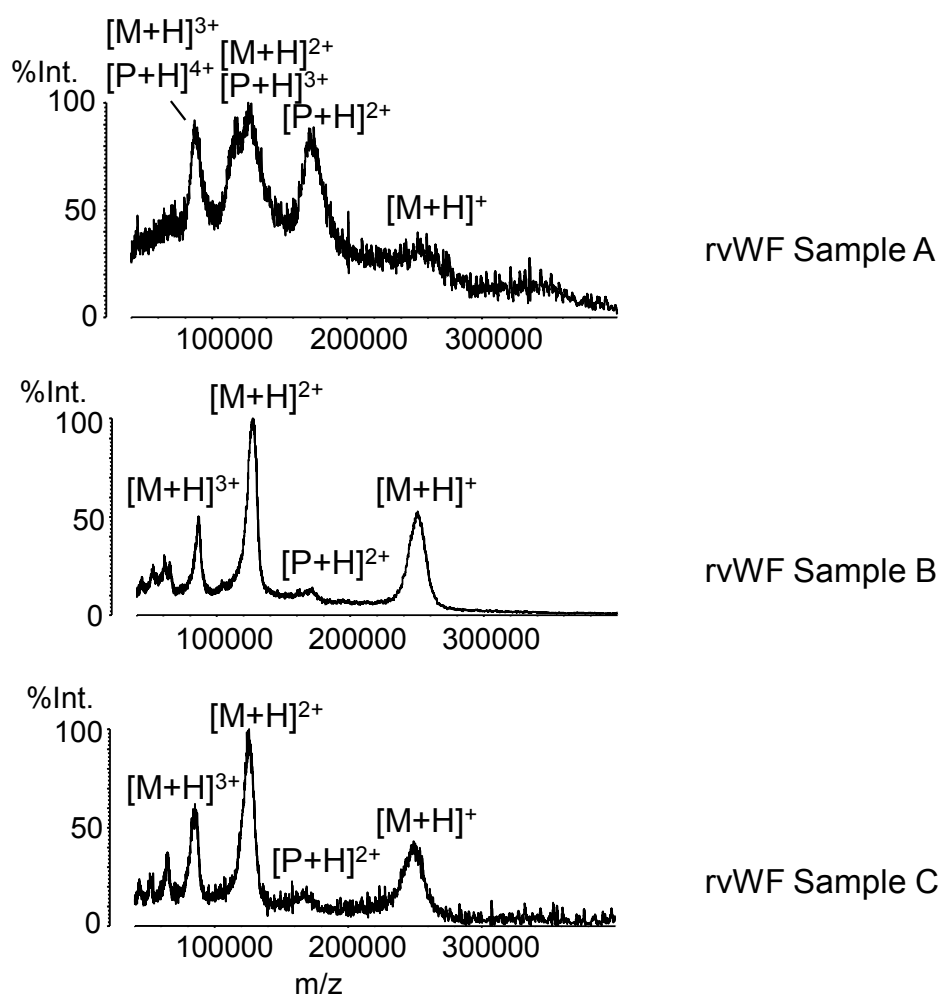
Figure 5.4: *Positive ion MALDI mass spectra obtained in the linear mode of rvWF samples A, B and C. M indicates mature rvWF and P indicates pro-rvWF.*

Figure 5.4 shows the positive ion MALDI mass spectra of rvWF samples A to C after the desalting step. Every mass spectrum yields singly as well as multiply charged molecular ions, complicating data interpretation in case of samples containing the already mentioned two rvWF species. $[M + H]^+$ (m/z 256100), $[M + 2H]^{2+}$ (m/z 127800) and $[M + 3H]^{3+}$ (m/z 87600) ions of mature rvWF and $[P + 2H]^{2+}$ (m/z 174400), $[P + 3H]^{3+}$ (m/z 118100) and $[P + 4H]^{4+}$ (m/z 87600) ions of pro-rvWF were detected in the positive ion mass spectrum of rvWF sample A (see Figure 5.4, top). The singly charged molecular ion of pro-rvWF could not be detected reliably. Due to the low mass spectrometric resolution doubly charged mature rvWF (m/z 127800) and triply charged pro-rvWF species (m/z 118100) could not be completely separated, resulting in a broad signal with two maxima (nevertheless a differentiation was possible). Triply charged mature and quadruply charged pro-rvWF species could not be separated at all, because the determined m/z values are practically

107

identical (m/z 87000). MALDI mass spectra of rvWF sample B and C (Figure 5.4, center and bottom) containing mainly mature rvWF (as already determined by CGE-on-the-chip, Figure 5.1) and only very low amounts of pro-rvWF, show singly (m/z 249000), doubly (m/z 125600) and triply (m/z 85600) charged molecular ions of mature rvWF with excellent S/N ratios, but also the doubly charged molecular ion of pro-rvWF (m/z 169300 sample B and m/z 167200 sample C) could be detected, but with very low abundance.

Sample	Nano ES GEMMA		MALDI-TOF MS		CGE-on-the-chip	
	Mature	Pro	Mature	Pro	Mature	Pro
A	298.8[1]		256.1	349.8	277.8	341.9
B	227.4	-	249.1	338.6	277.2	342.5
C	227.4	-	248.9	334.6	276.5	341.3

Table 5.1: *Summary of molecular weight data for rvWF obtained by nano ES GEMMA, MALDI-TOF MS and CGE-on-the-chip.* [1] *mixture of mature and pro-rvWF species.*

Table 5.1 summarizes molecular mass data obtained by nano ES GEMMA, MALDI-TOF MS and CGE-on-the-chip. By means of external mass calibration of the MALDI-TOF mass spectrometer an accurate molecular mass determination of rvWF species was possible with a mass precision of ± 0.8 %. Comparison of the obtained molecular mass values with calculated values (based on the amino acid sequence of vWF [38]) stated in literature [3], 307 kDa for the pro-vWF and 226 kDa for the mature vWF (both values without post translational modifications) results in a Δm of 27 to 43 kDa for pro-rvWF and a Δm of 30 to 34 kDa for mature rvWF. These Δm values account mainly for the carbohydrate moiety of the rvWF, yielding a glycosylation degree of 8 to 12 % for pro-rvWF and 12 to 14 % for mature rvWF. Contrary to MALDI TOF MS a separation of mature and pro-rvWF species present in sample A was not possible as already mentioned by the nanoES GEMMA analysis. Due to lower resolution, only a mixture of both species could be detected at 11.9 nm, resulting in a molecular mass of 298.8 kDa (± 1.6 %). This could be confirmed by back-calculation from MALDI MS data, 256.1 kDa (mature rvWF) and 349.8 kDa (pro-rvWF) yielding an EMD of 11.3 nm respectively 12.6 nm. A mixture of both species would yield an EMD of 11.95 nm corresponding to a molecular mass of

299.5 kDa. Also sample B and C contain mature and pro-rvWF species, but in contrast to sample A the concentration of the latter is very low, therefore only mature rvWF species was detected in nano ES GEMMA analysis resulting in a molecular mass of 227.4 kDa (± 2.5 %). Due to the great influence of post translational modifications of rvWF, particularly glycosylation and sulfation, on the capillary gel electrophoresis no reliable molecular mass data [39] could be obtained by CGE-on-the-chip, despite the following values could be determined: approx. 277 kDa for mature rvWF and 341 kDa for pro-rvWF.

Conclusion

Two analytical methods dedicated for molecular mass determination were used for characterization of three rvWF samples provided in differing glycoprotein concentrations and buffer systems, nano ES GEMMA and MALDI TOF MS. Prior to detailed characterization with MALDI TOF MS and nano ES GEMMA the sample homogeneity of the three rvWF solutions was investigated by means of CGE-on-the-chip with a laser induced fluorescence detector under reducing conditions revealing two compounds (molecular mass of approx. 277 kDa and 341 kDa) present in each sample at varying extent, namely mature and pro-rvWF.

External MS mass calibration allows determination of exact molecular mass, hence most accurate data, compared to literature (~226 kDa for mature and ~307 kDa for pro-vWF, based on the plain amino acid sequence), were achieved by MALDI-TOF MS, 256.1 kDa (± 0.8 %, based on singly charged molecular ions) for mature rvWF and 349.8 kDa (± 0.8 %, based on doubly charged molecular ions) for pro-rvWF. Hence compared to the molecular mass data stated in literature (based on the plain amino acid sequence), mass differences of 30 to 34 kDa (mature rvWF) and 27 to 43 kDa (pro-rvWF) were obtained, which correspond to the 22 N- and O-glycans of rvWF, resulting in a glycosylation degree of 12 to 14 % for mature and of 8 to 12 % for pro-rvWF. Due to the lower resolution of the nDMA no separation of mature and pro-rvWF was possible for nano ES GEMMA analysis of rvWF sample A. Only a mixture of both species could be detected at 11.9 nm corresponding to a molecular mass of 298.8 kDa (± 1.6 %), whereas nano ES GEMMA analysis of rvWF samples B and C containing pro-rvWF in a minor concentration resulted in the detection of the mature rvWF with a molecular mass of 227.4 kDa (± 2.5 %), corresponding to a size of 10.9 nm. In general, due to the required desalting/purification of

the rvWF samples determination of accurate molecular mass by means of nano ES GEMMA is more labor and time intensive (desalting with MicroSpin™ G-25 columns (1x), reduction and denaturation, desalting with MicroSpin™ G-25 columns (2x)) than by MALDI-TOF MS (reduction and denaturation, desalting/purification with ZipTip™ pipette tips). Hence, due to the faster and easier sample preparation MALDI-TOF MS is more suitable for accurate molecular mass determination of high molecular mass analytes provided in highly salt and detergents containing buffer systems.

Acknowledgements

References

[1]   Ruggeri Z.M. and Zimmerman T.S., von Willebrand factor and von Willebrand disease. Blood 1987; **70:** 895-904.

[2]   Sadler J.E., von Willebrand factor. The Journal of Biological Chemistry 1991; **266:** 22777-22780.

[3]   Dent J.A., Galbusera M. and Ruggeri Z.M., Heterogeneity of plasma von Willebrand factor multimers resulting from proteolysis of the constituent subunit. Journal of Clinical Investigation 1991; **88:** 774-782.

[4]   Ruggeri Z.M., Von Willebrand factor. Current Opinion in Hematology 2003; **10:** 142-149.

[5]   Furlan M., Von Willebrand factor: molecular size and functional activity. Annals of Hematology 1996; **72:** 341-348.

[6]   Jaffe E.A., Hoyer L.W. and Nachman R.L., Synthesis of antihemophilic factor antigen by cultured human endothelial cells. Journal of Clinical Investigation 1973; **52:** 2757-2764.

[7]   Wagner D.D. and Marder V.J., Biosynthesis of von Willebrand protein by human endothelial cells: processing steps and their intracellular localization. Journal of Cell Biology 1984; **99:** 2123-2130.

[8]   Nachman R., Levine R. and Jaffe E.A., Synthesis of factor VIII antigen by cultured guinea pig megakaryocytes. Journal of Clinical Investigation 1977; **60:** 914-921.

[9]   Titani K., Kumar S., Takio K., Ericsson L.H., Wade R.D., Ashida K., Walsh K.A., Chopek M.W., Sadler J.E. and Fujikawa K., Amino acid sequence of human von Willebrand factor. Biochemistry 1986; **25:** 3171-3184.

[10]   Marti T., Rosselet S.J., Titani K. and Walsh K.A., Identification of disulfide-bridged substructures within human von Willebrand factor. Biochemistry 1987; **26:** 8099-8109.

[11]   Wagner D.D., Lawrence S.O., Ohlsson-Wilhelm B.M., Fay P.J. and Marder V.J., Topology and order of formation of interchain disulfide bonds in von Willebrand factor. Blood 1987; **69:** 27-32.

[12]   Sodetz J.M., Paulson J.C. and McKee P.A., Carbohydrate composition and identification of blood group A, B, and H oligosaccharide structures on human Factor VIII/von Willebrand factor. The Journal of Biological Chemistry 1979; **254:** 10754-10760.

[13]   Matsui T., Titani K. and Mizuochi T., Structures of the asparagine-linked oligosaccharide chains of human von Willebrand factor. Occurrence of blood group A, B, and H(O) structures. The Journal of Biological Chemistry 1992; **267:** 8723-8731.

[14]   Millar C.M. and Brown S.A., Oligosaccharide structures of von Willebrand factor and their potential role in von Willebrand disease. Blood Reviews 2006; **20:** 83-92.

[15]   Carew J.A., Browning P.J. and Lynch D.C., Sulfation of von Willebrand factor. Blood 1990; **76:** 2530-2539.

[16]   Dent J.A., Berkowitz S.D., Ware J., Kasper C.K. and Ruggeri Z.M., Identification of a cleavage site directing the immunochemical detection of molecular abnormalities in type IIA von Willebrand factor. Proceedings of the National Academy of Sciences of the United States of America 1990; **87:** 6306-6310.

[17]   Carew J.A., Quinn S.M., Stoddart J.H. and Lynch D.C., O-linked carbohydrate of recombinant von Willebrand factor influences ristocetin-induced binding to platelet glycoprotein 1b. Journal of Clinical Investigation 1992; **90:** 2258-2267.

[18]   van Schooten C.J., Denis C.V., Lisman T., Eikenboom J.C., Leebeek F.W., Goudemand J., Fressinaud E., van den Berg H.M., de Groot P.G. and Lenting P.J., Variations in glycosylation of von Willebrand factor with O-linked sialylated T antigen are associated with its plasma levels. Blood 2007; **109:** 2430-2437.

[19]   Wagner D.D., Olmsted J.B. and Marder V.J., Immunolocalization of von Willebrand protein in Weibel-Palade bodies of human endothelial cells. Journal of Cell Biology 1982; **95:** 355-360.

[20]   Ruggeri Z.M., Von Willebrand factor, platelets and endothelial cell interactions. Journal of Thrombosis and Haemostasis 2003; **1:** 1335-1342.

[21]   Vlot A.J., Koppelman S.J., Bouma B.N. and Sixma J.J., Factor VIII and von Willebrand factor. Thrombosis and Haemostasis 1998; **79:** 456-465.

[22]   Budde U. and Schneppenheim R., Von Willebrand factor and von Willebrand disease. Reviews in clinical and experimental hematology 2001; **5:** 335-368.

[23]   Federici A.B., The use of desmopressin in von Willebrand disease: the experience of the first 30 years (1977-2007). Haemophilia 2008; **14 Suppl 1:** 5-14.

[24]   Menache D. and Aronson D.L., New treatments of von Willebrand disease: plasma derived von Willebrand factor concentrates. Thrombosis and Haemostasis 1997; **78:** 566-570.

[25]   Thompson A.R., Concentrated von Willebrand factor for treating patients with von Willebrand disease. Haematologica Reports 2005; **1:** 32-37.

[26]   Mannuccio P.M., Lattuada A. and Ruggeri Z.M., Proteolysis of von Willebrand factor in therapeutic plasma concentrates. Blood 1994; **83:** 3018-3027.

[27]   Fischer B.E., Recombinant von Willebrand factor: potential therapeutic use. Journal of Thrombosis and Thrombolysis 1999; **8:** 197-205.

[28]   Turecek P.L., Varadi K., Schlokat U., Pichler L., Dorner F. and Schwarz H.P., In vivo and in vitro processing of recombinant pro-von Willebrand factor. Histochemistry and Cell Biology 2002; **117:** 123-129.

[29]   Rand J.H., Chu S.V. and Potter B.J., In vitro multimerization of human von Willebrand factor from its subunits. British Journal of Haematology 1987; **67:** 433-436.

[30]   Fischer B., Mitterer A., Schlokat U., DenBouwmeester R. and Dorner F., Structural analysis of recombinant von Willebrand factor: identification of hetero- and homo-dimers. FEBS Letters 1994; **351:** 345-348.

[31]   Kaufman S.L., Skogen J.W., Dorman F.D. and Zarrin F., Macromolecule Analysis Based on Electrophoretic Mobility in Air: Globular Proteins. Analytical Chemistry 1996; **68:** 1895-1904.

[32]   Koropchak J.A., Sadain S., Yang X., Magnusson L.E., Heybroek M., Anisimov M. and Kaufman S.L., Nanoparticle detection technology for chemical analysis. Analytical Chemistry 1999; **71:** 386A-394A.

[33]   Kaddis C.S. and Loo J.A., Native protein MS and ion mobility large flying proteins with ESI. Analytical Chemistry 2007; **79:** 1778-1784.

[34]   Bacher G., Szymanski W.W., Kaufman S.L., Zollner P., Blaas D. and Allmaier G., Charge-reduced nano electrospray ionization combined with differential mobility analysis of peptides, proteins, glycoproteins, noncovalent protein complexes and viruses. Journal of Mass Spectrometry 2001; **36:** 1038-1052.

[35]   Muller R. and Allmaier G., Molecular weight determination of ultra-high mass compounds on a standard matrix-assisted laser desorption/ionization time-of-flight mass spectrometer: PAMAM dendrimer generation 10 and immunoglobulin M. Rapid Communication in Mass Spectrometry 2006; **20:** 3803-3806.

[36]   Karas M. and Hillenkamp F., Laser desorption ionization of proteins with molecular masses exceeding 10,000 daltons. Analytical Chemistry 1988; **60:** 2299-2301.

[37]   Laschober C., Wruss J., Blaas D., Szymanski W.W. and Allmaier G., Gas-phase electrophoretic molecular mobility analysis of size and stoichiometry of complexes of a common cold virus with antibody and soluble receptor molecules. Analytical Chemistry 2008; **80:** 2261-2264.

[38]   http://www.expasy.org/uniprot/P04275, May 2008;

[39]   Mueller R., Marchetti M., Kratzmeier M., Elgass H., Kuschel M., Zenker A. and Allmaier G., Comparison of planar SDS-PAGE, CGE-on-a-chip, and MALDI-TOF mass spectrometry for analysis of the enzymatic de-N-glycosylation of antithrombin III and coagulation factor IX with PNGase F. Analytical and Bioanalytical Chemistry 2007; **389:** 1859-1868.

Curriculum Vitae

Personal Information

Name:	Mag. JASMIN HIRSCHMANN
Address:	Stifterstraße 10a/2
	4663 Laakirchen
Phone:	0699/11118051
E-mail:	Jasmin.Hirschmann@gmx.at
Date of birth:	15. April 1980
Marital status:	Single
Nationality:	Austria

Education

1986 – 1990	Elementary school; 4663 Laakirchen
1990 – 1998	Grammar school Orth; 4810 Gmunden
1998	Enrollment in chemistry; University of Vienna
May 2004	Start of diploma thesis under the supervision of Univ.-Prof. Dr. Guenter Allmaier
	Institute of Analytical Chemistry; University of Vienna
	Characterisation of a Sambucus nigra allergen by mass spectrometry and two dimensional gel electrophoresis
April 2005	Diploma examination (with distinction)
May 2005:	Start of PhD thesis under the supervision of Univ.-Prof. Dr. Guenter Allmaier
	Institute of Chemical Technologies and Analytics; University of Technology, Vienna
	Sample preparation for matrix-assisted laser desorption/ionization mass spectrometry (MALDI MS) and gas phase electrophoretic macromolecula mobility analysis (GEMMA) related to proteins, polymers and intact Fusarium spores
June 2008:	Final examination

Working Experience

1995 – 2000   Temporary employment during summer holiday at Gmundner Zement Produktions- und Handels GmbH

2001 – 2002   Temporary employment during summer holiday at UPM-Kymmene Austria GmbH

Conference Participations and Contributions

September 2006   **Poster:** *Comparison of different protein staining protocols for SDS-PAGE of recombinant erythropoietin with respect to staining sensitivity and sequence coverage of MALDI-based peptide mass fingerprinting.* 7th Siena Meeting

September 2006   **Lecture:** *Comparison of different protein staining protocols for SDS-PAGE of rhEPO.* Österreichisches Proteomforschungssymposium

June 2007   **Poster:** *Comparison of different sample preparation techniques for differentiation of mycotoxin-producing Fusarium species by MALDI-TOF mass spectrometry.* 55th ASMS Conference on Mass Spectrometry and Allied Topics

February 2008   *MALDI-TOF-MS of intact Fusarium spores.* MassSpec-Forum-Vienna-2008

Publications

M. Marchetti, J. Hirschmann, E. Förster-Waldl, G. Allmaier, Mass spectrometry of proteinous allergens inducing human diseases. *Medial Applications of Mass Spectrometry*, Elsevier, 2008

J. Hirschmann, M. Marchetti, Ch. Reichel, G. Allmaier, Comparing standard and microwave assisted staining protocols for SDS-PAGE of glycoproteins followed by subsequent PMF with MALDI-MS. *Journal of Proteomics* (submitted April 2008)